Technical University of Darmstadt

Department of Materials and Earth Sciences

TECHNISCHE UNIVERSITÄT DARMSTADT

Spatial Distribution and Temporal Evolution of Polycyclic Aromatic Hydrocarbons in Sediment and Water in the Northern Part of Taihu Lake, China

Dissertation for the Degree of Doctor rerum naturalium (Dr. rer. nat)

Aili Li

From Xianyang, Shaanxi, V.R. China

Referee: Prof. Dr. Christoph Schüth

Co-referee: Prof. Dr. Wilhelm Urban

Examiner: Prof. Dr. Wolfgang Ensinger

Examiner: Prof. Dr. Matthias Hinderer

Darmstadt 2019 – D19

Submission date: 2019-06-03

Oral exam date: 2019-08-05

Declaration

The work presented in this dissertation was conducted in the Institute of Applied Geoscience, Technical University of Darmstadt within the period of November 2015 to May 2019. This dissertation represents the author's original work and no part of it has been submitted for a degree at any other university. Prior to the submission of this dissertation, part of the work has been published as described in the relevant chapter herein.

Aili Li

Darmstadt, April 30, 2019

Short CV

PhD 2014. 11 –

Technical University of Darmstadt

Institute of Applied Geosciences

Dissertation title: Spatial Distribution and Temporal Evolution of Polycyclic Aromatic Hydrocarbons in Sediment and Water in the Northern Part of Taihu Lake, China

Supervisor: Prof. Dr. Christoph Schüth

Master 2011.9 – 2014.6

Lanzhou University

College of Earth and Environmental Sciences

Dissertation title: Groundwater Flow Modeling with FEFLOW Model in Zhongwei Plain in Ningxia, China

Supervisor: Prof. Dr. Jianming Zhang

Bachelor 2007.9 – 2011.6

Northwest Agricultural and Forestry University

College of Water Resources and Architectural Engineering

Subject: Hydrology and Water Resources Engineering

Dissertation title: Analyses of the Effect of Irrigation Frequency on Soil Infiltration

Supervisor: Prof. Dr. Huanjie Cai

Table of content

List of figures

List of tables

Abbreviations

polycyclic aromatic hydrocarbon	PAH
persistent organic pollutant	POP
naphthalene	naph
2-methylnaphthalene	2methylnaph
1-methylnaphthalene	1methylnaph
acenaphthylene	acenaphthy
acenaphthene	acenaphthe
fluorene	fluorene
phenanthrene	phen
anthracene	anthra
fluoranthene	fluor
pyrene	pyrene
benzo[a]anthracene	BaA
chrysene	chry
benzo[b]fluoranthene	BbF
benzo[k]fluoranthene	BkF
benzo[e]pyrene	BeP
benzo[a]pyrene	BaP
perylene	perylene
dibenzo[a,h]anthracene	DahA
benzo[g,h,i]perylene	BghiP
indeno[1,2,3-c,d]pyrene	INcdP

Abstract

Taihu Lake is the third largest freshwater lake in China, playing an important role for flood control, tourism, shipping and especially as a drinking water source for its neighboring cities, but the lake has been seriously polluted and drinking water supply has been threatened. Polycyclic aromatic hydrocarbons (PAHs) are ubiquitously distributed in the environment with petrogenic and pyrogenic sources, and they are carcinogenic and mutagenic to humans and other organisms. With the development of economy and industries, the rapid increase of fuel and biomass consumption results in significant PAH emission to the environment. In this study, we focus on PAHs in the sediments and water body in the northern part of Taihu Lake where is more polluted than the other part of the lake.

We analyzed the concentration patterns of 20 PAHs in 25 surface sediments, 11 sediment cores and 41 water samples which were collected from the northern part of Taihu Lake during 4 times of field campaign (2015-11, 2016-06, 2017-02 and 2017-09). Three of the cores were dated based on ^{137}Cs activity for the deposition age of the sediment. The data on energy consumption and type of vehicles in the lake catchment in the last two decades were collected from regional official websites to explain potential PAH emission histories in the area. The literature data on PAH emissions from their potential sources and on PAH distributions in particle sizes were collected to generalize PAH emission and distribution features. PAH patterns from different emission sources and also from the sediment results of this study were combined to verify the two assumptions for the methods of PAH source track in the environment.

The spatial distributions of the PAH concentrations (perylene excluded) show that the inflow rivers into Zhushan bay and Meiliang bay were the main pathways for PAHs and sediments input into the northern part of the lake. This results in substantially higher PAH concentrations (up to 5000 ng/g) and sedimentation rates (higher than the average of 3 – 4 mm/a) in the area close to the river outlets. In addition, the results also show that PAH concentrations in the sediments considerably increased from the late 1950s due to the development of economy and industries, but the relatively decreased or stable concentrations in the upper layers of the sediments could be attributed to the gradual changes in energy structures, emission control in coal combustions since the 1990s and emission control in vehicle exhaust since ca. 2000 in this area.

PAHs determined in the sediment cores (perylene excluded) are dominated by 4 light ones (phenanthrene (phen), anthracene (anthra), fluoranthene (fluor), pyrene) and 6 heavy ones (benzo[k]fluoranthene (BkF), benzo[a]pyrene (BaP), benzo[b]fluoranthene (BbF), benzo[e]pyrene (BeP), indeno[1,2,3-c,d]pyrene (INcdP), benzo[g,h,i]perylene (BghiP)) whose concentrations typically reach up to 70% – 80% of that of the 19 PAHs. The concentration fractions of the 6 heavy PAHs are almost double of the fractions of the 4 light ones, and the fractions of the heavy PAHs increase with decreasing depth in the cores, but the fractions of the light PAHs show the opposite trends (except cores GH38 and ZS23 with special features). PAH emission patterns from wood combustion, coal combustion and vehicle exhausts together can, to a great extent, illustrate the distribution patterns of the concentration fractions between the light and the heavy PAHs in the cores. Wood combustion has evidently higher emission fractions of the 4 light PAHs than the fractions of the 6 heavy PAHs compared to the emission patterns from coal and oil combustions, but wood has been gradually phased out as an important energy source since the beginning of industrialization in the 1950s. PAH patterns from coal combustions can somewhat explain the concentration fraction distributions of the two groups of PAHs in the cores through four points: the continuous decrease of

residential coal consumption and the significantly increased consumption of emission-controlled coal combustion in this area during the last decades, relatively more ultrafine particles emitted from emission-controlled coal combustion, heavy PAHs bond more in ultrafine particles. Meanwhile, PAH patterns from vehicle exhausts contribute to the distributions of the concentration fractions in the cores through three points: the linear increase of oil consumption in transport, around 24-time increase in the number of light-duty vehicles but only 2-time increase in the number of heavy-duty vehicles in this area during the last two decades, and noticeably higher emission fraction of the heavy PAHs from light-duty vehicle exhausts than that from heavy-duty vehicle exhausts.

Several methods are frequently used to interpret PAH source track in the environment, and these methods are based on two assumptions: PAH patterns from different sources are specific and distinguishable from each other; the patterns maintain stable after emission to the environment. The first assumption was mainly verified by the PAH patterns from different emission sources, which shows that PAH patterns from different sources indistinguishably overlap from each other. The second assumption was verified by the spatial and temporal distributions of PAH patterns in the sediment of this study, which shows that PAH patterns in the sediment are ambiguous and variable. Therefore, both of the two assumptions are not valid for PAH source track in the sediment.

There were both anthropogenic and biogenic origins of perylene in the lake sediments, which were distinguished based on its spatial distribution patterns and also the concentration proportions of perylene to the sum of the 20 PAHs. In the cores collected close to the river outlets, the concentration proportions of perylene typically range from 0.02 to 0.18 and there are significant positive linear correlations between the concentration of perylene and three anthropogenic PAHs (BaP, BeP, Pyrene), suggesting that perylene was dominated by anthropogenic input. However, the cores collected further away from the river outlets show the concentration proportions between 0.13 and 0.96, and present significant negative correlations or no correlations between perylene and the three PAHs, suggesting that perylene was mainly formed by biogenic activities. Furthermore, the different perylene sources accompanied with the core location distributions imply that anthropogenic activities could inhibit its biogenic formation.

In the water samples, naphthalene (naph), 1-methylnaphthalene (1methylnaph) and 2-methylnaphthalene (2methylnaph) have considerably higher concentrations in the samples (2016-06 and 2017-09) taken in warm seasons than the concentrations in the samples (2015-11 and 2017-02) taken in cold seasons, but the concentrations of the other PAHs do not vary with seasonal variations. The distribution patterns of these PAHs might be mainly attributed to ambient temperature effects on the PAH solubility in the water body. It is noteworthy that in the campaign 2017-09, the concentrations of 2methylnaph are particularly around twice as high as the concentrations of naph and reach up to 1350 ng/L. As the emission rates of naph are generally higher than methylnaph from anthropogenic activities, so it is suspected that the relatively higher concentrations of 2methylnaph should be attributed to additional biogenic input in the lake water. Furthermore, the samples collected in cold seasons show that high concentrations are mostly located in the northwestern part of the lake and relatively low concentrations are in the northeastern part of lake, but the concentrations from the warm season samples are homogeneous in the whole sampling area. The reason for the different spatial distributions between the cold and warm seasons is that during the sampling campaigns in cold seasons, there was water recharge from the Yangtze River through the Wangyu River connecting the northeastern part of Taihu Lake, which diluted PAH concentrations in the northeastern part of the lake.

1 Introduction

1.1 Motivation

In the recent decades China has been rapidly industrialized and passed as the second largest economy in the world. This has led to increasing prosperity and living standards of a large fraction of the population, but also to a heavy exploitation, and even over-exploitation of natural resources, accompanied with a sharply increasing consumption of energy. As a result, significant and complex environmental problems arose, affecting all environmental compartments, from air pollution to contaminated soils and water resources. Especially, the contamination of water resources is of concern as China is partly a water scarce country with unevenly distributed water availability. The rapidly growing population in industrialized centers further amplifies local water demand, already resulting in serious water shortages in many cities.

The Taihu Lake catchment located in the Yangtze River Delta plain is one of the most developed areas in China with dense population and industries, hosting several large cities such as Changzhou, Wuxi, Suzhou and Shanghai (Fig. 1.1). Environmental pollution has been a major factor influencing the further development of the region and received ample attention over the last years. Taihu Lake itself is the third largest freshwater lake in China and it plays a crucial role for flood control, irrigation, tourism and especially as a drinking water source for the neighboring cities. However, due to high nutrient loads in inflowing rivers the Lake has experienced massive algal blooms, with the most severe ones in 1990 and 2007, causing the shutdown of several water supply facilities.

Fig. 1.1 Taihu Lake surrounded by densely populated cities, with the Yangtze River in the northeastern boundary of the catchment. Figure is from google earth. More information about the catchment is presented in Fig. 2.1.

Besides these obvious environmental impacts that require immediate environmental measures, the lake and its connected ecosystems are also threatened by the constant input of persistent organic pollutants (POPs) through contaminated inflowing rivers and atmospheric deposition. The long-term effects of these contaminant inputs are worrisome, as they may accumulate in the lake sediments and therefore pose a risk to ecosystems within. In addition, as Taihu Lake is very shallow with an average depth of less than 2 m only, contaminants might be mobilized through turbulences in the water column and reenter the water cycle.

PAHs are one group of POPs that ubiquitously exist in the environment. They are emitted since early history through open burning and wildfires, but individual PAHs, like perylene, might also be formed by microbial activities. However, industrialization and the associated combustion of tremendous amounts of organic materials have significantly raised their abundances in environmental compartments. Due to their hydrophobicity, PAHs tend to sorb on particulate matter after emission. As lakes are typically a final trap of particulate matter, lake sediment potentially contain an archive of PAH input from the catchment.

Due to their carcinogenicity and mutagenicity, once PAHs accumulate in environmental compartments, they might enter the food chain and pose a serious risk to human health and ecosystems. Therefore, some studies on PAH distributions in Taihu Lake have been conducted in the past. Most of these studies focus on PAHs in the surface sediment only, addressing the current PAH input into the lake. However, especially the evolution of PAH concentrations in the lake sediments and the alteration of background concentrations due to anthropogenic activities, have not been studied in detail. Also, a closer look into the distribution of individual PAHs might reveal potential emission sources or might allow to distinguish between anthropogenic or biogenic PAH formation.

The research presented in this dissertation was supported by the SIGN project (Sino-German water supply Network-Clean water from the source to the tap), funded by the German Ministry of Education and Research (BMBF-02WCL1336C), and by the International Science & Technology Cooperation Program of China (2016YFE0123700).

1.2 Objective

The main objective of this work was to investigate the spatial and temporal distribution of PAH concentrations and patterns in the sediments of the northern part of Taihu Lake. The intention of analyzing the spatial distribution of PAH concentrations was to conclude on their main input pathways. The temporal distribution of the PAH concentrations should allow to conclude anthropogenic impacts on PAH input and deposition in the lake over time. The PAH patterns in the sediment were compared with the patterns from different sources to explore the temporal changes of PAH emissions in Taihu Lake catchment in the last decades.

For this, surface sediments, sediment cores and also water samples were collected from the northern part of the lake during four field campaigns. The samples were analyzed for their PAH contents and patterns. In addition, three of the cores were dated using the artificial radionuclide ^{137}Cs to determine the deposition age of the sediments. PAH potential sources in the sediment were interpreted using literature data on energy consumptions in the area, PAH emission patterns from different sources and PAH distributions in particle size. Specific attention was paid to the concentration distribution of perylene in relation to the other PAHs in order to distinguish between biogenic and anthropogenic origins of perylene. Furthermore, PAHs in the water samples were analyzed to delineate their spatial and seasonal variations in the lake.

1.3 Framework of this dissertation

This dissertation consists of five chapters, the structure is described in Fig. 1.2.

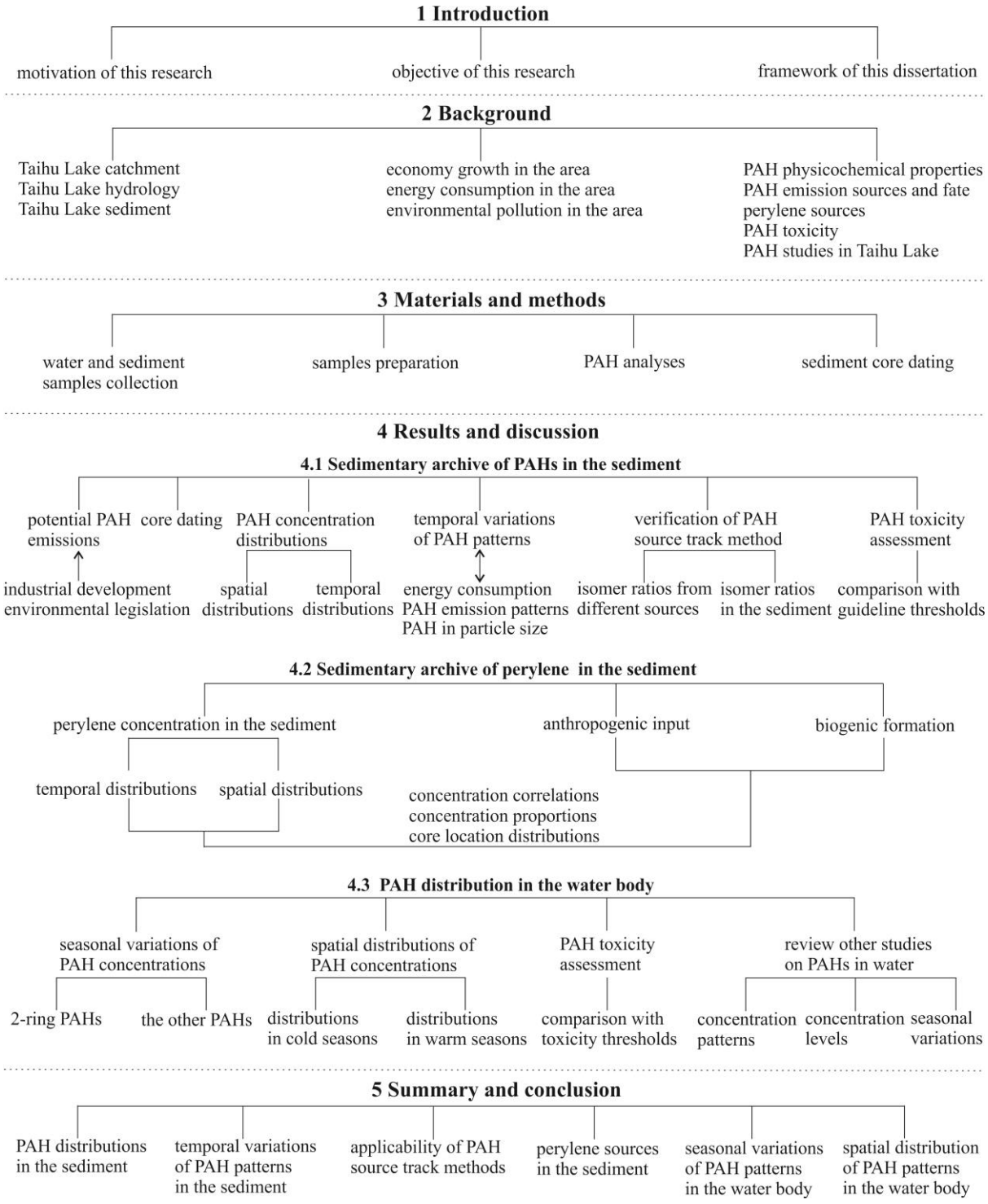

Fig. 1.2 Framework of this dissertation.

2 Background

2.1 Study area

The Taihu Lake catchment, located in the Yangtze River Delta plain, covers an area of about 36,500 km^2 in the southern part of the Jiangsu Province and in the northern part of the Zhejiang Province (Fig. 2.1). It is bound in the north and northeast by the Yangtze River, and in the south and west by mountainous ridges with altitudes reaching up to 1,200 m. The south-western part of the catchment is mainly covered by agriculture, while the lowland plains in the north-eastern part are densely populated with the cities of Changzhou, Wuxi, Suzhou and Shanghai, hosting large industries. Precipitation is the main surface water recharge in the catchment. Due to the topographic characteristics, the western area of the catchment receives more precipitation than the northeastern area. The average precipitation is ca. 1181 mm/a, of which 60% occurs in the month of May to September due to typhoon and southeastern monsoon. Monthly average temperature in the hot and humid summer can reach above 30°C. In the cold and dryer winters, average monthly temperature around the lake is as low as 1°C.

Taihu Lake is located in the center of the catchment, covering an area of about 2,340 km^2 with an average water depth of 1.9 m and a rather flat lake bottom. It is the third largest freshwater lake in China and plays an important role for flood control and irrigation in the region, also for tourism, shipping, aquaculture and especially as a drinking water source for its neighboring cities (Qin et al., 2007; Tao et al., 2010). There are more than 110 inflows and outflows around the lake. The inflows are mostly located in the northern and western part of the lake, while the outflows are in the eastern and southern part, partly connecting Taihu Lake with the Yangtze River (Qin, 2008). Some of the flow directions are occasionally reversing depending on the lake water level. The spatial distribution of the inflows and outflows results in a general water circulation in the lake from the northwest to the southeast. However, the shallowness of the lake and the hydraulic conditions lead to complex flow patterns, and the spatial and temporal current patterns in the lake are not fully understood (Qin et al., 2007). The water retention time in Taihu Lake is even longer than 10 months, which is rather longer than many other lakes and results in more potential of water deterioration (Qin, 2008). Due to the shallowness of the lake, hydrodynamics are important factors influencing sediment deposition and contaminants and nutrients release from sediment to water column, which can also threaten the improvement of its water quality and ecosystem. For example, the concentration of total phosphorus, total nitrogen and heavy metals in overlying water increase significantly because of sediment release and particle resuspension during water turbulence (Qin et al., 2006; Zheng et al., 2013).

The contaminants exchange between water and sediment is closely related to sediment distribution and physicochemical properties. In most parts of the lake, the soft sediment thickness varies between 0.5 and 2 m, and the greater sediment thicknesses are located in the northern and western parts, reflecting the prevailing wind and resulting water circulation patterns (Luo et al., 2004). The different thicknesses of the sediment indicate varying sedimentation rate in the lake. In the upper layers, sediment textures are dominated by clayey silt and clay, and the particle sizes are dominantly below 0.1 mm (Jin et al., 2006; Qin et al., 2004). The high water content and porosity occur in the surface around 5 cm in the northern and western part of the lake and in the surface around 15 cm in the southeastern part of the lake (Qin, 2008). It is, however, likely that during strong winds or floods sediment scouring and resuspension can alter the sediment stratigraphy (Qin et al., 2004).

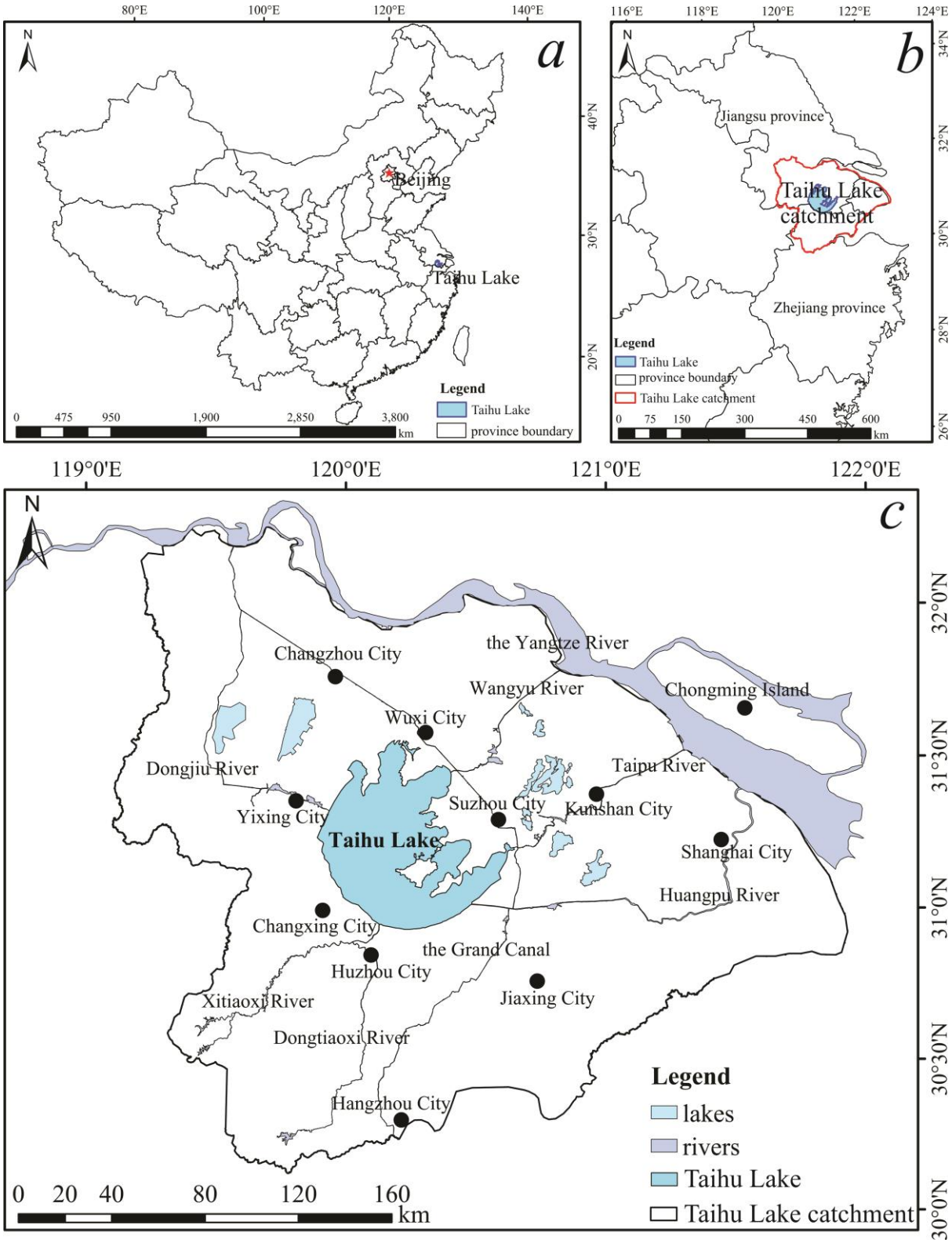

Fig. 2.1 Map of the study area, (a) location of Taihu Lake catchment in China; (b) the catchment boundary; (c) lakes, main inflowing and outflowing rivers, major cities in the catchment.

2.2 Energy consumption and environmental pollution in the catchment

In the last decades, China has achieved considerable growth in GDP (Wu, 2007), and has become the largest coal consumer and second-largest oil consumer in the world (Bloch et al., 2015). Especially, the eastern/costal area of China is in general more developed with several times higher energy consumption than the other areas of China (Hu and Wang, 2006). The over-consumption of

energies and natural resources has been inevitably accompanied with serious and complex environment degradation since the last 2 – 3 decades (Liu and Diamond, 2005; Shao et al., 2006). To mitigate environmental stress and deterioration, the Chinese government introduced a series of environmental measures and technologies (Wang and Chen, 2010; Zhang and Wen, 2008), and the indexes of energy intensity have greatly decreased since the 1980s (Feng et al., 2009; Wu, 2012). However, various contamination problems still occur in all environmental compartments and threaten the ecosystem and human health. For example, N-pollution in groundwater has posed a critical threat to drinking water safety and supply, especially in the northern area of China where the main drinking water source is groundwater (Zhang et al., 1996; Han et al., 2016); fuel combustion and mining contribute a risky amount of heavy metals to the atmosphere and soil in the eastern and middle area of China (Jiang et al., 2006; Li et al., 2014).

Taihu Lake catchment is one of the areas with the highest level of urbanization and rural industrialization in China (Yeh et al., 2011; Shen and Ma, 2005), and contributes around 10% of national GDP. It has a population of around 40 million accounting for more than 3% of the Chinese population. With the rapid development of economy and society, energy consumption has correspondingly increased. Coal is the main energy source and will continue to dominate the energy proportion in the near future in China (Wang and Feng, 2003). Jiangsu province is located in the developed East China and contributes significant GDP growth during the last decades of reform and opening-up policy implementation in China (Herrerias and Ordoñez, 2012; Zhang and Zou, 1998). The southern area of the province is severalfold developed in industries and economy than that in the northern area (Wei and Fan, 2000; Long and Ng, 2001; Huang and Leung, 2002). Therefore, the energy consumption of the whole province can, to a great extent, describe the situation in the developed southern area, and are reasonably used to explain the history of potential contaminant input to the northern part of Taihu Lake in the last decades. Considering the structure of energy consumption in this area, data are collected on coal consumption in residential combustion, coal coking, heating, industries and power generating, on oil consumption in industries and transport, and on the number of heavy-duty and light-duty vehicles (Fig. 2.2). Due to the limited data availability in the southern area of Jiangsu province, here the collected data is documented the consumption of the energies in the whole province.

Energy production from coal is orders of magnitude higher than from other sources in this province, and the total coal consumption remained rather stable with around 270 million tons after 2010 (Fig. 2.2a). The amount of coal used for power generating, heating and industries accounted for more than 90% of the total coal consumption in the period of 2000 – 2010, the rest consumption was in coal coking and residential coal combustion. After 2010, however, the proportion structure of coal consumptions somewhat changed. The consumptions in heating and power generating remained relatively stable, in coal coking kept slightly increasing, but in industries somewhat decreased. Especially, the consumption in residential coal combustion constantly decreased to negligible amount (from 3.88 million tons in 1995 to 0.063 million tons in 2015) compared to the coal consumption in the other compartments. The main oil consumption is gasoline and diesel in industries and transport and the amount of consumption in transport was linearly increasing, but the consumption in industries decreased after 2010 (Fig. 2.2b). From 2002 to 2016, there was an exponential increase in the number of light-duty vehicles (minimum number: 1.02 million in 2002 and maximum number: 25.80 million in 2016), but the number of heavy-duty vehicles only increased to around twice over (minimum number: 0.4 million in 2002 and maximum number: 0.96 million in 2013) (Fig. 2.2c).

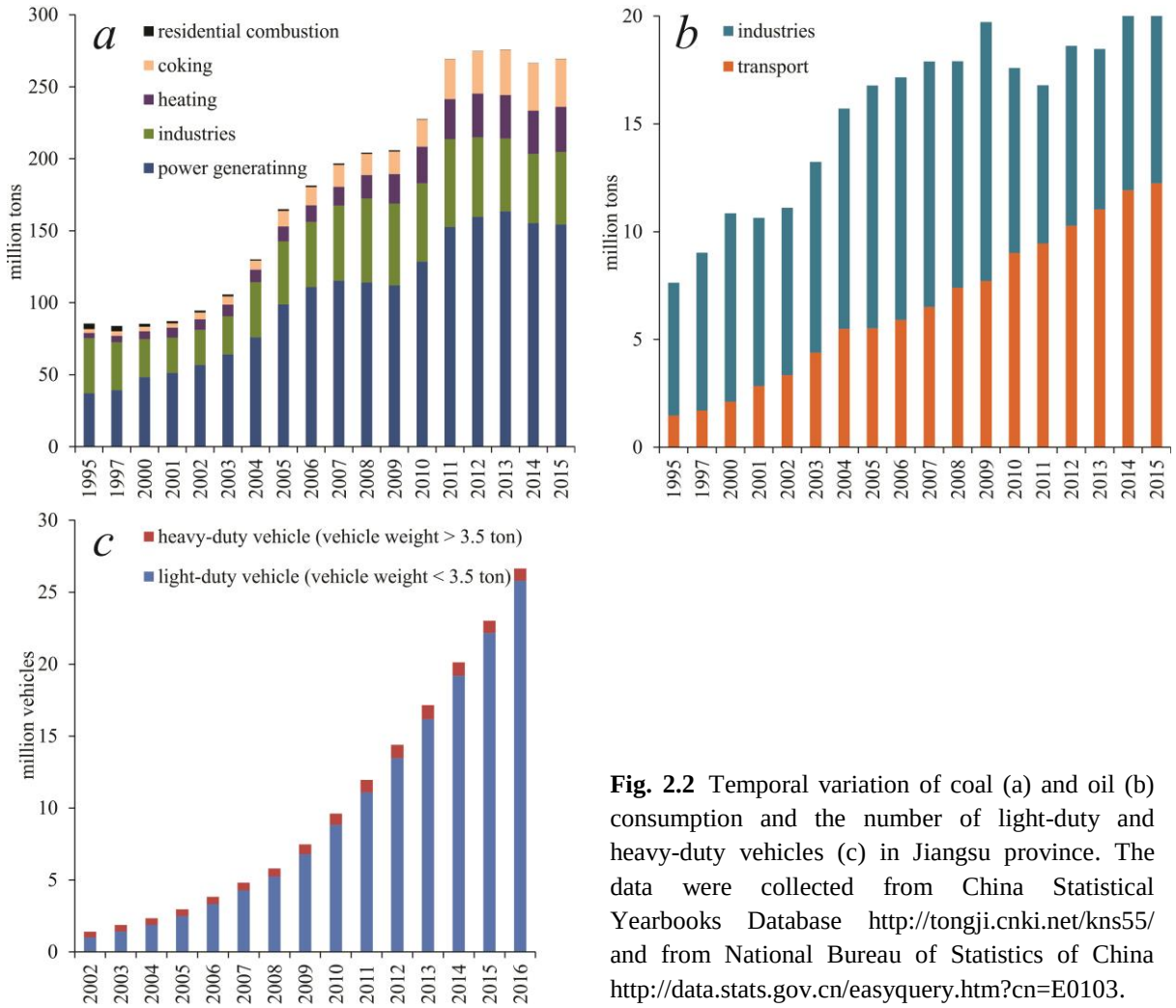

Fig. 2.2 Temporal variation of coal (a) and oil (b) consumption and the number of light-duty and heavy-duty vehicles (c) in Jiangsu province. The data were collected from China Statistical Yearbooks Database http://tongji.cnki.net/kns55/ and from National Bureau of Statistics of China http://data.stats.gov.cn/easyquery.htm?cn=E0103.

The significant amount of energy consumption is accompanied with serious and complex pollutants emission. For examples, one of the emissions is smoke which is composed of soot, aerosols, CO, VOC and some POPs; there are several kinds of NO_x formation during combustion, such as NO, NO_2, NH_3, HCN and HNCO; heavy metals and SO_x are also the alarming emissions, such as Pb, Cr, Mn, As, SO_2 and SO_3 (Williams et al., 2012; Zhao et al., 2008; Chan and Yao, 2008). Most of these pollutants initially emit to the atmosphere with both gaseous and particular phases, and part of the contaminants enter aquatic systems through wet and dry atmospheric deposition (Leister and Baker, 1994). River input and atmospheric deposition are the two main pathways transporting human-derived contaminants and particles to lake systems. Lake ecosystems are particularly sensitive to anthropogenic impacts as they can act as repositories for contaminants in the aquatic environment.

The inflows around Taihu Lake discharge a large amount of industrial effluents, improperly treated municipal sewage, diffused pollutants from agriculture and aquaculture, and accumulated atmospheric depositions into the lake. These discharges attaching complex pollutants gradually lead to serious ecological and water quality deterioration in the lake ecosystems, especially in the northern part of the lake where more inflows are located and which is surrounded by more developed areas (Wilhelm et al., 2011; Tao et al., 2018; Wang et al., 2003; Xu et al., 2014; Jiang et al., 2012). For example, it is found that nitrogen in the surface water in this region is mainly from urban domestic sewage and rural human and animal excreta (Xie et al., 2007), and water leachate from wheat crop also contains high concentration of nitrogen (Zhao et al., 2012); the concentrations of total phosphorus and nitrogen in

the Taihu Lake sediment increased significantly after the 1950s (Yuan et al., 2014); the duration and covering area of algal bloom were increasing in the last two decades (Duan et al., 2009; Qin et al., 2015); in 2007, excessive nutrient input into the lake caused a massive cyanobacterial bloom with the formation of volatile sulfide compounds, resulting in a serious drinking water crisis for half month in Wuxi City whose main drinking water intake is in Gonghu Bay (Zhang et al., 2010).

POPs are notable contaminants in aqueous environment and have had hazardous effects on water quality in China (Bao et al., 2012; Han and Currell, 2017; Wang et al., 2003). They are composed of many families of organic pollutants such as polychlorinated biphenyls (PCBs), polychlorinated dibenzo-p-dioxins and furans (PCDDs/PCFs), polybrominated diphenyl ethers (PBDEs), perfluorinated compounds (PFCs) and PAHs, and they mainly originate from deliberate manufacture and application, combustion processes and industrial activities (Jones and Voogt, 1999). These compounds are ubiquitously distributed in global environmental compartments, even in circumpolar arctic through atmospheric and oceanic transport (Muir and de Wit, 2010). Due to their hydrophobicity, POPs can easily bind to organic matter and then deposit in sediments. After deposition, such contaminants are less susceptible to microbial degradation due to their strong sorption and ageing, which reduces contaminant bioavailability (Erickson et al., 1993; Hatzinger and Alexander, 1995). Lake sediments therefore may contain continuous archives of such inputs with an annual to decadal resolution. With this, the analyses of lake sediments that may have accumulated over decades or centuries can provide insights into background conditions, and into historical, present and potentially future anthropogenic impacts (Hollert et al., 2018).

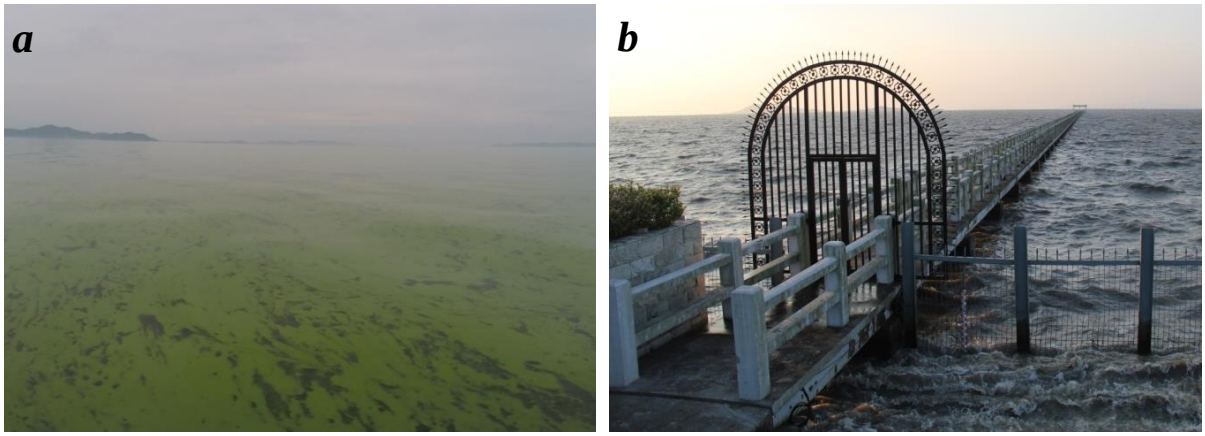

Fig. 2.3 Picture of the water body in Taihu Lake (a, general look; b, waterworks pump station in Gonghu bay).

2.2 PAHs

PAHs consist of two or more aromatic rings bound in linear, cluster or angular arrangement, and the simplest PAH structure is two-ring naph. The 2-ring and 3-ring PAHs are more volatile and hydrophilic, while with molecular mass increase PAHs become hydrophobic and lipophilic. The $\log K_{ow}$ ranges over 5 orders of magnitude from 3.4 for naph at 25 °C (Ma et al., 2010). PAHs are solid at ambient temperature, and their melting temperatures increase with the increase of molecular mass and rational symmetry number δ. 2-ring PAHs such as naph and alkyl naphs have half-lives of days in the atmosphere, weeks in water, months in soils and about a year in sediments (Mackay and Callcott, 1998). With molecular mass increase PAHs are more persistent and their half-lives are severalfold longer in environmental compartments.

PAHs are ubiquitously distributed in the environment. They have been emitted since prehistoric time through e.g. wild fires (Vila-Escalé et al., 2007) or volcanic eruption (Kozak et al., 2017). They are also indicators of anthropogenic activities resulting from incomplete combustion of fossil fuels (Zhang et al., 2008; Wu et al., 2017) and biomass such as wood (Shen et al., 2012), sewage sludge (Mininni et al., 2004), garbage (Besombes et al., 2001). In addition, they can also originate from wear of tires (Wik and Dave, 2009), asphalt pavements (Boonyatumanond et al., 2007), oil spills (Ke et al., 2002) or metallurgical industries (Yang et al., 2002). Nowadays, due to the considerable amount of energy consumption, PAH sources in the environment are mainly attributed to pyrogenic processes. Pyrogenic PAH emission rates and patterns are not only related to fuel types but also to combustion conditions such as combustion temperature, equipment used, oxygen access, catalyst addition. For example, PAH emission from vehicle exhaust is related not only to aromatic hydrocarbon content of added fuel but also to engine load, engine operating conditions and air-fuel ratios in the combustion chamber (Baek et al., 1991; Borras et al., 2009); PAH emission rates and patterns from lignite combustion vary with combustion temperatures ranging between 600 °C and 1000 °C, with air/coal ratios between 1 m^3/kg and 3.5 m^3/kg, and with lignite particle sizes ranging between 0.25 mm and 10 mm (Liu et al., 2012).

The broad anthropogenic emission sources have substantially raised PAH abundance in the environment since industrialization. After PAHs are emitted, gas-phase PAHs mainly contribute to the formation of PAH derivatives in the atmosphere (Tsapakis and Stephanou, 2007; Atkinson and Arey, 1994), and most particle-bound PAHs deposit on the ground (Bae et al., 2002; Demircioglu et al., 2011), so the partitioning of PAHs in gas and particle phase is a significant factor for PAH existence in the environment. The partitioning is dependent on both sub-cooled liquid vapor pressure (Fernandez et al., 2002; Sofowote et al., 2010; Tsapakis and Stephanou, 2005) and the properties of carbonaceous sorbents like soot and organic matter (Dachs and Eisenreich, 2000). Soil and aquatic sediments are sinks for the deposition of particle-bound PAHs. For the more volatile and hydrophilic 2-ring and 3-ring PAHs, the sinks are potentially the second sources for these compounds to escape to other compartments. Due to their physicochemical properties and bioavailabiliy in the sinks, however, the other heavier PAHs are particularly resistant to desorption and biodegradation in contaminated and aged soil and sediments (Readman et al., 1982; Cornelissen et al., 1998; Shuttleworth and Cerniglia, 1995). Therefore, the distribution of PAH contents in environmental matrixes can certainly play as an archive for PAH emission history.

As a specific PAH, perylene abundance in some investigations is noticeably higher than that of other anthropogenic PAHs, so it suggests that perylene can additionally originate from biogenic formation (Venkatesan and Kaplan, 1987; Slater et al., 2013; Fan et al., 2011). Due to the consistent presence of abundant perylene and anoxic indicators of elemental sulfur and pyrite in deep marine sediments, it is speculated that anoxic conditions are the requirement for biogenic formation of perylene (Venkatesan and Kaplan, 1987). On the contrast, it was also found that specifically high concentrations of perylene relative to that of the other PAHs occur in forest soils, surface sediments of wetlands and bird eggs around bird breeding colonies (Zamani et al., 2015). The potential origins of perylene currently raised are diatom (Louda and Baker, 1984), fossil wood degrading fungi (Suzuki et al., 2010; Marynowski et al., 2013; Bechtel et al., 2007), crinoids (Wolkenstein et al., 2006) and termite (Wilcke et al., 2000; Krauss et al., 2005). However, the suspicions on these potential sources are, to a large extent, based on the consistent occurrence and distribution of perylene and these potential sources, and there is no certain evidence for these biogenic formation processes of perylene. In addition, it was also suspected

that biogenic formation of perylene is probably more dependent on microbial activities rather than on aquatic or terrigenous sources of specific organic matter, as the concentration distribution of perylene is not correlated to that of biogenic silica, calcium carbonate, TOC or total phosphorus (Silliman et al., 1998; 2001; Hites et al., 1980). Therefore, a significant amount of research on biogenic perylene origins has been conducted so far, but the conclusions are still ambiguous.

Some of PAHs such as BaP, dibenzo[a,h]anthracene (DahA), benzo[a]anthracene (BaA) are classified as mutagenic, carcinogenic and genotoxic contaminants, and 16 of PAHs are listed as priority pollutants by US EPA (Boffetta et al., 1997; Kim et al., 2013; US EPA, 1993). It has been studied that bioconcentration factors of hydrophobic organic pollutants including PAHs are positively correlated with their partitioning coefficient K_{ow} (Geyer et al., 1984; Axelman et al., 1999), so heavier and more toxic PAHs have higher potentials to be bioaccumulated in organisms. In addition, cellular metabolism can be inhibited by catacondensed PAHs such as naph, phen and anthra rather than pericondensed PAHs probably due to molecular structure differences, tested with bioluminescent bacteria (Lee et al., 2003). Toxic equivalency factors/quotients are commonly adopted as indicators for toxicity assessment of mixed PAHs in environmental compartments, and the toxicity potential is expressed as BaP equivalent (Nisbet and Lagoy, 1992) or phen equivalent (Fisher et al., 2011). Humans can be exposed to PAHs through e.g., inhalation of PAHs from the atmosphere, oral uptake of PAH contaminated food and water, and dermal contact with PAH contaminated environmental compartments (Jongeneelen, 1994; Domingo and Nadal, 2015).

A significant amount of studies on PAHs in Taihu Lake have been conducted, covering PAH concentration distributions, sediment-water partitioning characteristics and toxicity assessment in both the water bodies and the sediments. PAHs in the surface sediments have been investigated in the whole lake and the higher concentrations mainly occur in the northern part of the lake (Qu et al., 2002; Qiao et al., 2006; Lei et al., 2014; Tao et al., 2010; Zhang et al., 2012; Tang et al., 2015). Meanwhile, a few sediment cores were analyzed for PAH deposition histories and the PAH concentration distributions are somewhat related to the regional GDP growth (Lei et al., 2016a; Tang et al., 2015; Peng et al., 2005). The PAH partitioning coefficient $\log K_{oc}$ between sediment and water in Taihu Lake is well correlated with their $\log K_{ow}$ (Zhang et al., 2011; Qiao et al., 2008). The biological thresholds and toxic equivalency factors are frequently used to assess the sediment toxicity in Taihu Lake, and the most results showed that PAHs in the lake sediments are not detrimental to benthic organisms (Qiao et al., 2006; Lei et al., 2014; Qu et al., 2002; Tao et al., 2010; Zhang et al., 2012; Zhang et al., 2011; Tang et al., 2015). In addition, PAH toxicity was also assessed in overlying water and sediment pore water in the northern and central part of the lake, and their hazard index values show no or rather low potential ecological risk (Lei et al., 2016b).

3 Materials and methods

3.1 Sample collection

3.1.1 Sediment sampling

During four sampling campaigns (2015-11, 2016-06, 2017-02 and 2017-09), a total of 25 grab surface sediments and 11 sediment cores ranging between 12 cm and 40 cm in length, were collected from the northern part of Taihu Lake, covering Gonghu Bay, Meiliang Bay and Zhushan Bay (Fig. 3.1 and Tab. 3.1). The cores were taken using a gravity corer with a core loss preventer (uwitec, Austria). The surface samples were stored in polyethylene bags, and the cores were sliced into 2 cm segments (147 in total) and were stored in aluminium screw top jars. Before further analysis, the samples were stored at –20 °C, except during the air shipping process from China to Germany.

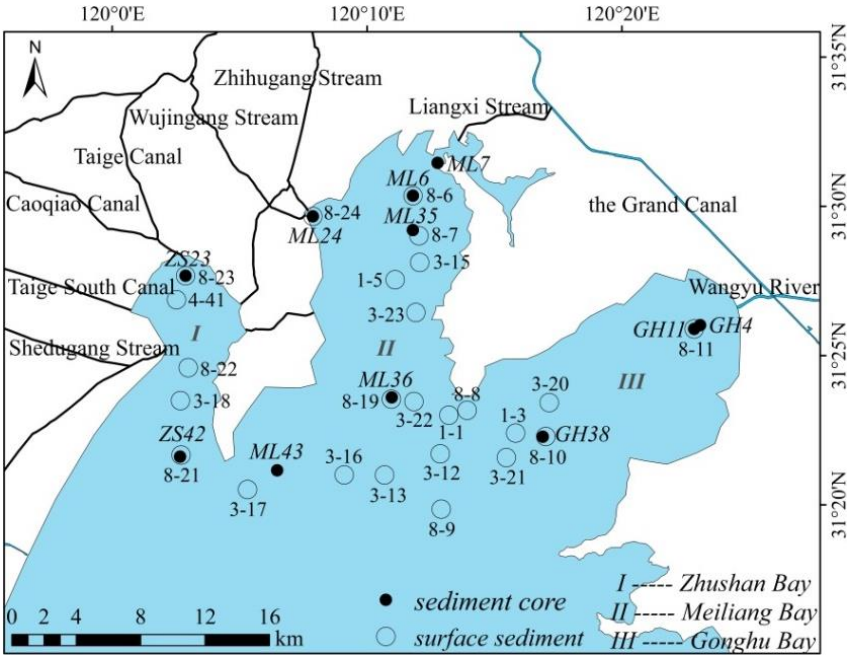

Fig. 3.1 Sampling location of the surface sediments and the sediment cores. The rivers and canals around the sampling area are generally only inflow, except the Wangyu River connecting Taihu Lake and the Yangtze River can act as an outflow in rainy season.

Tab. 3.1 Coordinate of the sampling locations of the surface sediments and the sediment cores

surface sediment				sediment core			
location	**sampling time**	**N**	**E**	**location**	**sampling time**	**N**	**E**
1-1	2015-05	31.3897	120.2127	**ML6**	2017-02	31.5128	120.1935
1-3	2015-05	31.3787	120.2559	**ML7**	2017-09	31.5310	120.2100
1-5	2015-05	31.4662	120.1802	**ML24**	2017-02	31.5029	120.1277
3-12	2015-11	31.3683	120.2064	**ML35**	2016-06	31.4936	120.1928
3-13	2015-11	31.3574	120.1697	**ML36**	2016-06	31.4006	120.1758
3-15	2015-11	31.4755	120.1966	**ML43**	2016-06	31.3617	120.0997
3-16	2015-11	31.3581	120.1434	**GH4**	2017-09	31.4362	120.3784
3-17	2015-11	31.3514	120.0800	**GH11**	2017-02	31.4337	120.3745
3-18	2015-11	31.4021	120.0379	**GH38**	2016-06	31.3761	120.2736
3-20	2015-11	31.3951	120.2784	**ZS23**	2017-02	31.4718	120.0435
3-21	2015-11	31.3651	120.2494	**ZS42**	2016-06	31.3708	120.0367
3-22	2015-11	31.3979	120.1902				
3-23	2015-11	31.4476	120.1931				
4-41	2016-06	31.4592	120.0372				
8-6	2017-02	31.5128	120.1935				
8-7	2017-02	31.4904	120.1966				
8-8	2017-02	31.3921	120.2247				
8-9	2017-02	31.3374	120.2060				
8-10	2017-02	31.3762	120.2756				
8-11	2017-02	31.4337	120.3745				
8-19	2017-02	31.3996	120.1755				
8-21	2017-02	31.3717	120.0373				
8-22	2017-02	31.4204	120.0436				
8-23	2017-02	31.4718	120.0435				
8-24	2017-02	31.5029	120.1277				

Geographic Coordinate System: GCS_WGS_1984.

3.1.2 Water sampling

During the 4 field campaigns, 41 water samples in total were collected from the northern part of Taihu Lake covering Gonghu bay, Meiliang bay and Zhushan bay (Fig. 3.2 and Tab. 3.2). In each location, 2 L of water samples were taken at 0.5 m depth and kept in 2 1-L amber glass bottles for PAH measurement and backup, respectively. After sampling, the samples were immediately transported to the laboratory for PAH extraction.

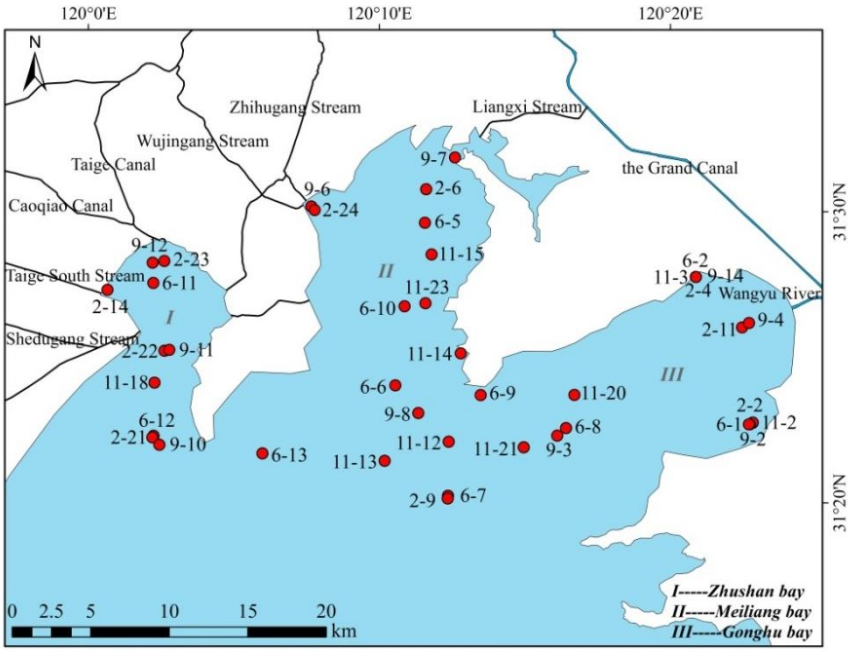

Fig. 3.2 Sampling location of the water samples.

Tab. 3.2 Coordinate of the sampling locations of the water samples

location	sampling time	N	E	location	sampling time	N	E
11-2	2015-11	31.3793	120.3805	2-2	2017-02	31.3753	120.3889
11-3	2015-11	31.4627	120.3479	2-4	2017-02	31.4627	120.3479
11-12	2015-11	31.3683	120.2064	2-6	2017-02	31.5128	120.1935
11-13	2015-11	31.3574	120.1697	2-9	2017-02	31.3374	120.2060
11-14	2015-11	31.4189	120.2133	2-11	2017-02	31.4337	120.3745
11-15	2015-11	31.4755	120.1966	2-14	2017-02	31.4552	120.0109
11-18	2015-11	31.4021	120.0379	2-21	2017-02	31.3717	120.0373
11-20	2015-11	31.3951	120.2784	2-22	2017-02	31.4204	120.0436
11-21	2015-11	31.3651	120.2494	2-23	2017-02	31.4718	120.0435
11-23	2015-11	31.4476	120.1931	2-24	2017-02	31.5029	120.1277
6-1	2016-06	31.0033	120.4681	9-2	2017-09	31.3753	120.3889
6-2	2016-06	31.4626	120.3480	9-3	2017-09	31.3718	120.2686
6-5	2016-06	31.4936	120.1928	9-4	2017-09	31.4362	120.3784
6-6	2016-06	31.4006	120.1758	9-6	2017-09	31.5009	120.1296
6-7	2016-06	31.3358	120.2058	9-7	2017-09	31.5310	120.2100
6-8	2016-06	31.3761	120.3761	9-8	2017-09	31.3847	120.1890
6-9	2016-06	31.3950	120.2247	9-10	2017-09	31.3666	120.0407
6-10	2016-06	31.4458	120.1811	9-11	2017-09	31.4209	120.0464
6-11	2016-06	31.4592	120.0372	9-12	2017-09	31.4708	120.0368
6-12	2016-06	31.3708	120.0367	9-14	2017-09	31.4626	120.3480
6-13	2016-06	31.3617	120.0997				

Geographic Coordinate System: GCS_WGS_1984.

3.2 Sample preparation

3.2.1 Sediment samples

The samples were freeze-dried and then milled in a vibratory disc mill. Between 7 – 12 g of each sample was then extracted using Accelerated Solvent Extraction (Dionex ASE 300) in static conditions (100 °C and 10 MPa) for 30 min with 35 mL of acetone. After the extraction, 100 µL of internal standard (4002.25 ug/L) was spiked to each sample extract. Extracts were then cleaned using

a glass column filled with glass wool, 2 g silica gel, 2 g Al_2O_3 and 0.5 g Na_2SO_4 to remove the residual water and interfering compounds. After the clean-up, the column was eluted with 15 mL of n-hexane, followed with 5 mL of a 9:1 (v/v) mixture of n-hexane and dichloromethane, and 20 mL of a 4:1 (v/v) mixture of n-hexane and dichloromethane. The eluate was concentrated to around 2 mL using an automatic evaporation-dryer with nitrogen. Then 1 µL of each concentrated eluate was injected into a gas chromatography-mass spectrometry (GC-MS) (Agilent 7890A/5975C) for PAH concentration measurement. Pictures on the collection and preparation of the surface sediments and the sediment cores are shown in Fig. 3.3 and Fig. 3.4, respectively.

3.2.2 Water samples

Around 1 liter of each sample were filtered with 0.45 µm pore size filters, then 1 ml (400.2 ng PAH standards) of stock solution was injected as internal standard to each sample before PAH extraction. PAHs were extracted with ISOLUTE® ENV+ 200 mg/3 mL SPE cartridge which was activated with 3 * 3 mL ethyl acetate before PAH loading, and the extraction speed was around 1 L/h. After extraction, the cartridge was dried naturally and then kept in sealed polyethylene bag. The loaded cartridges were transported to Germany by flight for further PAH analyses.

The cartridges were eluted with 3 * 3 mL of acetone, and the eluates were immediately concentrated to around 1 mL with nitrogen stream. Then 1 µL of the concentrated eluate was injected into a GC-MS (Agilent 7890A/5975C) for PAH concentration measurement. Pictures on the water sample collection and preparations are shown in Fig. 3.5.

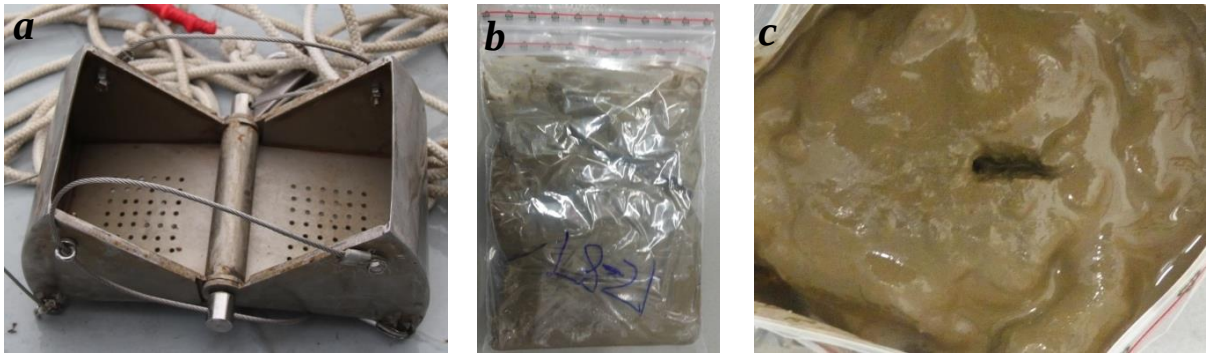

Fig. 3.3 Picture on the surface sediment sample collection (a, surface sediment sampler; b and c, surface sediment sample).

Fig. 3.4 Picture on the sediment core collection and process (a, sediment core sampler; b, core sampling; c and d, sediment core; e, core slicing; f, PAH extract; g, PAH concentrate).

Fig. 3.5 Picture on the water sample collection and process (a, raw water sample; b and c, water sample filtration; d, PAH extraction; e, cartridge with PAH loaded).

3.3 PAH analyses

PAH concentrations were measured with GC-MS and the compounds were carried by helium in pulsed splitless mode and detected in the selected ion monitoring (SIM) mode of the MS. The column is HP- 5MS 5% Phenyl Methyl Silox with 30 m length, 250 µm i.d. and 0.25 µm film thickness. The running time of one complete sequence is 43.333 min. The oven temperature is 75 °C for 3 min, and

is further programmed to 235 °C at 20 °C/min for 18 min and then to 300 °C at 15 °C/min for 8 min, finally to 320 °C at 10 °C/min.

For quantification, PAH standards (PAH-mix 14, PAH-mix 45 and deuterated PAH-mix 31) were obtained from Dr. Ehrenstorfer Augsburg, Germany. The three standards were diluted together in cyclohexane to four different concentrations for external calibration and response factors calculation. The internal standard (dilution of deuterated PAH-mix 31) with 5 deuterated PAHs was then used to quantify the analytes. All solvents and cleanup chemicals were purchased from Carl Roth GmbH + Co.KG, Germany.

Including 16 US EPA PAHs, a total of 20 PAHs were analyzed (2-ring: naph, 2methylnaph, 1methylnaph; 3-ring: acenaphthylene (acenaphthy), acenaphthene (acenaphthe), fluorene, phen, anthra; 4-ring: fluor, pyrene, BaA, chrysene (chry); 5-ring: BbF, BkF, BeP, BaP, perylene, DahA; 6-ring: BghiP, INcdP). The molecule structure and physicochemical properties of the 20 PAHs show in Fig. 3.6 and Tab. 3.4.

For testing the reliability of this method, a certified soil from a gas works site (European Reference Material ERM-CC013a) was purchased from the Federal Institute for Materials Research and Testing BAM (Berlin, Germany). The reported uncertainties for the concentrations of the different PAHs in the certified soil were between 5% and 20%. The certified soil was extracted and measured identically to the field samples. The recovery rates (9 replicates) in our tests were typically above 100% and higher than the reported recovery (Tab. 3.3), which might be because of more efficient extraction or other unknown reasons. However, the recovery rates are rather stable in the 9 replicates, so it still indicates reliable detection qualification.

Tab. 3.3 Average concentration recovery rate of the PAHs tested with certified soil

PAH compound	naph	fluorene	phen	anthra	fluor	pyrene	BaA
Recovery rate (%)	126.69	121.04	110.07	141.96	110.64	113.39	114.00
PAH compound	chry	BbF	BkF	BaP	IncdP	BghiP	
Recovery rate (%)	131.56	150.82	117.73	102.80	171.53	139.44	

The quantification limit for the GC-MS analysis was between 10 and 25 pg of injected mass in a standard, depending on the PAH compound. For soil samples the detection limit is also dependent on the background noise of chromatograms. This corresponds to 3 – 7 ng/g of individual PAHs in the soil samples, depending on the amount of soil extracted and the volume of the eluates concentrated. The limit corresponds to 10 – 25 ng/L of individual PAHs in the water samples.

3.4 Sediment core dating

Three of the cores were dated using the thermonuclear by-product ^{137}Cs with a half-life of 30.17 years. The three cores are located in Meiliang Bay (ML35 and ML36) and Zhushan Bay (ZS42) (Fig. 3.1). Since a certain mass was required for the determination of ^{137}Cs activities, some adjacent layers of core samples were combined and each dating sample ranges between 2 and 8 cm in length and between 15.1 and 29.9 g in weight. ^{137}Cs activity measurements were carried out with low-level gamma-spectroscopy based on the distinct ^{137}Cs gamma emission energy of 661 keV, using a n-type coaxial Low-Energy HPGe detector (ORTEC) with an active volume of 39 cm^3 and a 0.5 mm Be window. The detector efficiency and measuring geometry were calibrated with the certified reference material "IAEA-375 SOIL". Each of the samples was measured at least 24 hours in 32 cm^3 cylindrical capsules, and spectra analysis was performed with the software GAMMA-W®.

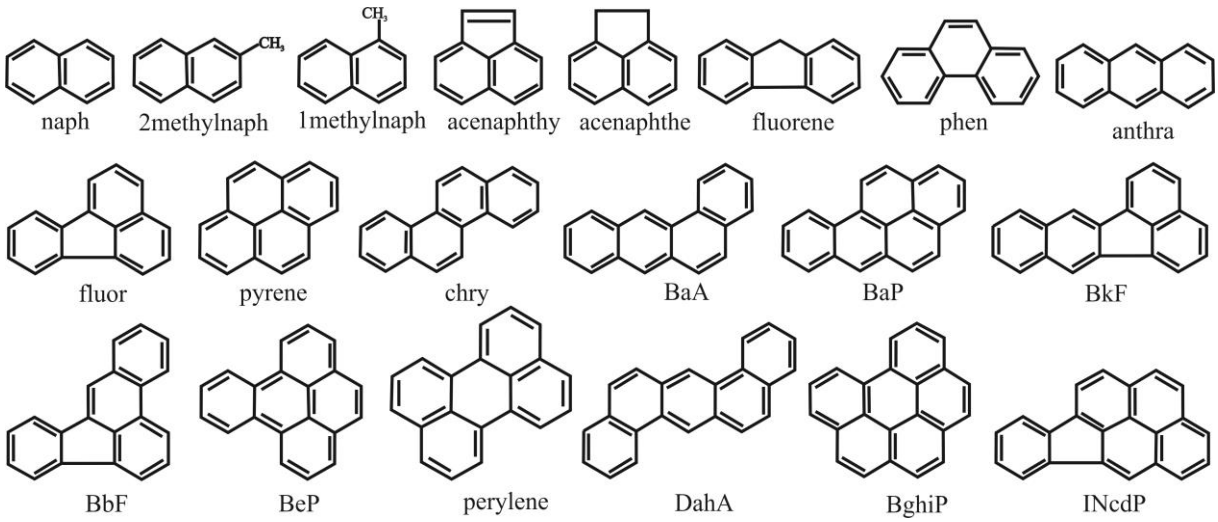

Fig. 3.6 Molecule structure of the 20 PAHs.

Tab. 3.4 Physicochemical properties of the 20 PAHs[*]

PAH compound	**molecular formula**	**molecular mass (g/mol)**	**vapor pressure (Pa) 25 °C**	**water solubility (mg/L) 25°C**	**Henry constant (–) 25 °C**	**logK_{ow} (–)**
naph	$C_{10}H_8$	128	11.3	31	$1.80*10^{-2}$	3.35
2methylnaph	$C_{11}H_{10}$	142	7.33	24.6	$2.12*10^{-2}$	4
1methylnaph	$C_{11}H_{10}$	142	8.93	25.8	$2.10*10^{-2}$	3.87
acenaphthy	$C_{12}H_8$	152	$8.90*10^{-1}$	16.1	$4.66*10^{-3}$	3.94
acenaphthe	$C_{12}H_{10}$	154	$2.87*10^{-1}$	3.9	$7.53*10^{-3}$	3.92
fluorene	$C_{13}H_{10}$	166	$8.00*10^{-2}$	1.69	$3.93*10^{-3}$	4.18
phen	$C_{14}H_{10}$	178	$1.61*10^{-2}$	1.15	$1.73*10^{-3}$	4.46
anthra	$C_{14}H_{10}$	178	$1.07*10^{-3}$	$4.34*10^{-2}$	$2.27*10^{-3}$	4.45
fluor	$C_{16}H_{10}$	202	$1.23*10^{-3}$	$2.6*10^{-1}$	$3.62*10^{-4}$	5.16
pyrene	$C_{16}H_{10}$	202	$6*10^{-4}$	$1.35*10^{-1}$	$4.87*10^{-4}$	4.88
BaA	$C_{18}H_{12}$	228	$2.8*10^{-5}$	$9.4*10^{-3}$	$4.91*10^{-4}$	5.76
chry	$C_{18}H_{12}$	228	$8.3*10^{-7}$	$2.00*10^{-3}$	$2.14*10^{-4}$	5.81
BbF	$C_{20}H_{12}$	252	$6.67*10^{-5}$	$1.5*10^{-3}$	$2.69*10^{-5}$	5.78
BkF	$C_{20}H_{12}$	252	$1.05*10^{-7}$	$8.00*10^{-4}$	$2.39*10^{-5}$	6.11
BaP	$C_{20}H_{12}$	252	$1.03*10^{-4}$	$1.62*10^{-3}$	$1.87*10^{-5}$	6.13
BeP	$C_{20}H_{12}$	252	$2.59*10^{-6}$	$6.3*10^{-3}$	$1.23*10^{-5}$	6.44
perylene	$C_{20}H_{12}$	252	$1.33*10^{-3}$	$4.00*10^{-4}$	$1.49*10^{-4}$	6.25
DahA	$C_{22}H_{14}$	278	$1.33*10^{-8}$	$2.19*10^{-3}$	$5.03*10^{-6}$	6.75
BghiP	$C_{22}H_{12}$	276	$1.33*10^{-8}$	$2.6*10^{-4}$	$1.35*10^{-5}$	6.63
INcdP	$C_{22}H_{12}$	276	$1.67*10^{-8}$	$1.9*10^{-4}$	$1.42*10^{-5}$	6.7

[*]: Achten, C. and Andersson, J.T., 2015. Overview of polycyclic aromatic compounds (PAC). *Polycyclic aromatic compounds*, *35*(2-4), pp.177-186.

4 Results and discussion

The results and discussion chapter consists of three parts. First, the spatial and temporal distribution of PAHs in the sediments is discussed without considering perylene (4.1). Then the perylene distributions in the sediments are interpreted (4.2). Finally, the PAHs in the water body are presented (4.3).

4.1 Sedimentary archive of PAHs in the sediments

To understand the PAH distribution in the sediments, first the results of a literature review on the industrial development with the associated emission sources in China and the region of Lake Taihu are presented. Also, the response of the Chinese government to the increased environmental pollution in terms of legislation that might have affected the PAH emissions and therefore deposition of PAHs in the sediments are explained (4.1.1). Then, the dating results of three sediment cores are presented that allow for a temporal resolution of the sediment deposition (4.1.2). Based on this, the spatial and temporal distributions of PAH concentrations in the sediments are discussed without considering perylene (4.1.3). In addition to the total PAH concentrations, also the profiles of PAH patterns (concentration fraction of 4 light PAHs and 6 heavy PAHs) in the cores are interpreted for the history of PAH input variations (4.1.4). Furthermore, concentration ratios of four groups of isomers (phen/anthra, fluor/pyrene, BaA/chry and INcdP/BghiP) were calculated from both the sediment results and literature data with different emission sources to validate the methods applied for PAH source track in the environment (4.1.5). Finally, the PAH concentrations were compared with toxicity thresholds from three national guidelines (4.1.6).

4.1.1 Potential PAH emissions in the area

In principal, the PAH concentration patterns together with the information on sediment age can be used to reveal the historical input of PAHs into the sediments. Coal and oil are the major energy sources in China (Crompton and Wu, 2005; Wang and Feng, 2003), hence PAH abundance in the sediments is a crucial indicator of energy consumption and industrial and economic development. After the People's Republic of China was established in 1949, China started intensifying the development of industry and economy, particularly in coastal areas (Fan, 1995), which was accompanied with a considerable increase in consumption of coal and oil (Liu, 2008; Jiang and Zhang, 2005). Furthermore, the reform and opening-up Policy in China, implemented from 1978, was associated with rapidly growing urbanization and industrialization (Yeh et al., 2011; Chen et al., 2013).

PAH concentration profiles in the sediment should be somewhat consistent with PAH emissions, energy consumptions, energy structure changes (Fig. 2.2) and also with the effects of environmental measures in this area. PAH emission rate (emissions per kg of coal) from residential coal combustion is generally two to three orders of magnitude higher than that from coal power plant and industrial coal boiler (Zhang et al., 2008; Liu et al., 2009; Yang et al., 1998), so PAHs from residential coal combustion should be carefully considered. In this area, the consumption of residential coal combustion continuously decreased from 3.88 million tons in 1995 to 0.06 million tons in 2015, and the sum of the consumptions in heating, power generating, industries and coking increased from 81.72 million tons in 1995 to the maximum 275.68 million tons in 2013. The decreased PAH emissions from residential combustion could therefore have at least partly compensated the increased emissions from the other coal combustion sources.

To control atmospheric pollution, the Chinese government enacted the first environmental standard "Discharge and emission standards of three industrial wastes" (GB J4-73) in 1973, and thereafter specifically introduced a series of updated emission standards for coal power plants and boilers (Yuan et al., 2017). Soot and dust emission is one of the main concerns in all of the standards, so the emission of PAHs bound in these particles are also controlled. Due to the dramatic increase of coal consumption and serious pollution situations in China, more stringent environmental policies and advanced technologies have been implemented to mitigate pollution since the late 1990s. For example, to develop clean coal technologies, Chinese government conducted some programs to replace small inefficient units with large power projects, and to apply supercritical and ultra-supercritical pulverized coal technology and coal transfer technologies in the last 2 – 3 decades (Chen and Xu, 2010; Chang et al., 2016; Qi et al., 2012; Horbach et al., 2014); some equipment have been installed to improve combustion efficiency and prevent particle emission from coal combustion after 2000, such as electrostatic precipitator (ESP), circulating fluidized beds (CFB), integrated gasification combined cycle (IGCC) and carbon capture and storage (CCS) (Chen and Xu, 2010; Qi and Yuan, 2011; Chang et al., 2016). Therefore, the structural change of coal consumption and the application of the clean coal measures might mitigate environmental pollution from the significant increase of coal consumption (Fig. 2.2a).

With the sharp increase in the number of vehicles (Fig. 2.2c), exhaust contamination also poses considerable stress on environmental quality in China, so great efforts have been made on the improvement of vehicle emission control and fuel quality in the last two decades. Emission factors of hydrocarbons and particles decrease noticeably from vehicle emission levels of China 0 to China V, the China I was implemented in around 2000, the China II was in around 2004, the China III was in around 2008, the China IV was after 2010, and the China V was started from 2018 (Shen et al., 2015; Lang et al., 2014; Wu et al., 2017). Accordingly, upgraded fuel quality standards have been promulgated step by step to meet vehicle emission standards (Yue et al., 2015; Wu et al., 2017). In addition, some typical control technologies have been gradually adopted to vehicles, such as electronic fuel injection, three-way catalyst and on-board diagnosis in gasoline passenger cars, and turbo-charge, inter-cooling, exhaust gas recirculation, diesel oxidation catalyst and diesel particulate filter in heavy-duty diesel vehicles (Wang et al., 2012).

Vehicle exhausts contain PAHs in both gas and particle phases, and their emission rates can also be reduced by the advanced environmental measures. For example, vehicles equipped with catalyst perform over 20-fold lower PAH emission rate than that without catalytic converter (Rogge et al., 1993; Westerholm et al., 1989; Schauer et al., 2002); vehicles equipped with diesel particle filter can significantly reduce hydrocarbon and particle/soot emissions (Tan et al., 2017; Tzamkiozis et al., 2010; Caliskan and Mori, 2017; Biswas et al., 2009; Ayala et al., 2002). In addition, heavy-duty vehicles present one to two orders of magnitude higher emission factor (per liter fuel) than light-duty ones in some specific PAHs (Marr et al., 1999; Phuleria et al., 2006). Therefore, due to these environmental measures on vehicle emissions, the increase of PAH emissions from vehicles could be lower as expected from the increase of oil consumption in transport from 1.47 million tons in 1995 to 12.25 million tons in 2015 (Fig. 2.2b) and the increase of the number of vehicles from 1.42 million in 2002 to 26.64 million in 2016 (Fig. 2.2c).

4.1.2 Dating of the cores

The presence of anthropogenic ^{137}Cs in the environment of the northern hemisphere can be traced both to the atmospheric testing of nuclear weapons in the late 1950s and the early 1960s and to major accidents in nuclear power stations, i.e. the Chernobyl accident in 1986. The latter produced a less uniform and laterally more limited pattern since the fallout was associated with complex short-term weather patterns (in particular rain). Whereas (for this reason) no Chernobyl fallout is known for the southern hemisphere, the nuclear weapon testing fallout is traceable in both the north and the south, appearing in the south about two years later (Rowntree and Foster, 2012).

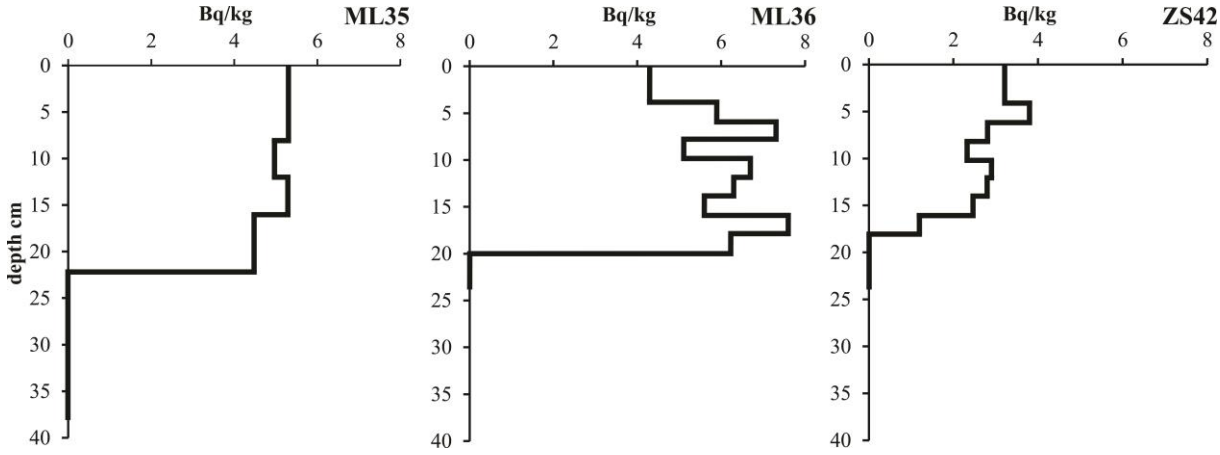

Fig. 4.1 Vertical distribution of ^{137}Cs activities in the three dated cores.

Sediment deposition rates in the three locations were measured based on ^{137}Cs activities in the cores taken from that locations. Fig. 4.1 shows that the ^{137}Cs activities are rather low and only detectable in the upper around 20 cm of the three cores, which is comparable to the results reported by others (Xue and Yao, 2011; Liu et al., 2004). Although the detected ^{137}Cs activities in the cores do not show any distinct peak related to any of the events, the deepest layer (at ca. 20 cm depth) at which ^{137}Cs was detected can be consequently dated to around the 1960s. This would indicate that an average sedimentation rate at these three locations is around 3 – 4 mm/a, which is similar to the rates reported by Xue and Yao (2011) and Liu et al. (2009), and is also reasonably consistent with the chronological results of spheroidal carbonaceous particles (Cao et al., 2013; Liu et al., 2012). These three locations are some km away from the lakefront and also away from the inflows into the lake. The sedimentation rates therefore represent most likely the average rate in the northern part of the lake, but might not be representative for the areas close to the lakefront and river outlets due to more intense sediment input.

4.1.3 PAHs in the surface sediments and the cores

Riverine runoff and atmospheric deposition are the two main pathways responsible for PAHs and sediment input to a lake (Zakaria et al., 2002; Ferrey et al., 2018). Riverine runoff may potentially contribute more significant pollutant and particle loads to lake systems, as rivers typically receive treated or untreated domestic wastewater, industrial effluents, and surface runoff (Pal et al., 2010; Wolf et al., 2013). These factors may lead to higher deposition rates and PAH concentrations in the sediment close to river inflows.

Fig. 4.2 shows the spatial distribution of the total PAH concentrations, without considering perylene, in the surface sediments. The concentrations range from around 150 ng/g to around 2300 ng/g. The higher concentrations (above 1000 ng/g) are found close to the inflow in Zhushan Bay (locations 8-23,

4-41 and 3-18) and in the northwestern part of Meiliang Bay (location 8-24). The concentrations at the other locations are typically below 1000 ng/g. These distribution patterns, with the higher concentrations located close to the inflows, reveal that the inflow rivers are the major current pathways for PAH input.

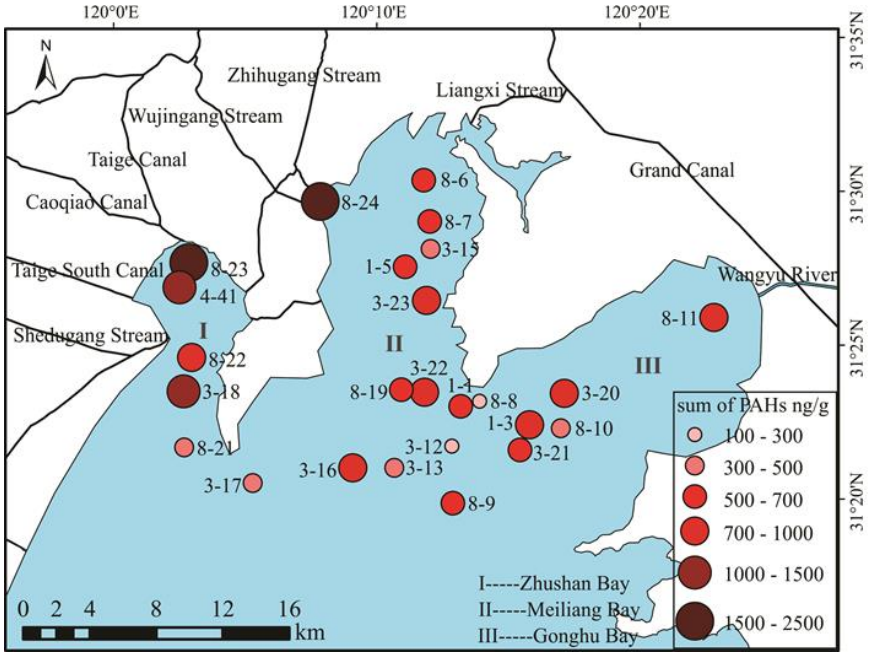

Fig. 4.2 Concentration distribution of the sum of the 19 PAHs (without perylene) in the surface sediments.

Three sediment cores were also taken close to the inflows in Zhushan Bay (ZS23), and in the northwestern and northeastern part of Meiliang Bay (ML7, ML24) (Fig. 3.1). In line with the results of the surface sediments, the three cores show the by far highest PAH concentrations (without perylene), reaching up to 5000 ng/g in core ML24 (Fig. 4.3). These three cores have a length of 40 cm (ZS23), 34 cm (ML7) and 18 cm (ML24), respectively, and their concentrations remain high throughout the cores. The other cores (ML6, ML35, ML36, ML43, ZS42) collected further away from the inflows in the two bays, however, show consistently low background concentrations (below around 150 ng/g) in the deeper layers and comparably high concentrations only in the upper 10 – 20 cm. These results suggest that the sedimentation rates in the area close to the inflows are substantially higher than the average rate of 3 – 4 mm/a in the other locations, and that the rivers connected to the northern part of these two bays are the main pathway for PAHs and sediment input into the lake.

These general findings are also reflected in the three cores (ML6, ML35 and ML36) located with increasing distances from the river outlets in Meiliang Bay (Fig. 3.1). These cores present similar concentration profiles, with background concentrations in the deeper layers and higher concentrations in the upper layers (Fig. 4.3). The concentrations increase from a depth of 28 cm (ML6), 26 cm (ML35) and 22 cm (ML36), respectively, which indicate that the sedimentation rates in the three locations decrease with increasing distances from the river outlets. In addition, core ML36 has lower concentrations in the upper layers compared to the other two cores, in line with the greater distance from river inflows. The two cores located in the south of Zhushan Bay (ZS42) and Meiliang Bay (ML43) show even lower sedimentation rates and also lower PAH concentrations (350 – 450 ng/g) in their upper layers. Their consistent concentration distributions coincide with their close location distribution and the water flow direction from the northwestern to the eastern area of the lake (Hu et al., 2010), that is, from location ZS42 to ML43. Consequently, combining the PAH concentration

profiles and the dating results with an average sedimentation rate of 3 – 4 mm/a in the sediments away from inflows, the significant increases of the PAH concentrations documented in cores ML6, ML35, ML36, ML43, and ZS42 would start from the late 1950s.

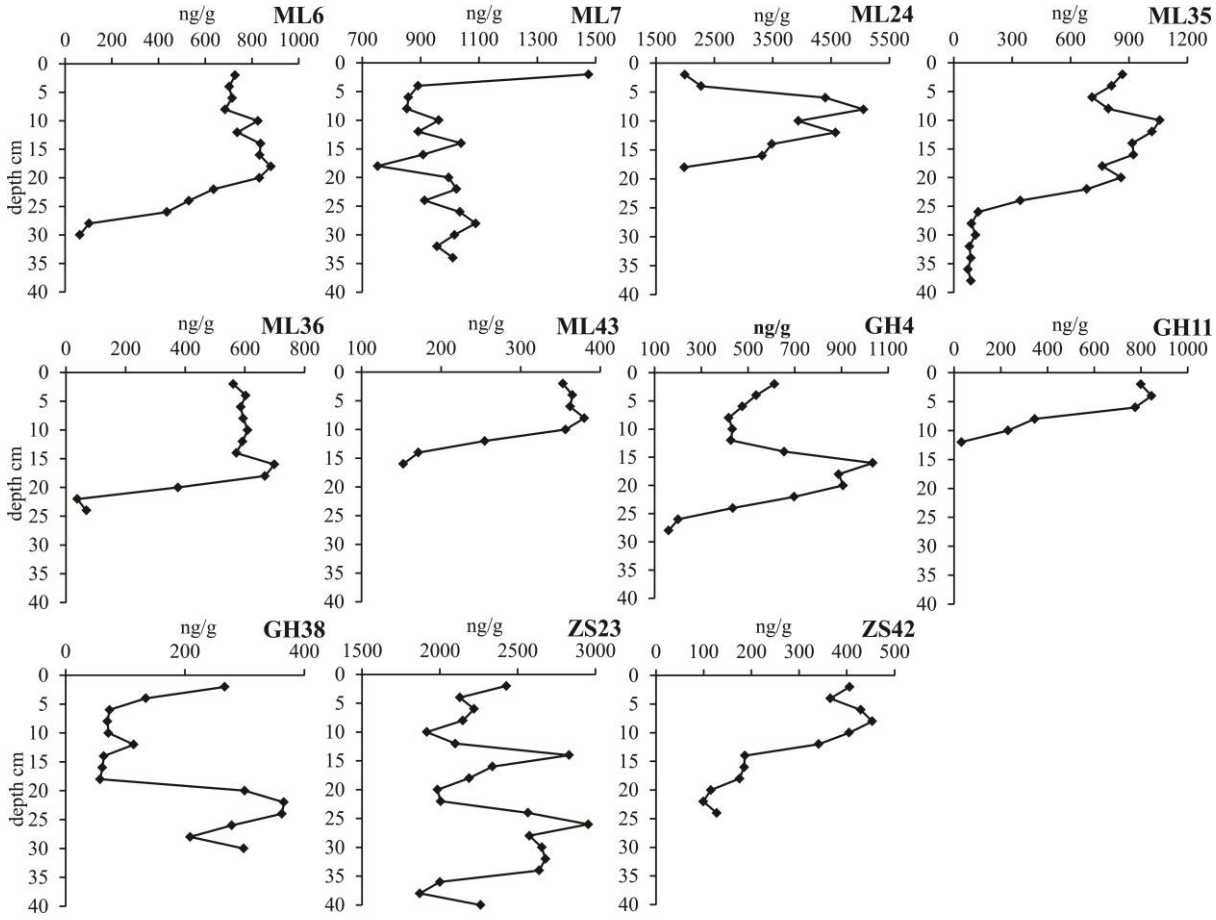

Fig. 4.3 Concentration profiles of the sum of the 19 PAHs (without perylene) in the cores.

Three cores (GH4, GH38 and GH11) were taken from Gonghu Bay (Fig. 3.1). Taihu Lake is a crucial drinking water source in this region, especially Gonghu Bay provides water to 4 major water treatment works covering 80% of drinking water supply in Wuxi City (Qin et al., 2010; Tao et al., 2010). Gonghu Bay is connected to the Yangtze River through the Wangyu River. In order to alleviate algae blooms in Taihu Lake, a project (WTYT project) was started in 2002 to transfer water from the comparatively low nutrient status Yangtze River to Taihu Lake through the Wangyu River (Zhai et al., 2010). In addition, sediment dredging was conducted around ten years ago to remove contaminated sediments from the bay (Liu et al., 2010; C. Liu et al., 2016; Chen et al., 2018). These activities likely had an impact on the contamination patterns and thickness of the sediments. The three cores show significantly different concentration profiles that consequently might be influenced by the activities in this bay and may not represent the original stratification.

As PAHs are mainly input by river runoff in the northern part of Taihu Lake, so PAHs in the sediment deposited after 2000 should, to a great extent, explain the same period of PAH input and discharge from the local area. The energy consumption increased significantly after 2000 (Fig. 2.2), but the sum of the 19 PAH concentrations are rather stable in the sediment layers deposited in the corresponding period (Fig. 4.3). In addition to the change of the energy structure and the environmental measures in coal combustion and vehicle exhaust (explained in 4.1.1), which could contribute to the rather stable PAH concentrations in the sections of the cores deposited in the last three to four decades, another

contribution might be sediment disturbance in the lake. Wind-driven waves can result in upper-layer sediment disturbance and resuspension in shallow aqueous environment (Bachmann et al., 2000; Cai et al., 2012; Li et al., 2018), which is accompanied with contaminants and nutrients release and remobilization in sediments (Qin et al., 2006; Søndergaard et al., 1992; Bogdan et al., 2002). Therefore, that the PAH concentration profiles do not match the significant increase of energy consumptions in this area might be somewhat attributed to the sediment disturbance and PAHs resettlement in the lake sediments. In addition, there might be other reasons which can explain the unmatched PAH concentrations in the sediment and the amount of energy consumptions in the study area, but they are not known yet.

4.1.4 PAH patterns in the cores

The concentration profiles of the sum of the 19 PAHs present the background level of PAH abundance in the deeper layers of the sediment and also confirm anthropogenic impacts on PAH existence and distributions in the upper layers of the sediment. Considering general PAH sources and the changes of the energy structures in the study area, PAH input to the sediment should be certainly altered corresponding to the potential sources during the last decades. Especially, in addition to the concentration profiles in the cores, there should be more interpretable information to explain PAH input resulting from energy consumptions. Based on this surmise, PAH patterns in the cores are further interpreted to illustrate the historical PAH input corresponding to the varying PAH sources and energy structures in the local area.

The concentrations of 4 light PAHs (phen, anthra, fluor, pyrene) and 6 heavy ones (BkF, BaP, BbF, BeP, INcdP, BghiP) typically account for 70% – 80% of the concentrations of the 19 PAHs determined in the cores (perylene is excluded) (Fig. 4.4b), so these ten PAHs are selected as references for PAH input interpretation in the sediment. The concentration profiles of the two groups of PAHs are shown in Fig. 4.4a. In Fig. 4.4b, except cores GH38 and ZS23, the concentration fractions of the heavy PAHs are typically double of the fractions of the light ones in the other cores, and it is consistent that the fractions of the heavy PAHs increase with decreasing depth of the cores, but the fractions of the light ones present the inverse trends. In core GH38, however, the fraction distributions of the two groups of PAHs are as opposite as that in most of the cores, but the reason for this remains unclear. In addition, the concentration fractions of the light PAHs in core ZS23 remain around 40% in the whole core, but the heavy ones present certain variations in the upper layers. According to the dating results (Fig. 4.1) and the PAH concentration profiles (Fig. 4.3), the deeper layers of cores ML35, ML36, ML6, ZS42, GH4 and GH11 with higher concentration fractions of the light PAHs compared to the fractions of the heavy PAHs were deposited before the 1950s (before industrialization).

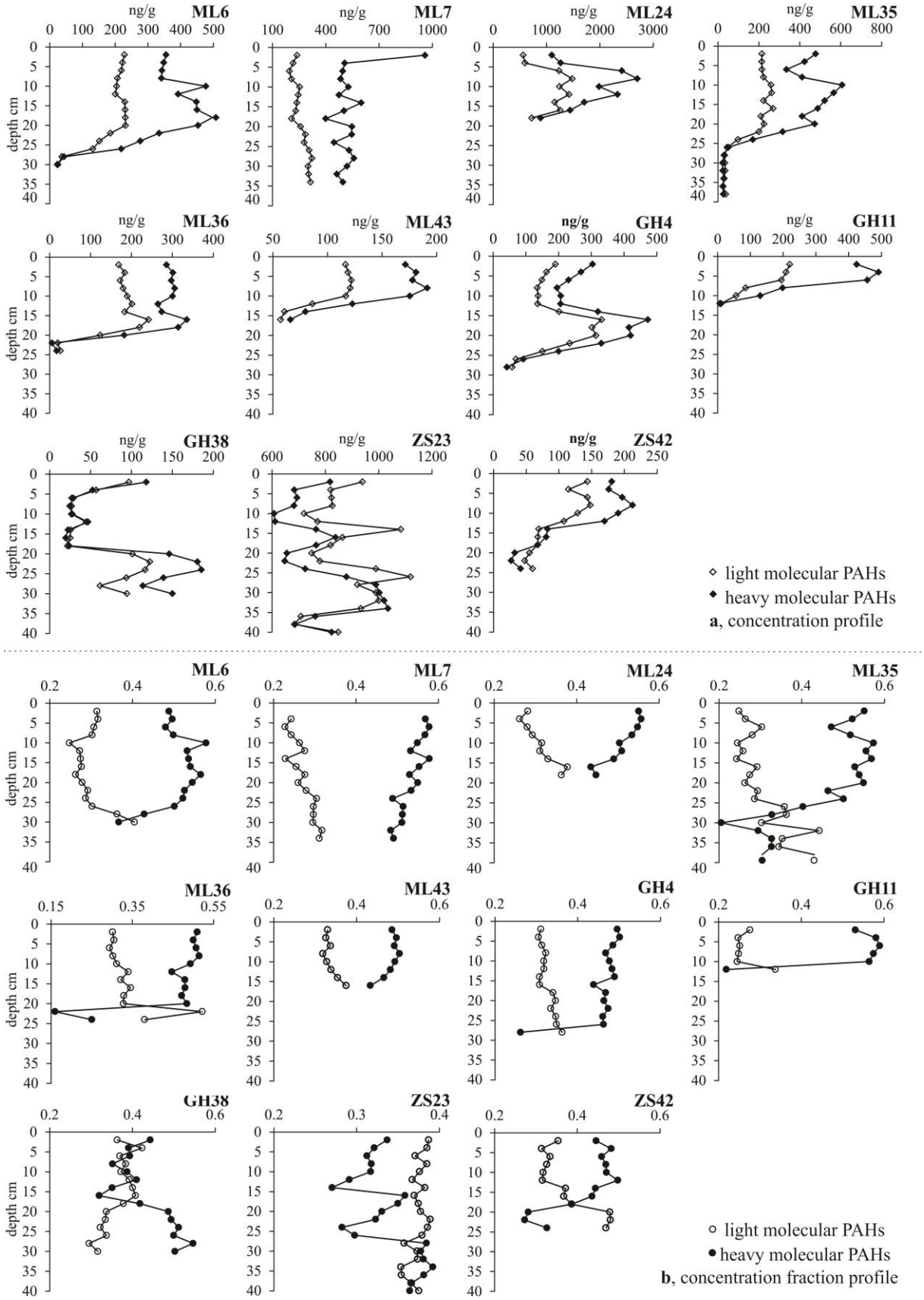

Fig. 4.4 Profile of concentrations (a) and concentration fractions (b) of the 4 light molecular PAHs (178 + 202: phen + anthra + fluor + pyrene) and of the 6 heavy ones (250 + 252 + 276: BkF + BaP + BbF + BeP + INcdP + BghiP) in the cores.

Since sediments can act as archives for contaminant input from anthropogenic activities, the trends of PAH patterns in these cores should strongly indicate the variations of PAH emissions in this area

during the last decades. As coal and oil have been the main energy sources and wood has been gradually phased out since industrialization in this area, their PAH emission patterns are specifically taken into account to explain the potential reasons for the variations of the PAH patterns in the sediment. Literature data on PAH emissions from heavy-duty vehicle exhaust (HDVE), light-duty vehicle exhaust (LDVE), coal coking (CC), coal power plant (CPP), residential coal combustion (RCC) and wood combustion (WC) were collected to show the differences of their emission patterns between the groups of the light and the heavy PAHs (Fig. 4.5a). Due to the gradual application of particle intercept equipment and their intercept effect on the emissions of particle fraction and PAHs, the distributions of the ten PAHs in ultrafine and fine particles are shown in Fig. 4.5b.

There is noticeably higher emission rate of the light PAHs than the emissions of the heavy ones from wood combustion compared to the emission patterns from the other sources shown in Fig. 4.5a. This could be the main reason that higher concentration fractions of the light PAHs occur in the deeper layers of cores ML35, ML36, ML6, ZS42, GH4 and GH11 with background PAH concentration levels, which were deposited before industrialization (the 1950s) when wood was an important energy source in this area. Thereafter, when industrialization started, coal and oil gradually took over the energy sources, especially coal was the dominant energy source, which changed the concentration profiles (Fig. 4.3) and the PAH patterns (Fig. 4.4b) in the sediment. Considering the energy structure and economic development, the consumption in RCC should continuously decrease, but the other parts of coal consumption should rapidly increase during the last decades, which should be, to a great extent, consistent with the structure trends of coal consumption before 2010 shown in Fig. 2.2a. Comparing the emission patterns from CC, CPP and RCC, the emission fraction of the heavy PAHs from CC and CPP are slightly higher than that from RCC (Fig. 4.5a). Therefore, combing the amount and the structure of coal consumption and their respective emission patterns, the emission fractions of the heavy PAHs from coal combustion are certainly increasing compared to their emission fractions of the light PAHs.

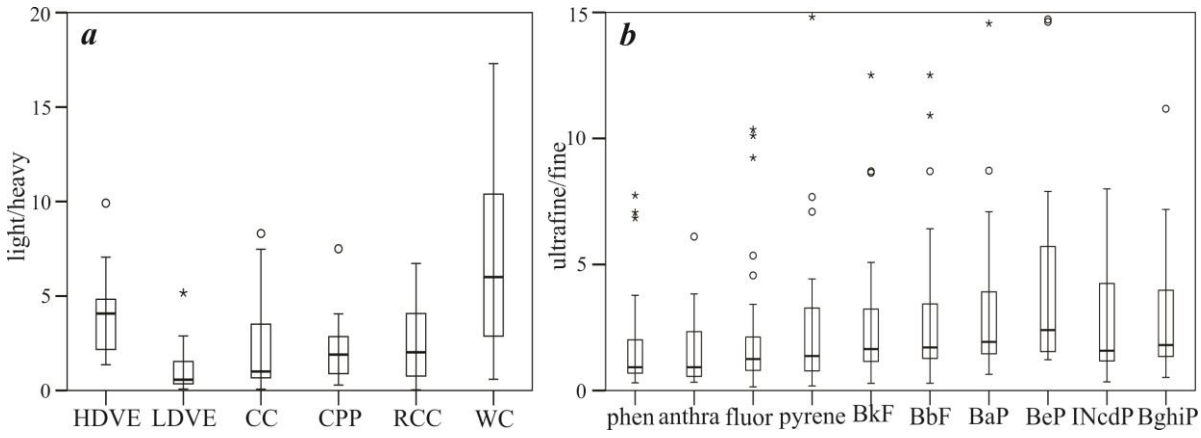

Fig. 4.5 a, Emission rate ratios between the 4 light molecular PAHs (178 + 202: phen + anthra + fluor + pyrene) and the 5 heavy ones (250 + 252 + 276: BkF + BaP + BbF + INcdP + BghiP) (BeP is not involved in the calculation due to data limit from literature data) from different emission sources (HDVE: heavy-duty vehicle exhaust; LDVE: light-duty vehicle exhaust; CC: coal coking; CPP: coal power plant; RCC: residential coal combustion; WC: wood combustion); **b**, concentration ratios of PAHs bound in ultrafine particles (1 µm + 0.35 µm/– 0.05 µm) and fine particles (> 1 µm). The number of data and literatures involved in these two figures are presented in Tab. 4.1 and Tab. 4.2, respectively.

Tab. 4.1 Number of literatures and data batches involved in the calculation of the emission ratio in Fig. 4.5a

data involved	LDVE	HDVE	CC	CPP	RCC	WC
number of literature	3	5	6	10	7	9
number of data batch	9	12	17	32	37	45

The data references are presented in literature data reference part (Fig. 4.5a data reference).

Tab. 4.2 Number of literatures and data batches involved in the calculation of PAH distribution patterns in particle size in Fig. 4.5b

data involved	phen	anthra	fluor	pyrene	BkF	BbF	BaP	BeP	INcdP	BghiP
number of literature	8	7	9	8	9	10	9	7	9	9
number of data batch	27	23	31	27	37	39	28	23	35	35

The data references are presented in literature data reference part (Fig. 4.5b data reference).

It is worthy to point out that the samples for PAH analyses from CPP were typically collected from combustion ash in the power plants rather than from the plant emissions in the environment. A series of particle intercept equipment have been applied to coal power plants and boilers in China, but these equipment cannot effectively intercept ultrafine particles (< l.0 μm) (You and Xu, 2010; Chen and Xu, 2010; Zhao et al., 2010; Yi et al., 2006). Around or even more than 50% of emitted PAHs are bound to organic particles with less than 1 μm diameter from the combustion of various fuels (Shen et al., 2010a; Chen et al., 2004; Wang et al., 2016a; Shen et al., 2011; Venkataraman et al., 2002; Venkataraman et al., 1994), hence a certain amount of PAHs associated with ultrafine particles are still emitted from coal combustion boiler with emission-controlled equipment to the environment. Meanwhile, the six heavy PAHs tend to be associated more with ultrafine particles rather than with fine particles compared to the distributions of the four light PAHs (Fig. 4.5b), that is, higher fractions of the heavy PAHs are emitted through the particle intercept equipment. Consequently, the factors from coal combustion contributing to the concentration fraction profiles of the heavy and the light PAHs in the sediments can be summed as the decrease in the consumption of RCC, the significant amount of coal consumption in CPP and other industrial boiler, the particle intercept effect on the emission fraction of particle size, and the heavy PAHs and the light PAHs distribution in the particle size.

Comparing the PAH patterns from LDVE and HDVE, there is noticeably higher emission fraction of the heavy PAHs from LDVE than the fractions from HDVE (Fig. 4.5a). Combing the linear increased oil consumption in transport (Fig. 2.2b), the exponentially increased number of the light-duty vehicles (Fig. 2.2c) and the differences of the emission patterns between LDVE and HDVE, vehicle exhaust, especially from light-duty vehicles should also contribute to the consistent concentration fraction profiles between the light and the heavy PAHs in the cores.

The reason is not clear for the different concentration fraction patterns of the two groups of PAHs in cores GH38 and ZS23 yet (Fig. 4.4). Core ZS23 is located close to the river outlet in Zhushan bay where is surrounded by agricultural area, so there still could be some straw burning activities, even though they have been banned in China. In addition, there should be residential coal combustion in the rural area. Straw burning and residential coal combustion can emit higher concentration fraction of the light PAHs than the heavy ones into the environment, which might be the reason that there are higher fractions of light PAHs than the fractions of the heavy ones in core ZS23. However, core GH38 shows the opposite trend as that in most of the cores. Some special activities should occur in this location, since the trend of the sum of the 19 PAH concentrations also presents differently from that of the other cores.

4.1.5 Applicability of PAH source track methods

With the intensive energy consumption, pyrogenic processes dominantly contribute PAH input to the environment, and environmental compartments act as sinks for PAH input from various sources. Some methods have been frequently employed to identify PAH input sources such as coal combustion, vehicle exhaust and wood combustion in the environment. The methods include isomer ratios (Pies et al., 2008; Liu et al., 2010; Yunker et al., 2002), chemical mass balance model (CMB) (Hanedar et al., 2011; Lee and Kim, 2007; Li and Kamens, 1993) and statistics such as principal component analysis, cluster analysis, positive matrix factorization, unmix (Liu et al., 2009; Pies et al., 2008; Liu et al., 2010; B. Yang et al., 2013; Zhang et al., 2012). The application of these methods is based on two assumptions: one is that PAH patterns emitted from different combustion materials are specifically distinguishable; another one is that PAH patterns maintain stable after emitted to the environment. To validate the efficiency of these methods, we use literature data on PAH emission patterns from different sources to validate the first assumption, and use our sediment results to validate the second assumption.

4.1.5.1 PAH patterns in potential emission sources

The emission ratios of four groups of isomers, phen/anthra, fluor/pyrene, BaA/chry and INcdP/BghiP from different sources are presented in Fig. 4.6, and the numbers of literatures and data batches involved in the calculations are shown in Tab. 4.3. These data are used to characterize the PAH emissions from various anthropogenic activities including coal coking (CC), coal power plant (CPP), residential coal combustion (RCC), vehicle exhaust (VE) and wood combustion (WC). The four groups of the isomer ratios from these sources overlap obviously and even cannot be qualitatively distinguished. Therefore, PAH patterns from different sources are not specific and the first assumption is not valid for the methods of PAH source track in the environment. This can also be somewhat supported by the ambiguity of the emission ratios between the four light PAHs and the six heavy PAHs from these sources in Fig. 4.5a.

The data describing the emission ratios from wood combustion are collected from the combustion of various kinds of wood with different combustion equipment, hence the wide range of the four isomer ratios should be attributed to the different wood and combustion condition involved in the experiments. By contrast, even though coal coking requires very strict coal quality and certain temperature (Díez et al., 2002), the four ratios are still in rather wide ranges comparable to that of the other sources, especially fluor/pyrene and INcdP/BghiP. The large variations of the ratios from coal power plant and residential coal combustion can be attributed to several factors such as the maturity and type of the coal (Chen et al., 2005; Masclet et al., 1987; Shen et al., 2010b), combustion temperature (Liu et al., 2009; Pergal et al., 2013), oxygen excess (Mastral et al., 2000; 1999), residence time (Liu et al., 2000) and the combustion equipment (Pergal et al., 2013; Wang et al., 2016b). The wide range of the ratios from vehicle emissions can result from different fuels, lubricant oil, catalyst effect, ambient temperature, engine model, operation mode, vehicle mileage (Westerholm et al., 1988; Rogge et al., 1993; Mi et al., 1996). Furthermore, the general reason for the wide variations of the emission ratios could be that the data were collected from a considerable number of literatures whose samples were processed in different laboratories. However, the variation ranges of the ratios from VE and WC with large number of data are comparable to the ranges of the ratios from the other sources with less number of data, so the variation ranges of the ratios are not significantly dependent on the number of literature and data involved. The reasons for

the ratio variations, therefore, should be principally attributed to combustion materials, equipment and conditions.

The isomer ratios from the sediment cores are also presented in the right side of each figure (Fig. 4.6). They are the concentration ratios from all of the sediment cores (ASC), from two cores ZS23 and ML24 with markedly high concentrations (SCHC), and also from the deepest layers of six cores ZS42 (19 – 24 cm), ML43 (15 – 16 cm), ML36 (21 – 24 cm), ML35 (27 – 38 cm), ML6 (27 – 30 cm) and GH11 (11 – 12 cm) with background PAH concentration level (SCBC). As explained in Fig. 4.3, the sediments in cores ZS23 and ML24 were probably only deposited during the last three to four decades and PAHs in the cores mainly originate from pyrogenic processes, but PAHs in the deepest layers of the six cores deposited before industrialization should have a high proportion of petrogenic origins. The ratios from the three groups of samples are plotted to explain that whether PAH sources can be somewhat distinguished with the isomer ratios. However, only the ratio of phen/anthra presents certain discrepancy between samples SCHC and SCBC, and the ratios from these sediment samples overlap with the ratios from all of the combustion sources.

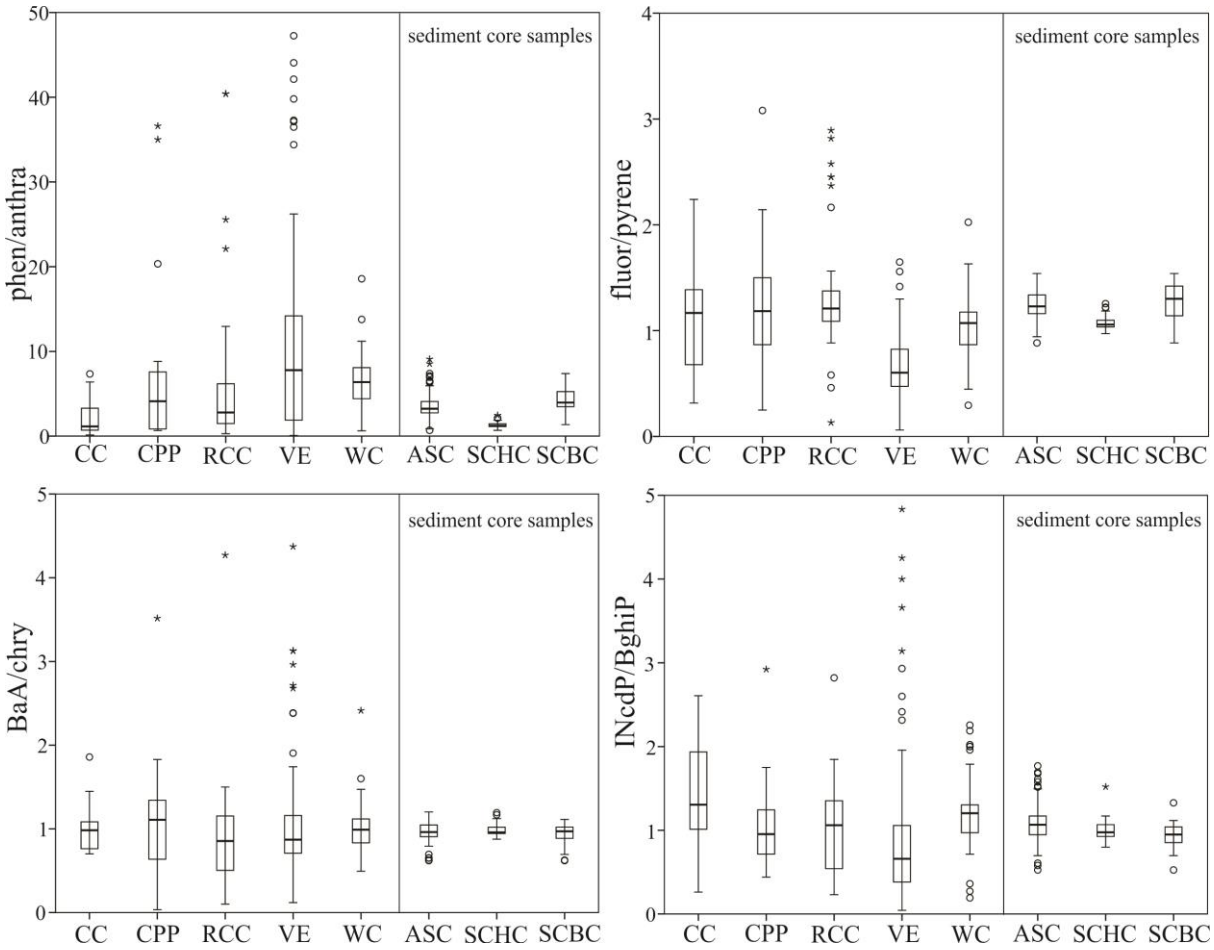

Fig. 4.6 Isomer ratios of PAH emissions from different sources (the circles are outliers and the asteroids are extreme outliers. The abbreviations, CC: coal coking; CPP: coal power plant; RCC: residential coal combustion; VE: vehicle exhaust; WC: wood combustion; ASC: all of the sediment core samples; SCHC: the sediment core samples with high concentrations; SCBC: the sediment core samples with background concentration level). The data and literatures involved in the figure are presented in Tab. 4.3.

In these literatures, their samples for PAH emission measurement were collected directly at the sources, so the ratios are assumed to be the initial values without alteration. However, the ratios from same source vary largely and there are in most cases no distinct differences among the different

sources in the four groups of ratios (Fig. 4.6). As a result, if different sources simultaneously emit PAHs and the emissions mix in the environment thereafter, then it will be even more complicated to distinguish the different sources based on the simple PAH source track methods. In addition, once PAHs enter the environment, the fractions of their homologues and the isomer ratios will keep altering during transport and deposition due to partitioning characteristics (Dachs and Eisenreich, 2000; Lohmann and Lammel, 2004), photolysis (Kim et al., 2009; Behymer and Hites, 1988) and biodegradation conducted by white-rot fungi, algae and bacteria (Wang et al., 2018; Ren et al., 2016; Haritash and Kaushik, 2009).

Tab. 4.3 Number of literatures and data batches involved in the calculations of the four groups of isomer ratios from different sources in Fig. 4.6

sources / ratios	CC		CPP		RCC		VE		WC		ASC	SCHC	SCBC
	a	b	a	b	a	b	a	b	a	b	a	a	a
phen/anthra	17	6	23	10	52	9	90	13	62	12	147	29	15
fluor/pyrene	17	6	40	12	58	10	101	15	83	13	147	29	15
BaA/chry	17	6	33	11	58	10	75	10	70	11	147	29	15
INcdP/BghiP	17	6	22	9	47	8	82	14	66	13	147	29	15

a: the number of data values; b: the number of literatures; the data references are presented in literature data reference part (Fig. 4.6 data reference)

Different combustion materials emit various size fractions of particles (Helble and Sarofim, 1989; Chang et al., 2004; Maricq et al., 1999) and PAH distributions in different particle sizes are somehow dependent on seasonality, for example, more PAHs were found in smaller particles in winter than in other seasons (Pierce and Katz, 1975; van Vaeck and van Cauwenberghe, 1978). Atmospheric deposition is one of the main pathways that contaminants bound to particles enter soils or aqueous environment compartments (Ferrey et al., 2018), and deposition processes incline to scavenge a certain size range of particles (Andronache, 2003; Kauppr and Mclachlan, 1999; Main and Friedlander, 1990). Therefore, the effect of particle bind and atmospheric deposition can, to a large extent, change the gas/particle partitioning and deposition rate of individual PAHs (Allen et al., 1996; Masclet et al., 1988). PAHs with longer-residence time in the atmosphere, either sorbed to particles or in gas phase have higher potential to be photodegraded. In addition, it has been found that PAHs bound to different adsorbent materials such as black carbon, coal fly ash, graphite and diesel particles with different carbon content or physicochemical properties, have different potentials to be degraded by NO_2 and OH radicals in the atmosphere (Behymer and Hites, 1988; Weissenfels et al., 1992; Esteve et al., 2006; Esteve et al., 2004). Consequently, before deposition into soil or aqueous environment, ambient effects in the atmosphere have changed initial PAH patterns depending on PAH properties and sorbent substrate, which should not be neglected in PAH source interpretation in the environment. The patterns change from emission sources to environmental receptor medias has also been verified by fugacity models in some selected PAHs (Zhang et al., 2005)

The general used isomer ratios phen/anthra < 10, fluor/pyrene > 1, INcdP/BghiP > 1 and BaA/chry > 0.5 suggest pyrogenic PAH sources (Yunker et al., 2002; Chen et al., 2012), but the isomer ratios originating from pyrogenic processes shown in Fig. 4.6 are not consistent with these indicator values. Especially, the ratios of fluor/pyrene and INcdP/BghiP are noticeably out of the thresholds of the common-used isomer ratios. As a consequence, the three aspects, the overlap of the isomer ratios

from different PAH sources, the indistinguishable ratios in the sediment and the ambient effect varying PAH patterns during transport and deposition, demonstrate that the two assumptions for the PAH source track methods (isomer ratios, CMB model, statistic analyses) are not reliable. Moreover, the spatial and temporal variations of the isomer ratios from the sediment results are further analyzed to verify this conclusion.

4.1.5.2 PAH patterns in the sediment

Spatial variation of the patterns

Considering the area of the northern part of Taihu Lake, it is reasonable to assume that PAH deposition from the atmosphere in this part of the lake is spatially similarly distributed, hence the different PAH patterns in this part of the lake should be attributed to different input by river runoff and/or to degradation/partitioning effects occurring in the lake system. Combing the inflow distributions around the northern part of the lake (Fig. 3.1) and the PAH concentration profiles in the sediment cores (Fig. 4.3), the cores (ML6, ML7, ML24, ML35, ML36, ML43 and ZS42) located in Meiliang bay and the southern area of Zhushan bay are taken into account to discuss the spatial variations of the PAH patterns in the lake. PAHs in these locations are related to distinct river inputs and transport pathways explained in 4.1.3 part, from the two locations ML24 and ML7 located close to the river outlets to locations ML6, ML35, ML36 with water flow direction, and from location ZS42 to ML43. To be temporal consistent, only the upper layers of cores ML6, ML35, ML36, ZS42 and ML43 with relatively stable and high PAH concentrations are considered to interpret the spatial variations of PAH patterns. The whole lengths of cores ML24 and ML7 are considered, as they show consistently high concentrations throughout the cores whose deposition age should correspond to the age of the upper layers of the five other cores. As a result, PAH patterns variation among these locations can be attributed to degradation/partitioning effects in the lake system rather than to input differences in these locations. Here, we use the four groups of the isomer ratios as indicators to verify the spatial variations of PAH patterns in the sediment (Fig. 4.7).

The four isomer ratios from the 7 cores vary noticeably from location to location (Fig. 4.7). There are some researches on the resistance differences between each group of the isomers. For example, Phen is more resistant than anthra in adsorbed particles under photolysis (Behymer and Hites, 1988; Bertilsson and Widenfalk, 2002), ozonation (Perraudin et al., 2007; Vollmuth and Niessner, 1995) and degradation and uptake by specific microorganisms (Schützendübel et al., 1999; Sanseverino et al., 1993; Moody et al., 2001; Tang et al., 2007); fluor is more resistant than pyrene by the degradation of some specific organisms (Schützendübel et al., 1999; Juhasz et al., 1997), but it is inverse by the degradation of some other organisms (Somtrakoon et al., 2008; Zhong et al., 2011); chry is more resistant than BaA in photochemical degradation (Behymer and Hites, 1988), atmospheric decay (Masclet et al., 1986; Kamens et al., 1988), ozonation (Vollmuth and Niessner, 1995) and biodegradation (Wolter et al., 1997; Baldrian et al., 2000) in various particles. In addition, there are rather consistent differences in the half-lives of phen and anthra (phen > anthra), fluor and pyrene (fluor > pyrene), BaA and chry (BaA < chry) bound in different substrates such as black carbon, cyclone dust, fly ash, silica gel, neutral alumina and biochar, but the half-lives differences between INcdP and BghiP are more related to the properties of these substrate they are bound (Behymer and Hites, 1988; Kuśmierz et al., 2016). Therefore, the differences in their resistance and half-lives between each group of the isomers should be the main reasons for the spatial variation of the isomer ratios from location to location.

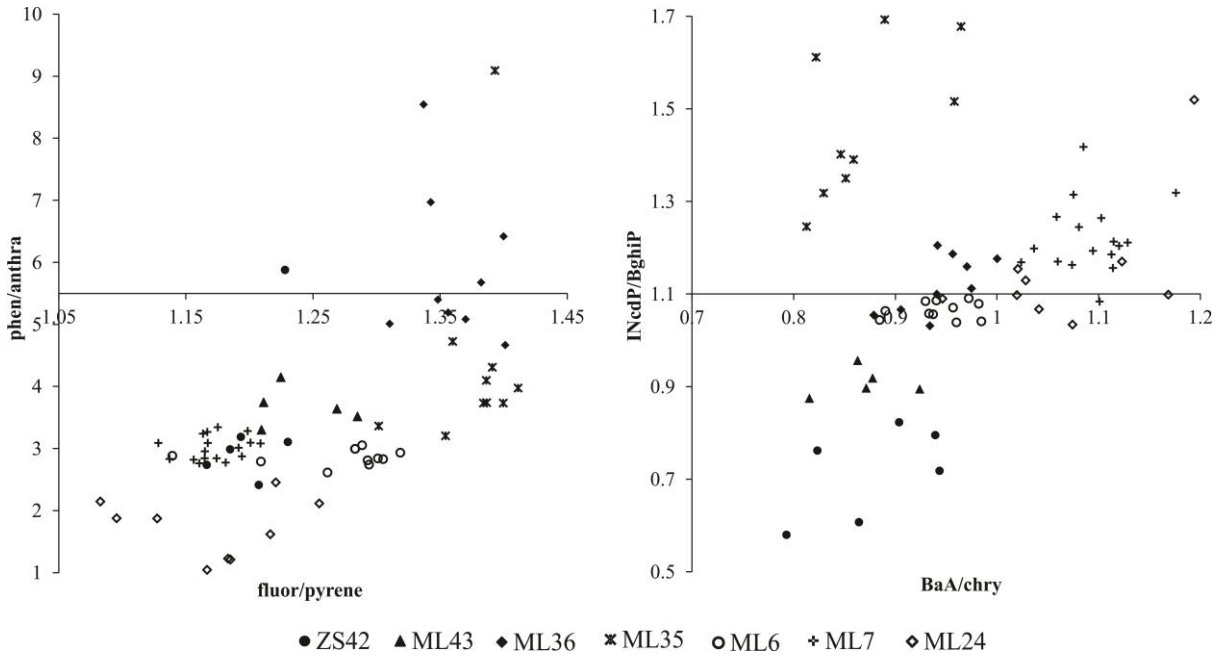

Fig. 4.7 Spatial variation of the concentration ratios of PAH isomers in the sediment cores.

It is noteworthy that the ratios of phen/anthra and fluor/pyrene in the cores typically increase with the PAH transport by water flow in both Zhushan bay and Meiliang bay, but there are no specific spatial variation trends in the ratios BaA/chry and INcdP/BghiP. As the light molecular PAHs (phen, anthra, fluor and pyrene) are several orders of magnitude more hydrophilic than the heavier PAHs (BaA, chry, BghiP and INcdP) (Tab. 3.4), the patterns of the light PAHs might be more influenced by water-particle partitioning effect during water transport, but the heavy ones might be more influenced by in situ degradation. As a consequence, it can be concluded that after PAHs are input to the lake sediment, their patterns are still variable during transport and/or after settlement, and the initial ratios calculated at emission sources are not applicable for emission source track in the sediment any more.

Temporal variation of the patterns

In line with the four groups of the isomer ratios explained above, the concentration ratios are also calculated and plotted in each of the cores with depth (Fig. 4.8 a, b, c, d). As explained in 4.1.3 and 4.1.4 part, PAH input patterns in the sediment have been changed during the last decades, so there should be certain trends in the isomer ratios with depth to imply the source changes. However, the isomer ratios do not show interpretable trends in all of the cores and the ranges of each of the isomer ratios vary significantly from core to core. Therefore, the spatial and temporal variations of the isomer ratios in the sediment suggest that PAH patterns maintain varying after settlement in the sediment. Consequently, after verifying the two assumptions, it indicates that isomer ratios, some statistics and CMB models are not the reliable methods for PAH source track in the sediment. The invalidity has also been affirmed by Kim et al. (2009) with illumination experiment in a laboratory, which shows that PAH patterns in same samples can imply different source input with varied duration of illumination, that is, photodegradation effect.

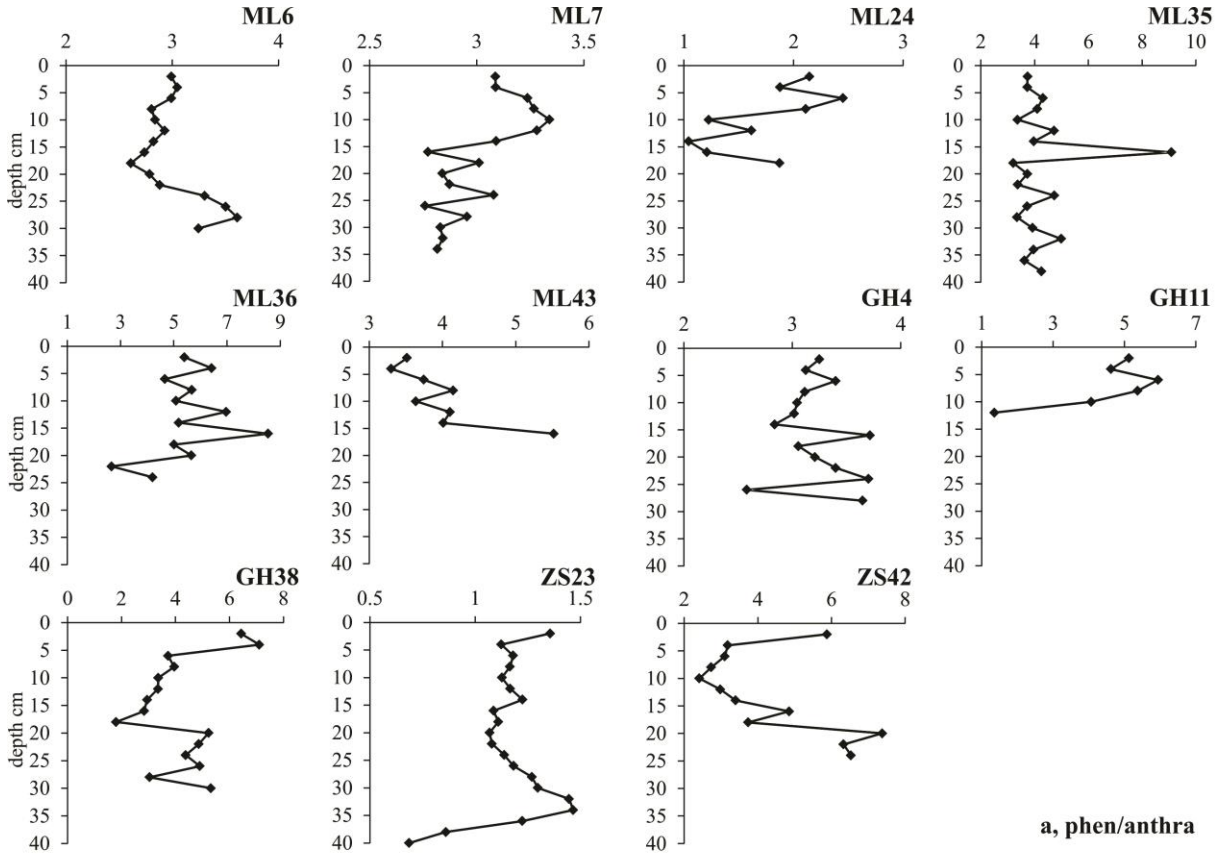
ML6
ML7
ML24
ML35
ML36
ML43
GH4
GH11
GH38
ZS23
ZS42
depth cm
a, phen/anthra

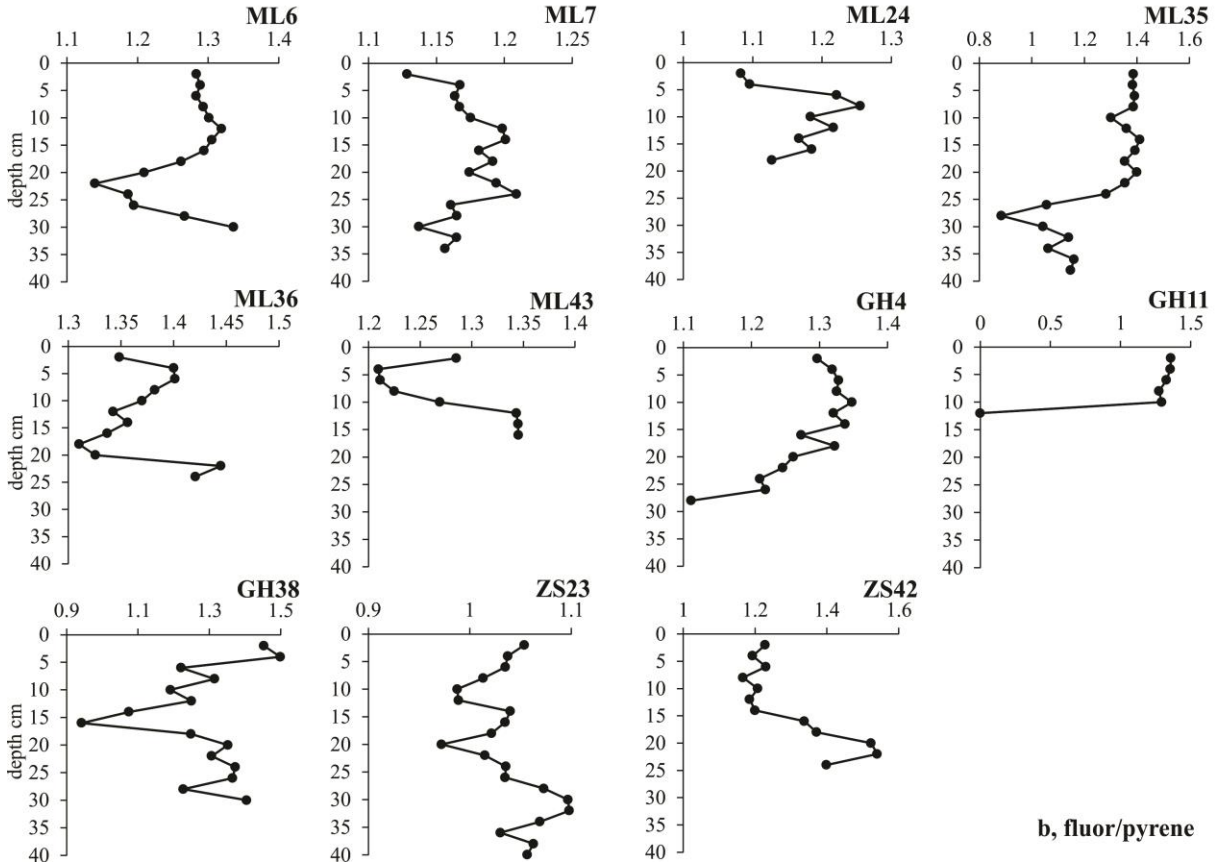
ML6
ML7
ML24
ML35
ML36
ML43
GH4
GH11
GH38
ZS23
ZS42
depth cm
b, fluor/pyrene

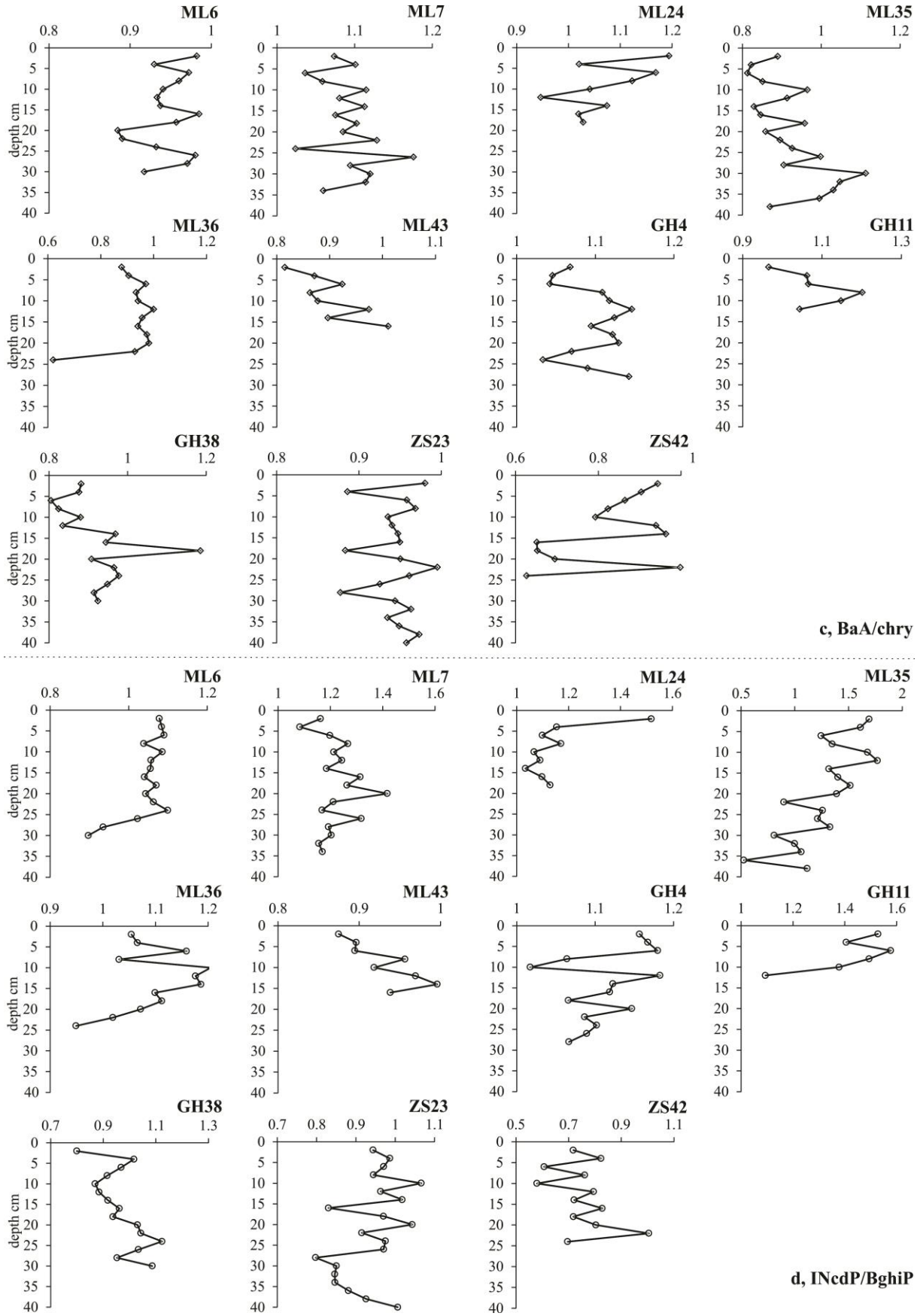

Fig. 4.8 Temporal variations of the concentration ratios of the PAH isomers in the sediment cores.

4.1.6 Toxicity assessment of the sediment

In general, sediment quality guidelines (SQGs) refer to the total concentration of a substance in the dry mass of the upper sediment layers (CCME, 1999). Several PAH SQGs have been proposed and the threshold concentrations of the concerned compounds vary in different countries or areas. The guideline from the Netherlands only concerns the total concentration of 10 PAHs, while Canadian Council of Ministers of the Environment (CCME) and consensus-based SQGs consider both the total PAH concentration and also the concentration of individual PAHs (Tab. 4.4).

The threshold value for sediments/soils in the Netherlands equals 1% of the HC5 (Hazardous Concentration for 5% of the species in the ecosystem), as this hazardous level is considered to pose a negligible risk to the ecosystems (Swartjes, 1999). According to this guideline, only 2 of the 25 surface sediments sampled in the northern part of Taihu Lake exceed the threshold value of 1000 ng/g and 72% of the samples are even below 500 ng/g. However, the guidelines from CCME are more stringent with lower threshold values. The concentrations of more than 50% of the concerned PAHs are higher than interim sediment quality guidelines (ISQG) in 3 locations 3-18, 8-23 and 8-24, especially the concentrations of all the compounds are above this threshold in 8-23. Among the 13 PAHs listed in CCME, fluorene, phen, pyrene, BaP and DahA are more risky in Taihu Lake, as their concentrations more frequently exceed the ISQG thresholds. Nevertheless, the concentrations of all the PAHs in the 25 samples are much lower than the probable effect level (PEL) values. In addition, compared to the consensus-based threshold effect concentration (TEC) and probable effect concentration (PEC), the concentrations of the concerned PAHs are much lower than TEC values except that the concentrations of some PAHs are slightly higher in locations 8-23 and 8-24, but the concentrations of all the PAHs are far below the PEC thresholds.

Tab. 4.4 PAH concentration levels of SQGs and the PAH concentration ranges in the sediments of this study

concerned PAH	Netherland	CCME		consensus-based SQG		range of this study
		ISQG	PEL	TEC	PEC	
naph		34.6	391	176	561	4.1 – 184.5
2methylnaph	–	20.2	201	–	–	ND – 83.1
acenaphthe	–	6.71	88.9	–	–	ND – 27.8
acenaphthy	–	5.87	128	–	–	ND – 35.6
fluorene	–	21.2	144	77.4	536	ND – 60.0
anthra		46.9	245	57.2	845	ND – 169.7
phen		41.9	515	204	1170	12.8 – 211.9
fluor		111	2355	423	2230	20.3 – 218.3
BaA		31.7	385	108	1050	4.5 – 107.1
chry		57.1	862	166	1290	5.6 – 122.9
pyrene	–	53	875	195	1520	15.3 – 208.4
BaP		31.9	782	150	1450	5.1 – 135.2
BkF		–	–	–	–	3.3 – 63.1
DahA		6.22	135	33	–	ND – 39.3
BghiP		–	–	–	–	9.1 – 153.3
INcdP		–	–	–	–	6.5 – 156.1
total PAHs	1000	468	7107	1610	22800	101.3 – 1466.7

–: the PAH compound is not considered; the guidelines of the first 7 light PAHs in CCME are provisionally derived from marine ISQGs and PELs use the modified National Status and Trends Program (NSTP) approach, because information was not sufficient; ND: concentration are below the quantification limit.

Therefore, combining the evaluations with the three guidelines, the sediment in Taihu Lake is rarely associated with adverse biological effects on sediment-dwelling organisms, although the concentration of some PAHs in one location (8-23) are risky compared to the threshold of ISQG and TEC. However, for safety and health concern, PAHs around location 8-23 need to be further studied and the inflow rivers should be the potential contaminant sources. What is more, the concentration of contaminants in sediments is not the single factor influencing the toxicity to aqueous organisms, the properties of organic compounds and the type of substrate in sediments are also significant factors (McGroddy et al., 1996).

4.2 Sedimentary archive of perylene in the sediment

4.2.1 Perylene in the surface sediment and the cores

Perylene concentrations in the surface sediments are typically below 200 ng/g, except in the five locations 8-6, 8-7, 8-21, 3-17 and 3-21 with higher concentrations (200 – 300 ng/g) (Fig. 4.9). Compared to the other PAHs (Fig. 4.2), perylene concentrations are relatively high in most of the sampling locations and the higher concentrations are generally located in the area close to the central part of the lake. The spatial distribution of perylene concentrations is somewhat inverse to the distribution of the other PAHs, which is especially obvious in Zhushan Bay.

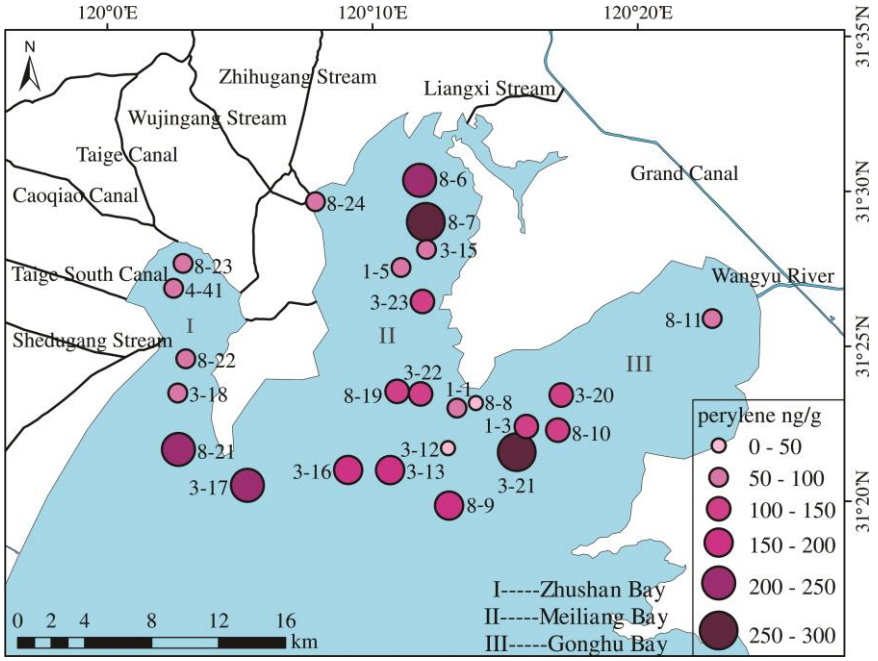

Fig. 4.9 Concentration distribution of perylene concentrations in the surface sediments.

As in the case of the surface sediments, perylene concentrations in the cores are generally below 200 ng/g, except cores ML35, GH38 and ZS42 (Fig. 4.10). In some sections of cores ML35 and GH38, perylene concentrations reach over 1000 ng/g, accounting for up to 96% of the sum of the 20 PAH concentrations. Concentration patterns, however, in the three cores are different. In core ML35, the high concentrations occur in the deeper layers and the relatively low and stable ones (around 200 ng/g) in the upper layers, while in core GH38 perylene concentrations generally increase from the deeper to the upper layer of the core with the highest concentration at 8 cm depth. In addition, the concentrations in core ZS42 decrease linearly from the deeper layer (around 450 ng/g) to the upper one (around 150 ng/g). Nevertheless, in the other cores, perylene concentrations are low and vary slightly, particularly in the upper 15 – 20 cm.

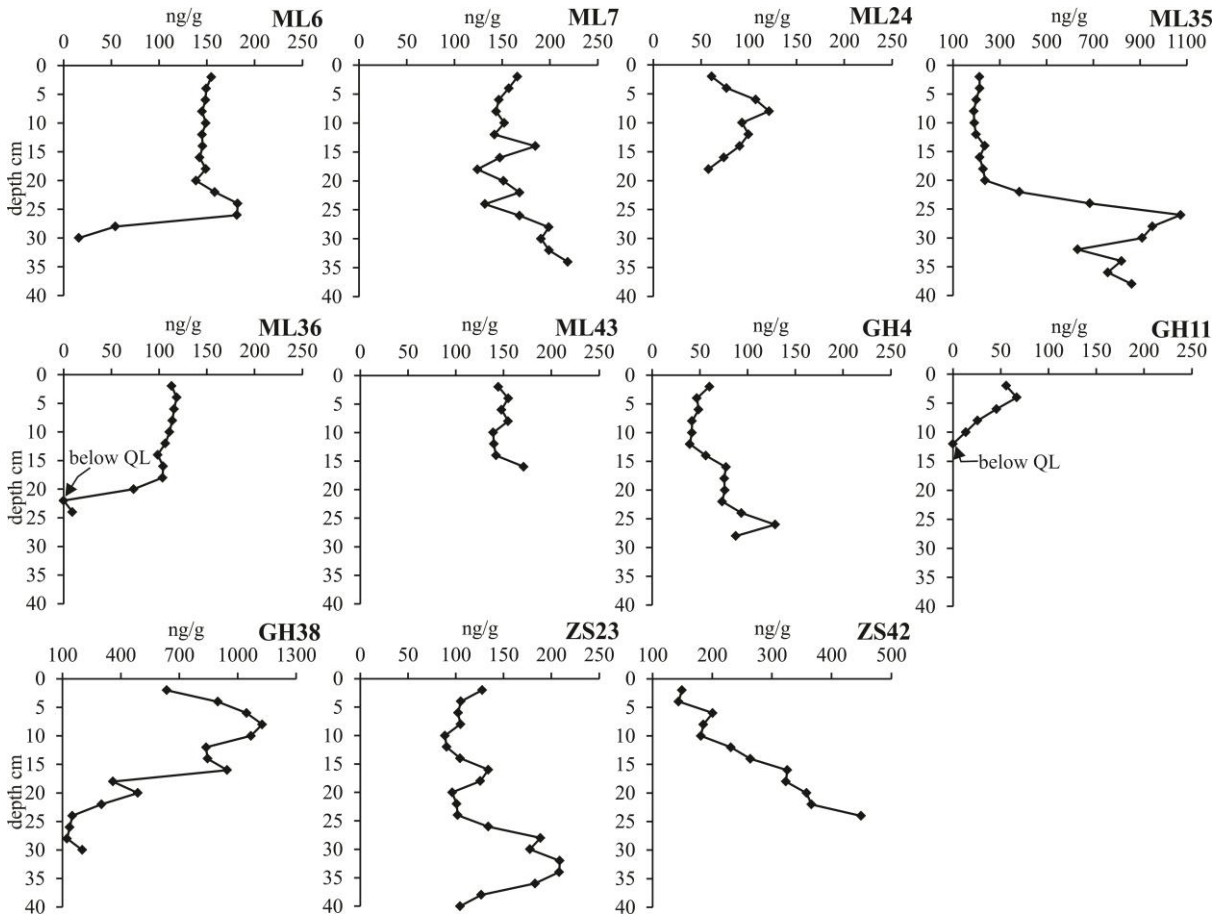

Fig. 4.10 Concentration profiles of perylene concentrations in the cores (QL--- quantification limit).

4.2.2 Perylene sources

Compared to the other PAHs, the concentration profiles of perylene are specific in each core, which might result from two potential sources, anthropogenic input together with the other PAHs and biogenic formation in the sediments after deposition. Three anthropogenic PAHs, BaP, BeP and pyrene are selected as references to distinguish anthropogenic and biogenic sources of perylene (Venkatesan, 1988). The five cores ZS23, ML24, ML7, GH11 and GH4 collected close to the river outlets show significant positive linear correlations with the three anthropogenic PAHs (Fig. 4.11a), while the other six cores ZS42, ML6, ML35, ML36, ML43 and GH38 collected far away from the river outlets show significant negative correlations (Fig. 4.11b) or no significant correlations (Fig. 4.11c). The significant positive linear correlations indicate that perylene, to a large extent, originated from the same sources as the three anthropogenic PAHs.

Tab. 4.5 describes the correlation calculations between the concentration of perylene and the three anthropogenic PAHs in the cores. The correlations were calculated with Pearson correlation method or Spearman's rho correlation method depending on the normality of the data set. The values labelled with $_{(p)}$ were calculated with Pearson correlation method and the values labelled with $_{(s)}$ were calculated with Spearman's rho correlation method. Meanwhile, the residual's normality was tested in the samples with significant positive correlations to confirm the linear regressions between the concentration of perylene and the three PAHs.

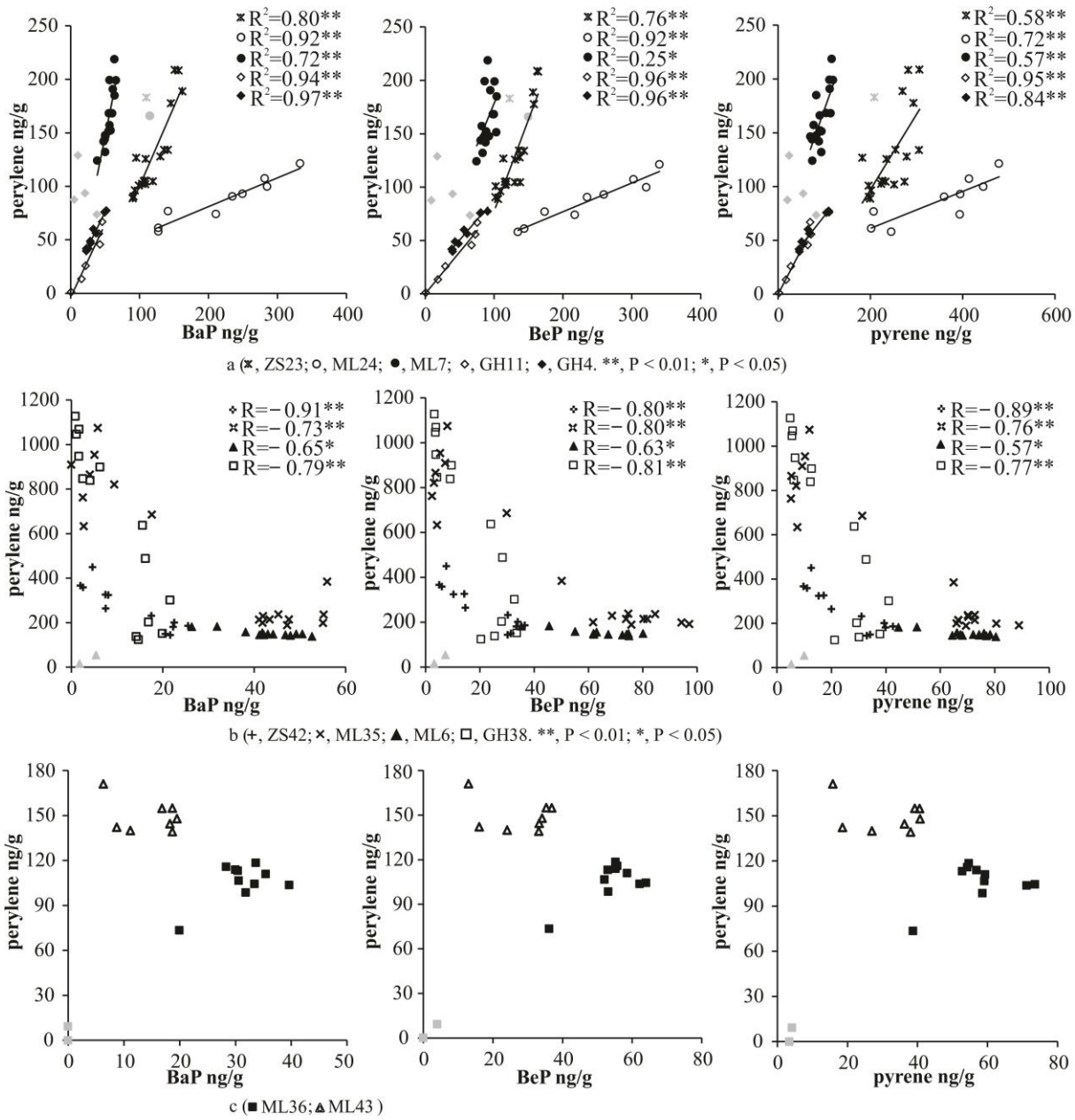

Fig. 4.11 Concentration correlations between perylene and the three anthropogenic PAHs (BaP, BeP and pyrene) with (a) significant positive linear correlations, (b) significant negative correlations and (c) no correlations (Four points from core GH4, one point from core ML7, one point from core ZS23, two points from core ML6, and two points from core ML36 (labeled with grey color) are outliers and were excluded from the correlation and regression calculations, the details about the outliers are explained as follows.).

In Fig. 4.11a, it is presented with determination coefficient R^2 in the significant positive linear correlations between the concentrations of perylene and the three PAHs. However, the significant negative correlated ones are described with correlation coefficient R (Fig. 4.11b). The correlations in cores ZS42 and ML6 could also be linear, but linear correlation cannot fit the distributions of the data points from cores ML35 and GH38, as their perylene concentrations are mainly distributed in high values and low values. Meanwhile, the negative correlations indicate perylene originated from biogenic formation, which implies that many possible and unknown factors could influence the formation processes. Therefore, considering the consistent data plot in one graph and also proper interpretation of the results, it is more reasonable to just show the correlation coefficient in the negative correlated groups. The concentration correlations are not significant only in cores ML36 and ML43 (Fig. 4.11c) with the furthest location distance from river outlets compared to the other cores

(Fig. 3.1), which might be explained by that anthropogenic impacts are minor and the inhibition effects are relieved in these areas. However, the perylene concentrations in these two cores are rather low compared to the other four cores with significant negative correlations, the conjecture for the unexpected low concentrations is that nutrient supply limited the biogenic formation of perylene in this area.

For the outliers in Fig. 4.11 a, b, c, except the one point in core ML7 from the surface layer, all the other outliers are from the deepest layers of the cores. The reason for the outliers from core GH4 could be that anthropogenic impacts were weak in the deeper layers of the sediment in this location, so perylene with higher concentrations in these layers could originate from both anthropogenic and biogenic activities. However, the reasons for the outliers with significantly low perylene concentrations in cores ML6 and ML36 could be that there was no proper nutrient supply for its biogenic formation.

Tab. 4.5 Statistic calculation results of the correlation and regression between the concentration of perylene and BaP, BeP, pyrene

location	perylene & BaP			perylene & BeP			perylene & pyrene		
	corre.	sig. of corre.	sig. of residuals' norm. test	corre.	sig. of corre.	sig. of residuals' norm. test	corre.	sig. of corre.	sig. of residuals' norm. test
ZS23	**0.893 (s)**	**	**0.336**	**0.874 (s)**	**	**0.446**	**0.758 (s)**	**	**0.099**
ML24	**0.957 (p)**	**	**0.460**	**0.961 (p)**	**	**0.460**	**0.849 (p)**	**	**0.755**
ML7	**0.846 (p)**	**	**0.217**	**0.503 (p)**	*	**0.066**	**0.758 (p)**	**	**0.963**
GH11	**0.971 (p)**	**	**0.840**	**0.982 (p)**	**	**0.884**	**0.974 (p)**	**	**0.878**
GH4	**0.986 (p)**	**	**0.064**	**0.979 (p)**	**	**0.834**	**0.915 (s)**	**	**0.142**
ZS42	**–0.905 (p)**	**	–	**–0.804 (s)**	**	–	**–0.894 (p)**	**	–
ML35	**–0.726 (s)**	**	–	**–0.800 (s)**	**	–	**–0.763 (s)**	**	–
ML6	**–0.654 (s)**	*	–	**–0.632 (s)**	*	–	**–0.571 (s)**	*	–
GH38	**–0.789 (s)**	**	–	**–0.811 (s)**	**	–	**–0.768 (P)**	**	–
ML43	–0.144 (s)	0.734	–	0.214 (s)	0.610	–	0.071 (s)	0.867	–
ML36	–0.030 (s)	0.934	–	0.188 (s)	0.603	–	–0.224 (s)	0.533	–

**: P < 0.01; *: P < 0.05. corre.: correlation; sig.: significance; norm: normality.

There are wide ranges of the concentration proportion of perylene to the sum of the 20 PAHs (Fig. 4.12). The concentration proportions are typically lower (0.02 to 0.18) in the five cores ZS23, ML7, ML24, GH4 and GH11 collected close to the inflow river outlets than that (0.13 to 0.96) in the other six cores ML6, ML35, ML36, ML43, GH38 and ZS42 collected far away from the river outlets. This is in agreement with the perylene concentration distributions in the surface sediment (Fig. 4.9) that the lower concentrations are generally located in the areas near the outlets of the inflow rivers, while the higher ones are mainly located far away from the outlets of the inflows. The lower perylene abundance relative to the other parent PAHs indicates perylene mainly originates from pyrogenic processes instead of diagenetic sources (Readman et al., 2002; Baumard et al., 1998).

Consequently, these three aspects, the lower concentration proportions, the positive linear concentration correlations and the locations with short distance from inflow river outlets, together strongly imply that perylene in these locations close to the river outlets originated mainly from anthropogenic activities and were input by river runoff. Furthermore, the different correlation slopes (Fig. 4.11a) and the different perylene proportions (Fig. 4.12) in the five cores suggest that there are different composition of anthropogenic PAH sources in the inflow rivers. In addition, the conclusion that anthropogenic perylene dominates the perylene origins in the river runoff indicates that there is

no or negligible amount of perylene input from terrigenous compartments by surface runoff, such as termite, wood substrate and wood-rotting fungi.

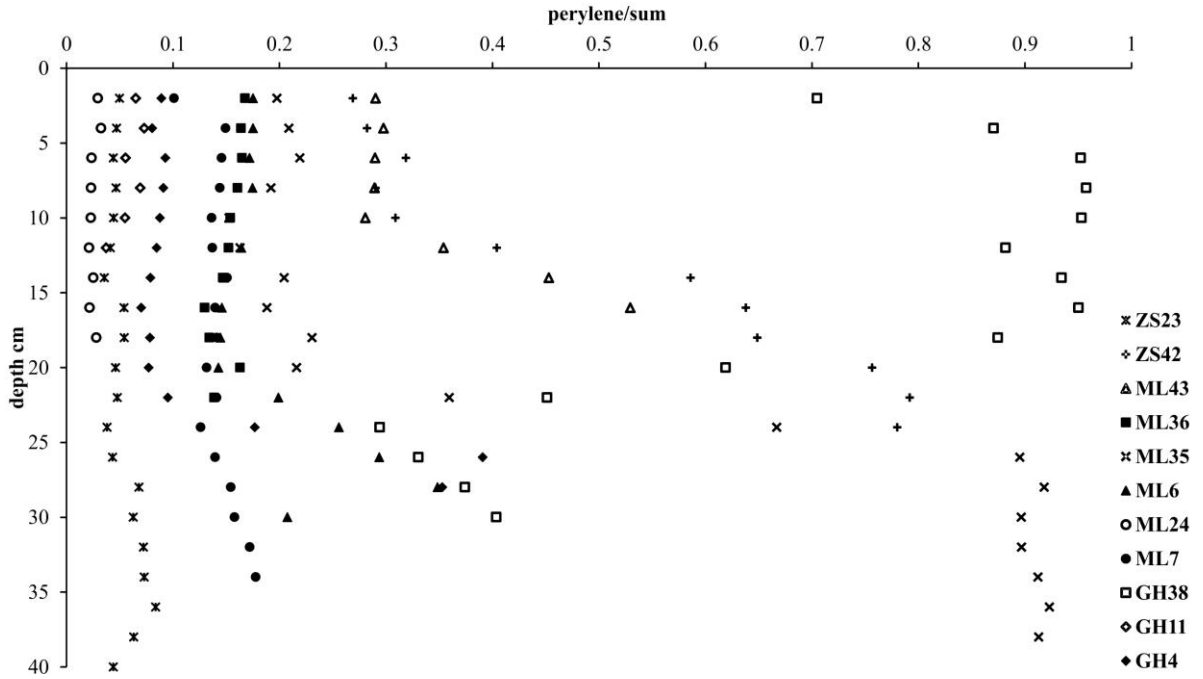

Fig. 4.12 Vertical distribution of the concentration proportions of perylene to the sum of the 20 PAHs in the cores.

However, in the other six locations ML6, ML35, ML36, ML43, GH38 and ZS42, perylene could be mainly formed in situ by biogenic activities without obvious spatial transport and interaction. This is supported by the negative or no correlations between the PAH concentrations and also the higher perylene concentration proportions on one hand, and on the other hand by the specific perylene concentration profiles. As explained, there are similar PAH concentration profiles between cores ML6 and ML7, cores ML6, ML35 and ML36, cores ML43 and ZS42, cores GH4 and GH38, due to the water flow direction and/or spatial distances of these core locations (Fig. 4.3), while the distributions of perylene concentration do not show the similarities in the core groups (Fig. 4.10).

Some studies suggested that phytoplankton, particularly diatom, could be perylene precursors in deep aquatic sediments (Venkatesan and Kaplan, 1987; Louda and Baker, 1984; Soma et al., 1996). Massive nutrient inputs have resulted in the rapid proliferation of phytoplankton in Taihu Lake since the 1980s and the occurrence of phytoplankton bloom became more frequent and severe after ca. 2000 (Duan et al., 2009; Duan et al., 2015; Dong et al., 2008). However, perylene concentrations fluctuate slightly or even decrease in the upper layers of the cores. This implies that the distribution of perylene is not consistent with the accumulation of phytoplankton, which agrees with Silliman's report (1998) that there is poor correlation between the mass accumulation rates of perylene and biogenic silica (an indicator of diatom production) in Lake Ontario.

Some researchers speculated that perylene was preferably formed in anaerobic condition in lake and marine sediment, as its concentrations showed increasing trend with depth in sediments (Tan and Heit, 1981; Silliman et al., 2001; Slater et al., 2013). In this study, however, perylene concentration distributions in the cores are not consistently related to depth. Taihu Lake is so shallow that the overlying water is usually under oxic condition (Jiang et al., 2008; Xu et al., 2010). Bioturbations modify the porosity, permeability and spatial heterogeneity of the upper sediment, which increase the

oxygen uptake from overlying water and create aerobic condition in the upper layer of the sediment (Zhang et al., 2011). Therefore, the distributions of perylene concentrations and the oxygen conditions in the sediment together imply that the biogenic formation perylene seems not to be so closely related to aerobic or anaerobic condition in Taihu Lake.

The results also indicate that biogenic formation of perylene might be inhibited in the sediments where anthropogenic impacts are stronger, which is close to the river inflows and also in the upper layer of the sediments. Nutrients, organic matter and pollution levels can influence the diversity of microbial communities and mineralization in sediments (Haller et al., 2011; Xu et al., 2018; Zeng et al., 2005) and therefore could also affect biogenic formation of perylene in sediments.

4.3 PAHs in the water body

4.3.1 Seasonal variation of PAH concentrations

The PAHs detectable in the water samples are dominated by naph, 2methylnaph and 1methylnaph, and then fluorene and phen are the relatively abundant molecules compared to the other heavy PAHs (Fig. 4.13). Comparing the four campaigns, the concentrations of naph, 2methylnaph and 1methylnaph in the samples collected in warm season (2016-06 and 2017-09) are up to one order of magnitude higher than that in the samples collected in cold season (2015-11 and 2017-02). Particularly, the concentrations of 2methylnaph in the campaign 2017-09 are even up to 20 folds higher compared to that in the samples collected in cold season. However, the concentrations of fluorene and phen do not show noticeable seasonal variations, and the concentrations of the other PAHs are typically below the quantification limit in both warm and cold seasons.

The water temperature in cold and warm seasons is around 10 °C and 30 °C, respectively. It has been studied that the water solubility of some PAHs including naph increase with the increase of temperature (Pérez-tejeda et al., 1990; Whitehouse, 1984), and also, the water partitioning of PAHs is temperature dependent (Slmonich and Hites, 1994; Tsapakis and Stephanou, 2005; Jenkins et al., 1996). For example, the partitioning of naph and methylnaph from diesel, gasoline and coal tar to water is significantly higher than the partitioning of the other heavier parent PAHs in ambient temperature, and the temperature effect on partitioning of the other PAH cannot be detected until 100 ^{o} C or even higher (Lee et al., 1992, a, b; Yang et al., 1997). Therefore, the noticeably high concentrations of naph and methylnaphs in warm seasons should be mainly attributed to temperature effect on PAH existence in the water body.

It is noteworthy that the concentration patterns between naph and methylnaphs are rather different in the cold and warm seasons. The concentration of naph is certainly higher than that of methylnaphs in the samples collected in cold seasons. On the contrary, the concentrations of methylnaphs, especially 2methylnaph, are notably high in the samples collected in warm season, and the concentrations of 2methylnaph from the campaign 2017-09 are typically double of the concentration of naph and reach up to 1350 ng/L. Generally, the combustion emission of methylnaph is severalfolds lower than that of naph (Jenkins et al., 1996; Herrington et al., 2012; Mcdonald et al., 2000), so it can be suspected that the dramatic abundance of methylnaphs in the warm season samples should originate from other additional sources besides from anthropogenic activities.

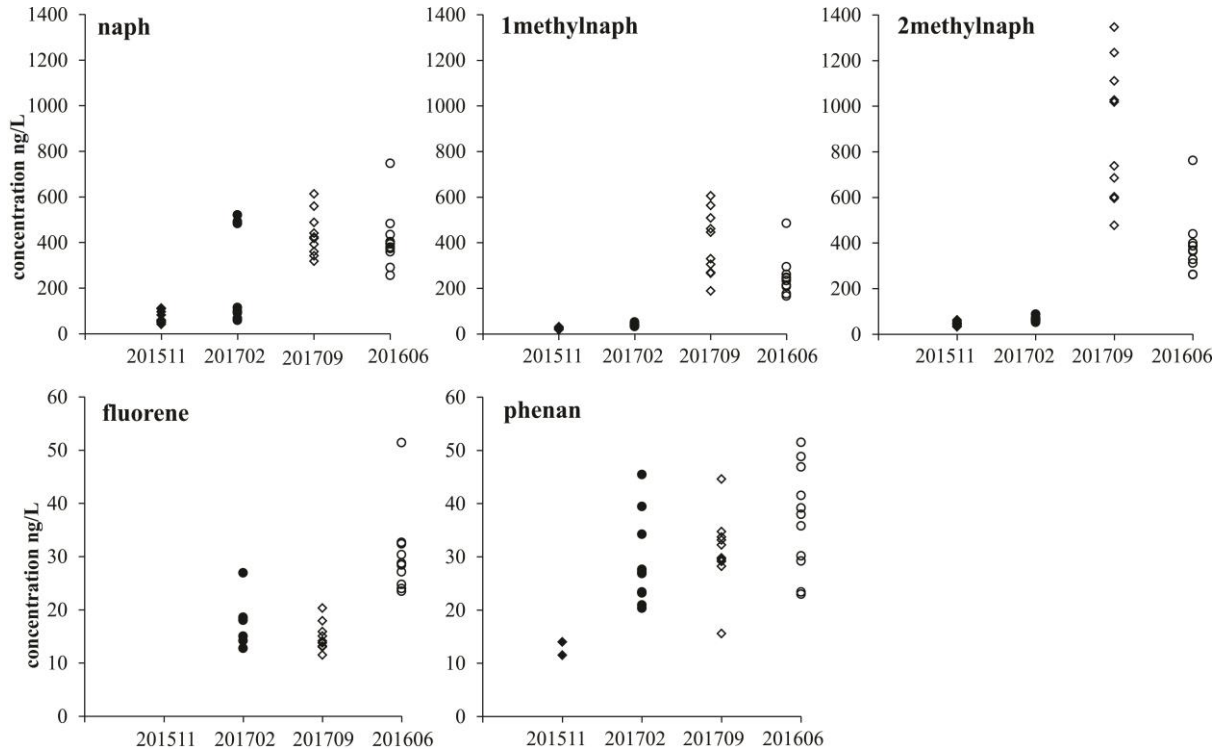

Fig. 4.13 Seasonal variation of PAH concentrations in the lake water (201511 and 201702 are the samples collected in cold season, 201909 and 201606 are the samples collected in warm season; there are 10 samples in 201511, 10 samples in 201702, 11 samples in 201606 and 10 samples in 201709 seen in Fig. 3.2)

4.3.2 Spatial distribution of PAH concentrations

It is rather consistent in the spatial concentration distributions of naph, methylnaphs and the other PAHs in cold seasons that the higher concentrations are located in Zhushan bay, and the lower concentrations are located in Gonghu bay and the eastern part of Meiliang bay (Fig. 4.14 a, c, e). The spatial concentration distributions of naph and the other PAHs in warm season, however, are somewhat homogeneous (Fig. 4.14 b, f). In addition, the spatial distribution of methylnaph concentrations in warm season does not show specific spatial patterns, but it presents marked differences between the two campaigns, that is, significantly high concentrations in samples 201709 and relatively low concentrations in samples 201606 (Fig. 4.14 d). The different distributions of methylnaphs with the other PAHs further support the suspicion that there are additional origins of methylnaphs particularly in September.

Generally, from Nov to the following April is the dry season in this area and the water level in the lake decreases significantly, while there is rather more precipitation in the other months in the catchment, especially monsoon occurs almost in every summer and results in heavy precipitation and flood (Chen et al., 2001; Xu et al., 2007; Tao et al., 2012). The water level in Taihu Lake is somehow adjusted by water recharge from the Yangtze River through the Wangyu River connecting the Yangtze River and the northeastern part of Taihu Lake (Gonghu bay) (Fig. 2.1c) (Zhai et al., 2010; Wang and Wang, 2014). The time allocation of the water recharge and the recharge duration mainly depend on the lake water level, which can be obtained in the documents of monthly and yearly water regime downloaded from Taihu Basin Authority of Ministry of Water Resources (http://www.tba.gov.cn/channels/48.html). The sampling campaigns 2015-11 and 2017-02 were during the period of water recharge from the Yangtze River, but the other two campaigns 2016-06 and 2017-09 were out of the period.

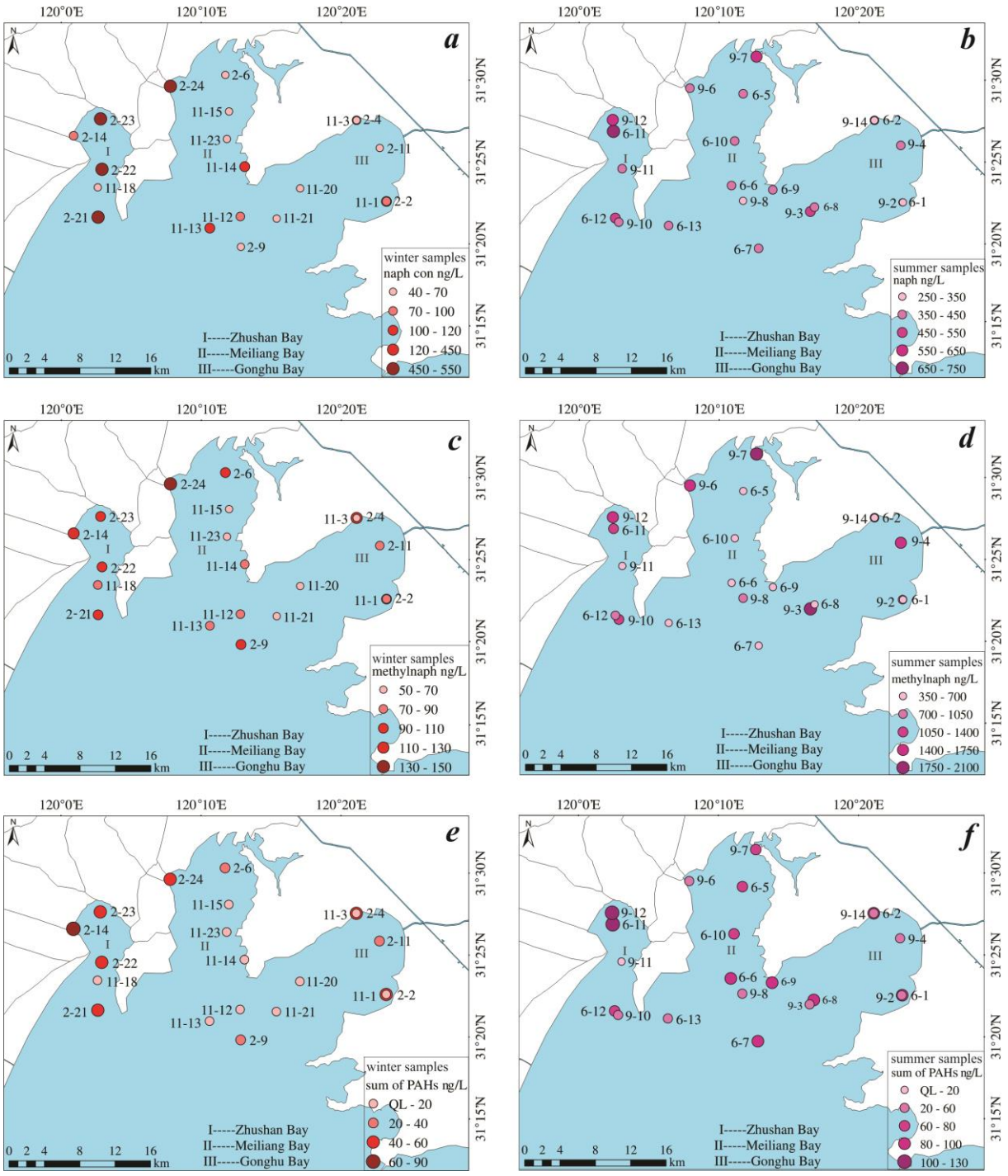

Fig. 4.14 Spatial variation of PAH concentrations in the water body (different scales in each of the figures).

The general inflows are located around the northern and the southwestern part of the lake and the outflows are around the eastern and southeastern part of the lake (Qin, 2008), which result in the water flow direction in the lake typically from the western part to the southeastern part. In dry season, there is less water input from the inflow rivers in the northern and western part of the lake, so the water recharge from the Yangtze River to the northeastern part of Taihu Lake can somewhat change the water flow directions in the northern part of the lake. Therefore, the water recharge from the Yangtze River can explain the spatial patterns of the PAH concentrations in samples 2015-11 and 2017-02 sampled within the water recharge period (Fig. 4.14 a, c, e). The higher concentrations are located in Zhushan bay and in the western of Meiliang bay close to the river outlet, and the lower concentrations are located in the eastern area of Meiliang bay and Gonghu bay. These spatial

distributions of the concentration patterns suggest that PAH abundance in the Yangtze River is lower than that in the northern part of Taihu Lake, and PAH concentrations in Gonghu bay and the eastern Meiliang were diluted by the water inflow from the Yangtze River. During the other two campaigns in rainy season, however, there is more water input from the other inflow rivers and high water dynamics in the lake homogenize PAH concentration distributions in the water body.

4.3.3 PAH toxicity in the water body

The carcinogenic and adverse PAH compounds mostly are the heavier molecules such as BaA, chry, BaP, BbF, DahA, BghiP (Kim et al., 2013) rather than the compounds detectable in these water samples. In addition, the measured concentrations in the samples are orders of magnitude lower than the concentrations with potential adverse effect tested with some organisms (Kalf et al., 1997; Couillard et al., 2005). However, it has been studied that the toxicity of some PAHs could significantly increase in the environment due to metabolism and oxidation, such as anthra, fluor and pyrene (Arfsten et al., 1996; Pelletier et al., 1997). Therefore, even though the compounds and their concentrations are not toxic in the water body, it is not sufficient to assess the PAH toxicity in the environment only considering the concentration of parent PAHs.

4.3.4 Review other studies on PAHs in water

As this research is focused on dissolved PAHs in the lake water, the comparison and discussion from other publications are also based on dissolved PAHs in surface water bodies. Most researches only measured the 16 PAHs listed by US EPA, and few researches also measured other PAHs such as 1mehtylnaph and 2methylnaph (Tongo et al., 2017; Guo et al., 2011). There are variable PAH patterns and orders of magnitude variations in their concentration levels in different studies. The detected PAHs are generally dominated by 2-ring and 3-ring PAHs, especially 2-ring naph and following with 3-ring phen, which is similar with the PAH patterns in the current study (Li et al., 2010; Li et al., 2006; Sun et al., 2009), but the concentrations of 3-ring acenaphthy and acenaphthe in some studies are also found rather high even as the concentration of naph (Kabziński et al., 2002; Tongo et al., 2017; Sarria-villa et al., 2016; Kafilzadeh, 2015). The 4-ring fluor and pyrene are generally the heaviest PAH compounds detected in water samples (Li et al., 2010; Li et al., 2006; Sun et al., 2009), but in some researches 5-ring and 6-ring PAHs also show relatively high concentrations (Dhananjayan et al., 2012; Guo et al., 2011). In addition, markedly high concentrations of 1methylnaph and 2methylnaph as found in current study have not been investigated and/or discovered in previous studies. The concentrations of individual PAHs range from several ng/L to thousands ng/L in different studies, and the variations mostly occur in the 2-ring and 3-ring PAHs (Tongo et al., 2017; Dhananjayan et al., 2012; Patrolecco et al., 2010; Sarria-villa et al., 2016; Yang et al., 2013; Kafilzadeh, 2015). Furthermore, seasonal variations of PAH concentrations in water are also not consistent: higher PAH concentrations in warm season than in cold season (Qin et al., 2014; Montuori et al., 2016; Deng et al., 2006), which is similar to this study; higher concentrations in cold season than in warm season (Guigue et al., 2014; S. Liu et al., 2016; Mzoughi and Chouba, 2011); no obvious differences between cold and warm seasons (Guigue et al., 2011; Kafilzadeh, 2015; M. Liu et al., 2016). Meanwhile, it was also found that naph was the dominant in cold season, but the 3-ring PAHs were the dominant in warm season (P. Li et al., 2015; Y. Li et al., 2015). Therefore, even though there are significant amount of researches on PAHs in water phase, it is difficult to conclude general characteristics of PAH distribution and existence in water bodies.

5 Summary and conclusion

The sediment and water samples were collected from the northern part of Taihu Lake for PAH concentration analyses. The PAHs in the surface sediments and the sediment cores were interpreted for the current and historical PAH depositions in the lake. In addition, the four aspects, PAH patterns in the cores, energy consumption in this catchment, literature data on PAH emission patterns from different sources and PAH distributions in fine and ultrafine particle sizes together reveal anthropogenic impacts on the PAH existence and distributions in the sediments. ^{137}Cs was used as a time indicator of the late 1950s for the sediment age measurement. Perylene in the sediment was interpreted separately to distinguish its biogenic and anthropogenic origins. Water samples were analyzed to interpret the seasonal variations of PAH concentrations and the spatial distributions in the lake.

The spatial distributions of the PAH concentrations in both, the surface sediments and sediment cores, show that noticeably higher concentrations are located close to the inflow outlets in Zhushan bay and Meiliang bay, so the inflow rivers mainly contribute the PAH input to this area of the lake. This coincides with higher sedimentation rates close to the inflow rivers. Comparing the concentrations in the three bays, Meiliang bay is more polluted with PAHs than the other two bays. The temporal analyses of PAH concentrations in the cores show that increasing PAH input into the lake started from the late 1950s due to economic and industrial development. Over the years, PAH concentrations in the sediments increased fairly quickly by a factor of 10 or more compared to the background concentrations. However, quite stable PAH concentrations in the upper 10 to 20 cm of the sediments in several cores might indicate sediment resuspension due to currents and turbulences in the shallow water column of Taihu Lake. The resulting redistribution of the sediments could, to some extent have spoiled the functioning of the sediments as a temporal archive. This assumption is further supported by the quite rapid increase and then more or less constant ^{137}Cs activities in the upper parts of the three dated cores. In addition, bioturbation could have further influenced the stratification of the sediments. To what extent the environmental measures implemented by the Chinese government since ca. 2000 are reflected in these concentration profiles is difficult to quantify. Some cores show even a decrease in concentrations in the uppermost parts, but local effects or sediment resuspension are also likely causes.

PAHs in the cores are dominated by 4 light PAHs (phen, anthra, fluor, pyrene) and 6 heavy ones (BkF, BaP, BbF, BeP, INcdP, BghiP), and the concentration fractions of the light PAHs are decreasing with decreasing depth, but the fractions of the heavy PAHs are increasing. The structure change of energy consumptions in this area is considered as one of the reasons for the distribution trends of the PAH concentration fractions. The changes could be explained by three aspects, (i) the continuously increasing consumption of coal in emission-controlled combustion, (ii) the linear increase of oil consumption in transport and (iii) the exponential increase of the number of light-duty vehicles in the study area during the last decades. Another reason could be the introduction of particle intercept equipment for emission control, resulting in the emission of relatively more ultrafine particles, as heavy PAHs preferable bind to these ultrafine particles. In addition, the methods of PAH source track in the environment are verified with PAH emission patterns from their main sources and also with the PAH patterns in the sediments of this study. The methods are not applicable in this study area, because the two assumptions for the methods are not satisfied with the indistinguishable PAH patterns from different PAH emission sources and the varying patterns in the sediments.

The spatial distributions of perylene concentrations in the sediments and its concentrations in relation to the other PAHs suggest that perylene can originate from the same sources as the other anthropogenic PAHs in the locations close to the river inflows. However, in locations far away from inflows it may result from biogenic processes, as concentrations are typically higher compared to the other PAHs and in addition are not positively correlated to typical anthropogenic PAHs. Consequently, this could imply that the biogenic formation of perylene is inhibited by anthropogenic activities.

There are markedly higher concentrations of naph, 1methylnaph and 2methylnaph in the summer water samples than in winter samples from the lake, which is most probably because of temperature effect on the solubility of these three PAHs in warm seasons. The spatial distribution of the PAH concentrations in cold seasons indicate that the water recharge from the Yangtze River through the Wangyu River diluted the PAH concentrations in the northeastern part of the lake.

As it was shown, high PAH concentrations occur typically in the upper around 20 cm of the sediments in the northern part of Taihu Lake. If sediment dredging is applied to reduce PAH loading and improve the quality of the ecosystem in this part of the lake, the dredging depth should be below the layer with high PAH concentration. The importance of dredging depth has been verified by others in lab experiments (Liu et al., 2015; Zhong et al., 2008). The two different proposed perylene sources, anthropogenic input and biogenic formation, result in its distinctly different spatial distribution. This may serve as a tool to investigate which factors inhibit or promote the biogenic formation of perylene, such as the hydrochemical conditions, nutrient availability, or pollutants. Moreover, PAH distribution characteristics should be further investigated in the other areas of Taihu Lake to generate comprehensive information on the PAH distribution in the lake sediments. This could result in more effective strategies for environmental protection and governance in the basin.

Reference

Allen, J.O., Dookeran, N.M., Smith, K.A., Sarofim, A.F., Taghizadeh, K., Lafleur, A.L., 1996. Measurement of polycyclic aromatic hydrocarbons associated with size-segregated atmospheric aerosols in Massachusetts. Environ. Sci. Technol. 30, 1023–1031. https://doi.org/10.1021/es950517o

Andronache, C., 2003. Estimated variability of below-cloud aerosol removal by rainfall for observed aerosol size distributions. Atmos. Chem. Phys. 3, 131–143. https://doi.org/10.5194/acp-3-131-2003

Arfsten, D.P., Schaeffer, D.J., Mulveny, D.C., 1996. The effects of near ultraviolet radiation on the toxic effects of polycyclic aromatic hydrocarbons in animals and plants: A review. Ecotoxicol. Environ. Saf. 33, 1–24. https://doi.org/10.1006/eesa.1996.0001

Atkinson, R., Arey, J., 1994. Atmospheric Chemistry of Gas-phase Polycyclic Aromatic Hydrocarbons : Formation of Atmospheric Mutagens. Environ. Health Perspect. 03, 29–32. https://doi.org/10.1289/ehp.94102s4117

Axelman, J., Naes, K., Naf, C., Broman, D., 1999. Accumulation of polycyclic aromatic hydrocarbons in membrane devices and caged mussels (mytilus edulis L.) in relation to water column phase distribution. Environ. Toxicol. 18, 2454–2461. https://doi.org/10.1002/etc.5620181111

Ayala, A., Kado, N.Y., Okamoto, R.A., Homen, B.A., Kuzmicky, P.A., Kobayashi, R., Stiglitz, K.E., 2002. Diesel and CNG heavy-duty transit bus emissions over multiple driving schedules: Regulated pollutants and project overview,. Soc. Automot. Eng. 2002-01–17, 1–13. https://doi.org/10.4271/2002-01-1722

Bachmann, R.W., Hoyer, M. V., Canfield, D.E., 2000. The potential for wave disturbance in shallow Florida Lakes. Lake Reserv. Manag. 16, 281–291. https://doi.org/10.1080/07438140009354236

Bae, S.Y., Yi, S.M., Kim, Y.P., 2002. Temporal and spatial variations of the particle size distribution of PAHs and their dry deposition fluxes in Korea. Atmos. Environ. 36, 5491–5500. https://doi.org/10.1016/S1352-2310(02)00666-0

Baek, S.O., Field, R.A., Goldstone, M.E., Kirk, P.W., Lester, J.N., Perry, R., 1991. A review of atmospheric polycyclic aromatic hydrocabons: sources , fate and behavior. Water. Air. Soil Pollut. 60, 279–300. https://doi.org/10.1007/BF00282628

Baldrian, P., in der Wiesche, C., Gabriel, J., Nerud, F., Zadrazil, F., 2000. Influence of cadmium and mercury on activities of lignolytic enzimes and degradation of polycyclic aromatic hydrocarbons by Pleurotus ostreatus in soil. Appl. Environ. Microbiol. 66, 2471–2478. https://doi.org/10.1128/AEM.66.6.2471-2478.2000

Bao, L., Maruya, K.A., Snyder, S.A., Zeng, E.Y., 2012. China's water pollution by persistent organic pollutants. Environ. Pollut. 163, 100–108. https://doi.org/10.1016/j.envpol.2011.12.022

Baumard, P., Budzinski, H., Michon, Q., Garrigues, P., Burgeot, T., Bellocq, J., 1998. Origin and Bioavailability of PAHs in the Mediterranean Sea from Mussel and Sediment Records. Estuar. Coast. Shelf Sci. 47, 77–90. https://doi.org/10.1006/ecss.1998.0337

Bechtel, A., Widera, M., Sachsenhofer, R.F., Gratzer, R., Luecke, A., Woszcyk, M., 2007. Biomarker and stable carbon isotope systematics of fossil wood from the second Lusatian lignite seam of the Lubstow deposit (Poland). Org. Geochem. 38, 1850–1864. https://doi.org/10.1016/j.orggeochem.2007.06.018

Behymer, T.D., Hites, R.A., 1988. Photolysis of polycyclic aromatic hydrocarbons adsorbed on fly ash. Environ. Sci. Technol. 22, 1311–1319. https://doi.org/10.1021/es00176a011

Bertilsson, S., Widenfalk, A., 2002. Photochemical degradation of PAHs in freshwaters and their impact on bacterial growth – influence of water chemistry. Hydrobiologia 469, 23–32. https://doi.org/10.1023/A:1015579628189

Besombes, J., Maitre, A., Patissier, O., Marchand, N., Chevron, N., Stoklov, M., Masclet, P., 2001. Particulate PAHs observed in the surrounding of a municipal incinerator. Atmos. Environ. 35, 6093–6104. https://doi.org/10.1016/S1352-2310(01)00399-5

Biswas, S., Verma, V., Schauer, J.J., Sioutas, C., 2009. Chemical speciation of PM emissions from heavy-duty diesel vehicles equipped with diesel particulate filter (DPF) and selective catalytic reduction (SCR) retrofits. Atmos. Environ. 43, 1917–1925. https://doi.org/10.1016/j.atmosenv.2008.12.040

Bloch, H., Rafiq, S., Salim, R., 2015. Economic growth with coal , oil and renewable energy consumption in

China : Prospects for fuel substitution. Econ. Model. 44, 104–115. https://doi.org/10.1016/j.econmod.2014.09.017

Boffetta, P., Jourenkova, N., Gustavsson, P., 1997. Cancer risk from occupational and environmental exposure to polycyclic aromatic hydrocarbons. Cancer Causes Control 8, 444–472. https://doi.org/10.1023/A:1018465507029

Bogdan, J.J., Budd, J.W., Eadie, B.J., Hornbuckle, K.C., 2002. The effect of a large resuspension event in southern Lake Michigan on the short-term cycling of organic contaminants. J. Great Lakes Res. 28, 338–351. https://doi.org/10.1016/S0380-1330(02)70589-3

Boonyatumanond, R., Murakami, M., Wattayakorn, G., Togo, A., Takada, H., 2007. Sources of polycyclic aromatic hydrocarbons (PAHs) in street dust in a tropical Asian mega-city , Bangkok , Thailand. Sci. Total Environ. 384, 420–432. https://doi.org/10.1016/j.scitotenv.2007.06.046

Borras, E., Tortajada-genaro, L.A., Vazquez, M., Zielinska, B., 2009. Polycyclic aromatic hydrocarbon exhaust emissions from different reformulated diesel fuels and engine operating conditions. Atmos. Environ. 43, 5944–5952. https://doi.org/10.1016/j.atmosenv.2009.08.010

Cai, Y., Gong, Z., Qin, B., 2012. Benthic macroinvertebrate community structure in Lake Taihu, China: Effects of trophic status, wind-induced disturbance and habitat complexity. J. Great Lakes Res. 38, 39–48. https://doi.org/10.1016/j.jglr.2011.12.009

Caliskan, H., Mori, K., 2017. Environmental, enviroeconomic and enhanced thermodynamic analyses of a diesel engine with diesel oxidation catalyst (DOC) and diesel particulate filter (DPF) after treatment systems. Energy 128, 128–144. https://doi.org/10.1016/j.energy.2017.04.014

Cao, Y., Zhang, E., Langdon, P., Liu, E., Shen, J., 2013. Spatially different nutrient histories recorded by multiple cores and implications for management in Taihu Lake, eastern China. Chinese Geogr. Sci. 23, 537–549. https://doi.org/10.1007/s11769-013-0625-6

CCME, 1999. Protocol for the derivation of canadian sediment quality guidelines for the protection of aquatic life.

Chan, C.K., Yao, X., 2008. Air pollution in mega cities in China. Atmos. Environ. 42, 1–42. https://doi.org/10.1016/j.atmosenv.2007.09.003

Chang, M.-C.O., Chow, J.C., Watson, J.G., Hopke, P.K., Yi, S.-M., England, G.C., Chang, O., 2004. Measurement of Ultrafine Particle Size Distributions from Coal-, Oil-, and Gas-Fired Stationary Combustion Sources. J. Air Waste Manage. Assoc. 54, 1494–1505. https://doi.org/10.1080/10473289.2004.10471010org/10.1080/10473289.2004.10471010

Chang, S., Zhuo, J., Meng, S., Qin, S., Yao, Q., 2016. Clean Coal Technologies in China: Current Status and Future Perspectives. Engineering 2, 447–459. https://doi.org/10.1016/j.eng.2016.04.015

Chen, H., Teng, Y., Wang, J., 2012. Source apportionment of polycyclic aromatic hydrocarbons (PAHs) in surface sediments of the Rizhao coastal area (China) using diagnostic ratios and factor analysis with nonnegative constraints. Sci. Total Environ. 414, 293–300. https://doi.org/10.1016/j.scitotenv.2011.10.057

Chen, M., Cui, J., Lin, J., Ding, S., Gong, M., Ren, M., Tsang, D.C.W., 2018. Successful control of internal phosphorus loading after sediment dredging for 6 years: A field assessment using high-resolution sampling techniques. Sci. Total Environ. 616–617, 927–936. https://doi.org/10.1016/j.scitotenv.2017.10.227

Chen, M., Liu, W., Tao, X., 2013. Evolution and assessment on China's urbanization 1960-2010: Under-urbanization or over-urbanization? Habitat Int. 38, 25–33. https://doi.org/10.1016/j.habitatint.2012.09.007

Chen, W., Xu, R., 2010. Clean coal technology development in China. Energy Policy 38, 2123–2130. https://doi.org/10.1016/j.enpol.2009.06.003

Chen, X., Zong, Y., Zhang, E., Xu, J., Li, S., 2001. Human impacts on the Changjiang ž Yangtze / River basin , China , with special reference to the impacts on the dry season water discharges into the sea. geomorphology 41, 111–123. https://doi.org/10.1016/S0169-555X(01)00109-X

Chen, Y., Bi, X., Mai, B., Sheng, G., Fu, J., 2004. Emission characterization of particulate/gaseous phases and size association for polycyclic aromatic hydrocarbons from residential coal combustion. Fuel 83, 781–790. https://doi.org/10.1016/j.fuel.2003.11.003

Chen, Y., Sheng, G., Bi, X., Feng, Y., Mai, B., Fu, J., 2005. Emission factors for carbonaceous particles and polycyclic aromatic hydrocarbons from residential coal combustion in China. Environ. Sci. Technol. 39, 1861–1867. https://doi.org/10.1021/es0493650

Cornelissen, G., Rigterink, H., Ferdinandy, M.M.A., Noort, P.C.M. Van, 1998. Rapidly Desorbing Fractions of PAHs in Contaminated Sediments as a Predictor of the Extent of Bioremediation. Environ. Sci. Technol 32, 966–970. https://doi.org/10.1021/es9704038

Couillard, C.M., Lee, K., Legare, B., King, T.L., 2005. Effect of dispersant on the composition of the water-accommodated fraction of crude oil and its toxicity to larval marine fish. Environ. Toxicol. Chem. 24, 1496–1504. https://doi.org/10.1897/04-267R.1

Crompton, P., Wu, Y., 2005. Energy consumption in China: Past trends and future directions. Energy Econ. 27, 195–208. https://doi.org/10.1016/j.eneco.2004.10.006

Dachs, J., Eisenreich, S.J., 2000. Adsorption onto Aerosol Soot Carbon Dominates Gas-Particle Partitioning of Polycyclic Aromatic Hydrocarbons. Environ. Sci. Technol 34, 3690–3697. https://doi.org/10.1021/es991201+

Demircioglu, E., Sofuoglu, A., Odabasi, M., 2011. Particle-phase dry deposition and air – soil gas exchange of polycyclic aromatic hydrocarbons (PAHs) in Izmir , Turkey. J. Hazard. Mater. 186, 328–335. https://doi.org/10.1016/j.jhazmat.2010.11.005

Deng, H., Peng, P., Huang, W., Song, J., 2006. Distribution and loadings of polycyclic aromatic hydrocarbons in the Xijiang River in Guangdong, South China. Chemosphere 64, 1401–1411. https://doi.org/10.1016/j.chemosphere.2005.12.027

Dennis Wei, Y., Cindy Fan, C., 2000. The Professional Geographer Regional Inequality in China: A Case Study of Jiangsu Province Regional Inequality in China: A Case Study of Jiangsu Province*. Prof. Geogr. 523, 455–469. https://doi.org/10.1111/0033-0124.00238

Dhananjayan, V., Muralidharan, S., Peter, V.R., 2012. Occurrence and Distribution of Polycyclic Aromatic Hydrocarbons in Water and Sediment Collected along the Harbour Line, Mumbai, India. Int. J. Oceanogr. 2012, 1–7. https://doi.org/10.1155/2012/403615

Díez, M.A., Alvarez, R., Barriocanal, C., 2002. Coal for metallurgical coke production: Predictions of coke quality and future requirements for cokemaking. Int. J. Coal Geol. 50, 389–412. https://doi.org/10.1016/S0166-5162(02)00123-4

Domingo, J.L., Nadal, M., 2015. Human dietary exposure to polycyclic aromatic hydrocarbons : A review of the scientific literature. Food Chem. Toxicol. 86, 144–153. https://doi.org/10.1016/j.fct.2015.10.002

Dong, X., Bennion, H., Battarbee, R., Yang, X., Yang, H., Liu, E., 2008. Tracking eutrophication in Taihu Lake using the diatom record: potential and problems. J. Paleolimnol. 40, 413–429. https://doi.org/10.1007/s10933-007-9170-6

Duan, H., Loiselle, S.A., Zhu, L., Feng, L., Zhang, Y., Ma, R., 2015. Distribution and incidence of algal blooms in Lake Taihu. Aquat. Sci. 77, 9–16. https://doi.org/10.1007/s00027-014-0367-2

Duan, H., Ma, R., Xu, X., Kong, F., Zhang, S., Kong, W., Hao, J., Shang, L., 2009. Two-decade reconstruction of algal blooms in China's Lake Taihu. Environ. Sci. Technol. 43, 3522–3528. https://doi.org/10.1021/es8031852

Erickson, D.C., Loehr, R.C., Neuhauser, E.F., 1993. PAH loss during bioremediation of manufactured gas plant site soils. Water Res. 27, 911–919. https://doi.org/10.1016/0043-1354(93)90157-D

Esteve, W., Budzinski, H., Villenave, E., 2006. Relative rate constants for the heterogeneous reactions of NO 2 and OH radicals with polycyclic aromatic hydrocarbons adsorbed on carbonaceous particles. Part 2: PAHs adsorbed on diesel particulate exhaust SRM 1650a. Atmos. Environ. 40, 201–211. https://doi.org/10.1016/j.atmosenv.2005.07.053

Esteve, W., Budzinski, H., Villenave, E., 2004. Relative rate constants for the heterogeneous reactions of OH, NO2and NO radicals with polycyclic aromatic hydrocarbons adsorbed on carbonaceous particles. Part 1: PAHs adsorbed on 1-2 μm calibrated graphite particles. Atmos. Environ. 38, 6063–6072. https://doi.org/10.1016/j.atmosenv.2004.05.059

Fan, C., Shiue, J., Wu, Cheng-yi, Wu, Cheng-yu, 2011. Perylene dominance in sediments from a subtropical high mountain lake. Org. Geochem. 42, 116–119. https://doi.org/10.1016/j.orggeochem.2010.10.008

Fan, C.C., 1995. Of Belts and Ladders: State Policy and Uneven Regional Development in Post-Mao China. Ann. Assoc. Am. Geogr. 85, 421–449. https://doi.org/10.1111/j.1467-8306.1995.tb01807.x

Feng, T., Sun, L., Zhang, Y., 2009. The relationship between energy consumption and economic structure in China. Energy Policy 37, 5475–5483. https://doi.org/10.1016/j.enpol.2009.08.008

Fernandez, P., Grimalt, J.O., Vilanova, R.M., 2002. Atmospheric Gas-Particle Partitioning of Polycyclic Aromatic Hydrocarbons in High Mountain Regions of Europe. Environ. Sci. Technol 36, 1162–1168. https://doi.org/10.1021/es010190t

Ferrey, M.L., Hamilton, C.M., Backe, W.J., Anderson, K.E., 2018. Pharmaceuticals and other anthropogenic chemicals in atmospheric particulates and precipitation. Sci. Total Environ. 612, 1488–1497. https://doi.org/10.1016/j.scitotenv.2017.06.201

Fisher, T.T., Law, R.J., Rumney, H.S., Kirby, M.F., Kelly, C., 2011. Towards a scheme of toxic equivalency factors (TEFs) for the acute toxicity of PAHs in sediment. Ecotoxicol. Environ. Saf. 74, 2245–2251. https://doi.org/10.1016/j.ecoenv.2011.07.023

Geyer, H., Politzki, G., Freitag, D., 1984. Prediction of ecotoxicological behaviour of chemicals: relationship between n-octanol/water partirion coefficient and bioaccumulation of organic chemicals by alga chlorella. Chemosphere 13, 269–284. https://doi.org/10.1016/0045-6535(84)90134-6

Guigue, C., Tedetti, M., Ferretto, N., Garcia, N., Méjanelle, L., Goutx, M., 2014. Spatial and seasonal variabilities of dissolved hydrocarbons in surface waters from the Northwestern Mediterranean Sea : Results from one year intensive sampling. Sci. Total Environ. 466–467, 650–662. https://doi.org/10.1016/j.scitotenv.2013.07.082

Guigue, C., Tedetti, M., Giorgi, S., Goutx, M., 2011. Occurrence and distribution of hydrocarbons in the surface microlayer and subsurface water from the urban coastal marine area off Marseilles , Northwestern Mediterranean Sea. Mar. Pollut. Bull. 62, 2741–2752. https://doi.org/10.1016/j.marpolbul.2011.09.013

Guo, W., He, M., Yang, Z., Lin, C., Quan, X., 2011. Aliphatic and polycyclic aromatic hydrocarbons in the Xihe River , an urban river in China ' s Shenyang City : Distribution and risk assessment. J. Hazard. Mater. 186, 1193–1199. https://doi.org/10.1016/j.jhazmat.2010.11.122

Haller, L., Tonolla, M., Zopfi, J., Peduzzi, R., Wildi, W., Poté, J., 2011. Composition of bacterial and archaeal communities in freshwater sediments with different contamination levels (Lake Geneva, Switzerland). Water Res. 45, 1213–1228. https://doi.org/10.1016/j.watres.2010.11.018

Han, D., Currell, M.J., 2017. Persistent organic pollutants in China ' s surface water systems. Sci. Total Environ. 580, 602–625. https://doi.org/10.1016/j.scitotenv.2016.12.007

Han, D., Currell, M.J., Cao, G., 2016. Deep challenges for China ' s war on water pollution *. Environ. Pollut. 218, 1222–1233. https://doi.org/10.1016/j.envpol.2016.08.078

Hanedar, A., Alp, K., Kaynak, B., Baek, J., Avsar, E., Odman, M.T., 2011. Concentrations and sources of PAHs at three stations in Istanbul, Turkey. Atmos. Res. 99, 391–399. https://doi.org/10.1016/j.atmosres.2010.11.017

Haritash, A.K., Kaushik, C.P., 2009. Biodegradation aspects of Polycyclic Aromatic Hydrocarbons (PAHs): A review. J. Hazard. Mater. 169, 1–15. https://doi.org/10.1016/j.jhazmat.2009.03.137

Hatzinger, P.B., Alexander, M., 1995. Effect of Aging of Chemicals in Soil on Their Biodegradability and Extiactability. Environ. Sci. Technol 29, 537–545. https://doi.org/10.1021/es00002a033

Helble, J.J., Sarofim, A.F., 1989. Influence of char fragmentation on ash particle size distributions. Combust. Flame 76, 183–196. https://doi.org/10.1016/0010-2180(89)90066-7

Herrerias, M.J., Ordoñez, J., 2012. New evidence on the role of regional clusters and convergence in China (1952-2008). China Econ. Rev. 23, 1120–1133. https://doi.org/10.1016/j.chieco.2012.08.001

Herrington, J.S., Hays, M.D., George, B.J., Baldauf, R.W., 2012. The effects of operating conditions on semivolatile organic compounds emitted from light-duty , gasoline-powered motor vehicles. Atmos. Environ. 54, 53–59. https://doi.org/10.1016/j.atmosenv.2012.02.043

Hites, R.A., Laflamme, R.E., Windsor, J.J.G., Farrington, J.W., Deuser, W.G., 1980. Poiycyclic aromatic hydrocarbons in an anoxic sediment core from the Pettaquamscutt River (Rhode Island , U . S . A .). Geochim. Cosmochim. Acta 44, 873–878. https://doi.org/10.1016/0016-7037(80)90267-7

Hollert, H., Crawford, S.E., Brack, W., Brinkmann, M., Fischer, E., Hartmann, K., Keiter, S., Ottermanns, R., Ouellet, J.D., Rinke, K., Rösch, M., Roß-nickoll, M., Schäffer, A., Schüth, C., Schulze, T., Schwarz, A., Seiler, T., Wessels, M., Hinderer, M., Schwalb, A., 2018. Looking back - Looking forward : A novel multi-time slice weight-of- evidence approach for de fi ning reference conditions to assess the impact of human activities on lake systems Signal generation : Climate Signal transformation : Control by filters Dire. Sci. Total Environ. 626, 1036–1046. https://doi.org/10.1016/j.scitotenv.2018.01.113

Horbach, J., Chen, Q., Rennings, K., Vögele, S., 2014. Do lead markets for clean coal technology follow market demand? A case study for China, Germany, Japan and the US. Environ. Innov. Soc. Transitions 10, 42–58. https://doi.org/10.1016/j.eist.2013.08.002

Hu, J.-L., Wang, S.-C., 2006. Total-factor energy efficiency of regions in China. Energy Policy 34, 3206–3217. https://doi.org/10.1016/j.enpol.2005.06.015

Hu, L., Hu, W., Zhai, S., Wu, H., 2010. Effects on water quality following water transfer in Lake Taihu, China. Ecol. Eng. 36, 471–481. https://doi.org/10.1016/j.ecoleng.2009.11.016

Huang, V., Leung, Y., 2002. Analysing regional industrialisation in Jiangsu province using geographically weighted regression. J. Geogr. Syst. 4, 233–249. https://doi.org/10.1007/s101090200081

Jenkins, B.M., Jones, D.A., Turn, S.Q., Williams, R.B., 1996. Particle concentrations, gas-particle partitioning, and species intercorrelations for polycyclic aromatic hydrocarbons (PAH) emitted during biomass burning. Atmos. Environ. 30, 3825–3835. https://doi.org/10.1016/1352-2310(96)00084-2

Jiang, G., Shi, J., Feng, X., 2006. Merccury pollution in China. Am. Chem. Soc. 3672–3678. https://doi.org/10.1021/es062707c

Jiang, W., Zhang, L., 2005. China energy consumption change and its spatial-temporal effect analysis. J. Liaoning Tech. Univ. (Natural Sci. Ed. 24, 612–615. https://doi.org/1008-0562(2005)04-0612-04

Jiang, X., Jin, X., Yao, Y., Li, L., Wu, F., 2008. Effects of biological activity, light, temperature and oxygen on phosphorus release processes at the sediment and water interface of Taihu Lake, China. Water Res. 42, 2251–2259. https://doi.org/10.1016/j.watres.2007.12.003

Jiang, X., Wang, W., Wang, S., Zhang, B., Hu, J., 2012. Initial identification of heavy metals contamination in Taihu Lake, a eutrophic lake in China. J. Environ. Sci. 24, 1539–1548. https://doi.org/10.1016/S1001-0742(11)60986-8

Jin, X., Wang, S., Pang, Y., Wu, F., 2006. Phosphorus fractions and the effect of pH on the phosphorus release of the sediments from different trophic areas. Environ. Pollut. 139, 288–295. https://doi.org/10.1016/j.envpol.2005.05.010

Jones, K.C., Voogt, P. de, 1999. Persistent organic pollutants (POPs): state of the science. Environ. Pollut. 100, 209–221. https://doi.org/10.1016/S0269-7491(99)00098-6

Jongeneelen, F.J., 1994. Biological monitoring of environmental exposure to polycyclic aromatic hydrocarbons ; 1-hydroxypyrene in urine of people. Toxicol. Lett. 72, 205–211. https://doi.org/10.1016/0378-4274(94)90030-2

Juhasz, A.L., Britz, M.L., Stanley, G.A., 1997. Degradation of fluoranthene, pyrene, benz [a] anthracene and dibenz [a,h] anthracene by Burkholderia cepacia. J. Appl. Microbiol. 83, 189–198. https://doi.org/10.1046/j.1365-2672.1997.00220.x

Kabziński, A.K.M., Cyran, J., Juszczak, R., 2002. Determination of Polycyclic Aromatic Hydrocarbons in Water (Including Drinking Water) of Łódź. Polish J. Environ. Stud. 11, 695–706.

Kafilzadeh, F., 2015. Distribution and sources of polycyclic aromatic hydrocarbons in water and sediments of the Soltan Abad River, Iran. Egypt. J. Aquat. Res. 41, 227–231. https://doi.org/10.1016/j.ejar.2015.06.004

Kalf, D.F., Crommentuijn, T., VAN DE Plassche, E.J., 1997. Environmental Quality Objectives for 10 Polycyclic Aromatic Hydrocarbons (PAHs). Ecotoxicol. Environ. Saf. 36, 89–97. https://doi.org/10.1006/eesa.1996.1495

Kamens, R.M., Guo, Z., Fulcher, J.N., Bell, D.A., 1988. Influence of Humidity, Sunlight, and Temperature on the Daytime Decay of Polyaromatic Hydrocarbons on Atmospheric Soot Particles. Environ. Sci. Technol. 22, 103–108. https://doi.org/10.1021/es00166a012

Kauppr, H., Mclachlan, M.S., 1999. Atmospheric particle size distributions of polychlorinated dibenzo-p-

dioxins and dibenzofurans (PCDD/Fs) and polycyclic aromatic hydrocarbons (PAHs) and their implications for wet and dry deposition. Atmos. Environ. 33, 85–95. https://doi.org/https://doi.org/10.1016/S1352-2310(98)00129-0

Ke, L., Wong, T.W.Y., Wong, Y.S., Tam, N.F.Y., 2002. Fate of polycyclic aromatic hydrocarbon (PAH) contamination in a mangrove swamp in Hong Kong following an oil spill. Mar. Pollut. Bull. 45, 339–347. https://doi.org/10.1016/S0025-326X(02)00117-0

Kim, D., Kumfer, B.M., Anastasio, C., Kennedy, I.M., Young, T.M., 2009. Environmental aging of polycyclic aromatic hydrocarbons on soot and its effect on source identification. Chemosphere 76, 1075–1081. https://doi.org/10.1016/j.chemosphere.2009.04.031

Kim, K.-H., Jahan, S.A., Kabir, E., Brown, R.J.C., 2013. A review of airborne polycyclic aromatic hydrocarbons (PAHs) and their human health effects. Environ. Int. 60, 71–80. https://doi.org/10.1016/J.ENVINT.2013.07.019

Kozak, K., Ruman, M., Kosek, K., Karasinski, G., Stachnik, L., Polkowska, Z., 2017. Impact of Volcanic Eruptions on the Occurrence of PAHs Compounds in the Aquatic Ecosystem of the Southern Part of West Spitsbergen (Hornsund Fjord, Svalbard). Water 9, 1–21. https://doi.org/10.3390/w9010042

Krauss, M., Wilcke, W., Martius, C., Bandeira, A.G., Garcia, M.V.B., Amelung, W., 2005. Atmospheric versus biological sources of polycyclic aromatic hydrocarbons (PAHs) in a tropical rain forest environment. Environ. Pollut. 135, 143–154. https://doi.org/10.1016/j.envpol.2004.09.012

Kuśmierz, M., Oleszczuk, P., Kraska, P., Pałys, E., Andruszczak, S., 2016. Persistence of polycyclic aromatic hydrocarbons (PAHs) in biochar-amended soil. Chemosphere 146, 272–279. https://doi.org/10.1016/j.chemosphere.2015.12.010

Lang, J., Cheng, S., Zhou, Y., Zhang, Y., Wang, G., 2014. Air pollutant emissions from on-road vehicles in China, 1999-2011. Sci. Total Environ. 496, 1–10. https://doi.org/10.1016/j.scitotenv.2014.07.021

Lee, H.J., Villaume, J., Cullen, D.C., Kim, B.C., Gu, M.B., 2003. Monitoring and classification of PAH toxicity using an immobilized bioluminescent bacteria. Biosens. Bioelectron. 18, 571–577. https://doi.org/10.1016/S0956-5663(03)00039-3

Lee, J.Y., Kim, Y.P., 2007. Source apportionment of the particulate PAHs at Seoul, Korea: Impact of long range transport to a megacity. Atmos. Chem. Phys. 7, 3587–3596. https://doi.org/10.5194/acp-7-3587-2007

Lee, L.S., Hagwall, M., Delflno, J.J., Raot, P.S.C., 1992a. Partitioning of Polycyclic Aromatic Hydrocarbons from Diesel Fuel into Water. Environ. Sci. Techno 26, 2104–2110. https://doi.org/10.1021/es00035a005

Lee, L.S., Rao, P.S.C., Okuda, I., 1992b. Equilibrium Partitioning of Polycyclic Aromatic Hydrocarbons from Coal Tar into Water. Environ. Sci. Techno 2115, 2110–2115. https://doi.org/10.1021/es00035a006

Lei, B., Kang, J., Wang, X., Yu, Y., Zhang, X., Wen, Y., Wang, Y., 2014. The levels of PAHs and aryl hydrocarbon receptor effects in sediments of Taihu Lake , China. Env. Sci Pollut Res 21, 6547–6557. https://doi.org/10.1007/s11356-014-2542-3

Lei, P., Zhang, H., Shan, B., 2016a. Vertical records of sedimentary PAHs and their freely dissolved fractions in porewater profiles from the northern bays of Taihu Lake, Eastern China. RSC Adv. 6, 98835–98844. https://doi.org/10.1039/C6RA11180G

Lei, P., Zhang, H., Shan, B., Zhang, B., 2016b. Distribution , diffusive fluxes , and toxicity of heavy metals and PAHs in pore water profiles from the northern bays of Taihu Lake. Environ. Sci. Pollut. Res. 23, 22072–22083. https://doi.org/10.1007/s11356-016-7467-6

Leister, D.L., Baker, J.E., 1994. Atmospheric contaminants deposition of organic to the chesapeake. Atmos. Environ. 28, 1499–1520. https://doi.org/10.1016/1352-2310(94)90210-0

Li, C.K., Kamens, R.M., 1993. The use of polycyclic aromatic hydrocarbons as source signatures in receptor modeling. Atmos. Environ. Part A. Gen. Top. 27, 523–532. https://doi.org/10.1016/0960-1686(93)90209-H

Li, G., Xia, X., Yang, Z., Wang, R., Voulvoulis, N., 2006. Distribution and sources of polycyclic aromatic hydrocarbons in the middle and lower reaches of the Yellow River, China. Environ. Pollut. 144, 985–993. https://doi.org/10.1016/j.envpol.2006.01.047

Li, J., Shang, X., Zhao, Z., Tanguay, R.L., Dong, Q., Huang, C., 2010. Polycyclic aromatic hydrocarbons in

water , sediment , soil , and plants of the Aojiang River waterway in Wenzhou , China. J. Hazard. Mater. 173, 75–81. https://doi.org/10.1016/j.jhazmat.2009.08.050

Li, P., Cao, J., Diao, X., Wang, B., Zhou, H., Han, Q., Zheng, P., 2015. Spatial distribution , sources and ecological risk assessment of polycyclic aromatic hydrocarbons in surface seawater from Yangpu Bay , China. Mar. Pollut. Bull. 93, 53–60. https://doi.org/10.1016/j.marpolbul.2015.02.015

Li, Y., Li, P., Ma, W., Song, Q., Zhou, H., Han, Q., Diao, X., 2015. Spatial and temporal distribution and risk assessment of polycyclic aromatic hydrocarbons in surface seawater from the Haikou Bay , China. Mar. Pollut. Bull. 92, 244–251. https://doi.org/10.1016/j.marpolbul.2014.12.014

Li, Y., Wei, J., Gao, X., Chen, D., Weng, S., Du, W., Wang, W., Wang, J., Tang, C., Zhang, S., 2018. Turbulent bursting and sediment resuspension in hyper-eutrophic Lake Taihu, China. J. Hydrol. 565, 581–588. https://doi.org/10.1016/j.jhydrol.2018.08.067

Li, Z., Ma, Z., Jan, T., Kuijp, V. Der, Yuan, Z., Huang, L., 2014. A review of soil heavy metal pollution from mines in China : Pollution and health risk assessment. Sci. Total Environ. 468–469, 843–853. https://doi.org/10.1016/j.scitotenv.2013.08.090

Liu, C., Shen, Q., Zhou, Q., Fan, C., Shao, S., 2015. Precontrol of algae-induced black blooms through sediment dredging at appropriate depth in a typical eutrophic shallow lake. Ecol. Eng. 77, 139–145. https://doi.org/10.1016/j.ecoleng.2015.01.030

Liu, C., Zhong, J., Wang, J., Zhang, L., Fan, C., 2016. Fifteen-year study of environmental dredging effect on variation of nitrogen and phosphorus exchange across the sediment-water interface of an urban lake. Environ. Pollut. 219, 639–648. https://doi.org/10.1016/j.envpol.2016.06.040

Liu, E., Birch, G.F., Shen, J., Yuan, H., Zhang, E., Cao, Y., 2012. Comprehensive evaluation of heavy metal contamination in surface and core sediments of Taihu Lake, the third largest freshwater lake in China. Env. Earth Sci 67, 39–51. https://doi.org/10.1007/s12665-011-1478-x

Liu, E., Ji, S., Zhu, Y., Xia, W., Zhu, G., 2004. Source Analysis of Heavy Metals in Surface Sediments of Lake Taihu. J. Lake Sci. 16, 113–119.

Liu, G., Zhang, G., Jin, Z., Li, J., 2009. Sedimentary record of hydrophobic organic compounds in relation to regional economic development: A study of Taihu Lake, East China. Environ. Pollut. 157, 2994–3000. https://doi.org/10.1016/J.ENVPOL.2009.05.056

Liu, G., Zhang, Z., Liu, H., Zhong, J., Yan, S., Fan, C., 2010. Effects of sediment dredging on benthos community structure and water quality in Zhushan Bay. J. Environ. Sci. 31, 2645–2651. https://doi.org/10.13227/j.hjkx.2010.11.016

Liu, H., 2008. Time-dependent analysis of relation between oil consumption and economic growth in China. J. Northeast. Univ. (Social Sci. 10, 121–126. https://doi.org/1008-3758(2008) 02-0121-06

Liu, J., Diamond, J., 2005. China ' s environment in a globalizing world. Nature 435, 1179–1186.

Liu, K., Xie, W., Zhao, Z.B., Pan, W.P., Riley, J.T., 2000. Investigation of polycyclic aromatic hydrocarbons in fly ash from fluidized bed combustion systems. Environ. Sci. Technol. 34, 2273–2279. https://doi.org/10.1021/es990944s

Liu, M., Feng, J., Hu, P., Tan, L., Zhang, X., Sun, J., 2016. Spatial-temporal distributions , sources of polycyclic aromatic hydrocarbons (PAHs) in surface water and suspended particular matter from the upper reach of Huaihe River , China. Ecol. Eng. 95, 143–151. https://doi.org/10.1016/j.ecoleng.2016.06.045

Liu, S., Liu, X., Liu, M., Yang, B., Cheng, L., Li, Y., Qadeer, A., 2016. Levels , sources and risk assessment of PAHs in multi-phases from urbanized river network system in Shanghai. Environ. Pollut. J. 219, 555–567. https://doi.org/10.1016/j.envpol.2016.06.010

Liu, S., Wang, C., Zhang, S., Liang, J., Chen, F., Zhao, K., 2012. International Journal of Coal Geology Formation and distribution of polycyclic aromatic hydrocarbons (PAHs) derived from coal seam combustion : A case study of the Ulanqab lignite from Inner Mongolia , northern China. Int. J. Coal Geol. 90–91, 126–134. https://doi.org/10.1016/j.coal.2011.11.005

Liu, Wen X, Dou, H., Wei, Z.C., Chang, B., Qiu, W.X., Liu, Y., Tao, S., 2009. Emission characteristics of polycyclic aromatic hydrocarbons from combustion of different residential coals in North China. Sci. Total Environ. 407, 1436–1446. https://doi.org/10.1016/j.scitotenv.2008.10.055

Liu, Wen X., Dou, H., Wei, Z.C., Chang, B., Qiu, W.X., Liu, Y., Tao, S., 2009. Emission characteristics of polycyclic aromatic hydrocarbons from combustion of different residential coals in North China. Sci. Total Environ. 407, 1436–1446. https://doi.org/10.1016/J.SCITOTENV.2008.10.055

Liu, Y., Chen, L., Huang, Q., Li, W., Tang, Y., Zhao, J., 2009. Source apportionment of polycyclic aromatic hydrocarbons (PAHs) in surface sediments of the Huangpu River, Shanghai, China. Sci. Total Environ. 407, 2931–2938. https://doi.org/10.1016/j.scitotenv.2008.12.046

Liu, Y., Chen, L., Zhao, J., Wei, Y., Pan, Z., Meng, X., Huang, Q., Li, W., 2010. Polycyclic aromatic hydrocarbons in the surface soil of Shanghai, China: Concentrations, distribution and sources. Org. Geochem. 41, 355–362. https://doi.org/10.1016/j.orggeochem.2009.12.009

Lohmann, R., Lammel, G., 2004. Adsorptive and absorptive contributions to the gas-particle partitioning of polycyclic aromatic hydrocarbons: State of knowledge and recommended parametrization for modeling. Environ. Sci. Technol. 38, 3793–3803. https://doi.org/10.1021/es035337q

Long, G., Ng, M.K., 2001. The political economy of intra-provincial disparities in post-reform China: A case study of Jiangsu province. Geoforum 32, 215–234. https://doi.org/10.1016/S0016-7185(00)00030-0

Louda, J.W., Baker, E.W., 1984. Perylene occurrence, alkylation and possible sources in deep-ocean sediments. Geochim. Cosmochim. Acta 48, 1043–1058. https://doi.org/10.1016/0016-7037(84)90195-9

Luo, L., Qin, B., Zhu, G., 2004. Sediment distribution pattern mapped from the combination of objective analysis and geostatistics in the large shallow Taihu Lake, China. J. Environ. Sci. 16, 908–911.

Ma, Y., Lei, Y.D., Xiao, H., Wania, F., Wang, W., 2010. Critical Review and Recommended Values for the Physical-Chemical Property Data of 15 Polycyclic Aromatic Hydrocarbons at 25 ° C. J. Chem. Eng. Data 55, 819–825. https://doi.org/10.1021/je900477x

Mackay, D., Callcott, D., 1998. Partitioning and Physical Chemical Properties of PAHs, in: In PAHs and Related Compounds. pp. 325–345. https://doi.org/10.1007/978-3-540-49697-7_8

Main, H.H., Friedlander, S.K., 1990. Dry Deposition of Atmospheric Aerosols by Dual Tracer Method--I. Area Source. Atmos. Environ. 24, 103–108. https://doi.org/10.1016/0960-1686(90)90445-S

Maricq, M.M., Podsiadlik, H.D., Chase, E.R., 1999. Gasoline Vehicle Particle Size Distributions: Comparison of Steady State, FTP, and US06 Measurements. Environ. Sci. Technol. 33(12), 2007–2015. https://doi.org/10.1021/es981005n

Marr, L.C., Kirchstetter, T.W., Harley, R.A., Miguel, A.H., Hering, S. V., Hammond, S.K., 1999. Characterization of polycyclic aromatic hydrocarbons in motor vehicle fuels and exhaust emissions. Environ. Sci. Technol. 33, 3091–3099. https://doi.org/10.1021/es981227l

Marynowski, L., Smolarek, J., Bechtel, A., Philippe, M., Kurkiewicz, S., Simoneit, B.R.T., 2013. Perylene as an indicator of conifer fossil wood degradation by wood-degrading fungi. Org. Geochem. 59, 143–151. https://doi.org/10.1016/j.orggeochem.2013.04.006

Masclet, P., Bresson, M.A., Mouvier, G., 1987. Polycyclic aromatic hydrocarbons emitted by power stations, and influence of combustion conditions. Fuel 66, 556–562. https://doi.org/10.1016/0016-2361(87)90163-3

Masclet, P., Mouvier, G., Nikolaou, K., 1986. Relative decay index and sources of polycyclic aromatic hydrocarbons. Atmos. Environ. 20, 439–446. https://doi.org/10.1016/0004-6981(86)90083-1

Masclet, P., Pistikopoulos, P., Beyne, S., Mouvier, G., 1988. Long range transport and gas/particle distribution of polycyclic aromatic hydrocarbons at a remote site in the mediterranean sea. Atmos. Environ. 22, 639–550. https://doi.org/10.1016/0004-6981(88)90002-9

Mastral, A., Calle, M., Murillo, R., Garcia, T., Vinas, M., 1999. Influence on PAH emissions of the air flow in AFB coal combustion. Fuel 78, 1553–1557. https://doi.org/10.1016/S0016-2361(99)00079-4

Mastral, A.M., Callén, M.S., Garcia, T., 2000. Toxic organic emissions from coal combustion. Fuel Process. Technol. 67, 1–10. https://doi.org/10.1016/S0378-3820(00)00088-6

Mcdonald, J.D., Zielinska, B., Fujita, E.M., Sagebiel, J.C., Chow, J.C., Watson, J.G., 2000. Fine Particle and Gaseous Emission Rates from Residential Wood Combustion. Environ. Sci. Technol 34, 2080–2091. https://doi.org/10.1021/es9909632

McGroddy, S.E., Farrington, J.W., Gschwend, P.M., 1996. Comparison of the in Situ and Desorption Sediment−Water Partitioning of Polycyclic Aromatic Hydrocarbons and Polychlorinated Biphenyls.

Environ. Sci. Technol. 30, 172–177. https://doi.org/10.1021/es950218z

Mi, H., Lee, W., Wu, T., Lin, T., Wang, L., Chao, H., 1996. PAH emission from a gasoline-powered engine. J. Environ. Sci. Heal. . Part A Environ. Sci. Eng. Toxicol. 31, 1981–2003. https://doi.org/10.1080/10934529609376469

Mininni, G., Sbrilli, A., Guerriero, E., Rotatori, M., 2004. Polycyclic aromatic hydrocarbons formation in in sludge incineration by fluidised bed and rotary kiln furnace. Water. Air. Soil Pollut. 154, 3–18. https://doi.org/10.1023/B:WATE.0000022923.99488.c7

Montuori, P., Aurino, S., Garzonio, F., Sarnacchiaro, P., Nardone, A., Triassi, M., 2016. Distribution, sources and ecological risk assessment of polycyclic aromatic hydrocarbons in water and sediments from Tiber River and estuary, Italy. Sci. Total Environ. 566–567, 1254–1267. https://doi.org/10.1016/j.scitotenv.2016.05.183

Moody, J.D., Freeman, J.P., Doerge, D.R., Cerniglia, C.E., 2001. Degradation of Phenanthrene and Anthracene by Cell Suspensions of Mycobacterium sp. Strain PYR-1. Appl. Environ. Microbiol. 67, 1476–1483. https://doi.org/10.1128/AEM.67.4.1476-1483.2001

Muir, D.C.G., de Wit, C.A., 2010. Trends of legacy and new persistent organic pollutants in the circumpolar arctic: Overview, conclusions, and recommendations. Sci. Total Environ. 408, 3044–3051. https://doi.org/10.1016/j.scitotenv.2009.11.032

Mzoughi, N., Chouba, L., 2011. Distribution and partitioning of aliphatic hydrocarbons and polycyclic aromatic hydrocarbons between water, suspended particulate matter, and sediment in harbours of the West coastal of the Gulf of Tunis (Tunisia). J. Environ. Monit. 13, 689–698. https://doi.org/10.1039/c0em00616e

Nisbet, I.C.T., Lagoy, P.K., 1992. Toxic Equivalency Factors (TEFs) for Polycyclic Aromatic Hydrocarbons (PAHs). Regul. Toxicol. Pharmacol. 16, 290–300. https://doi.org/10.1016/0273-2300(92)90009-X

Pal, A., Gin, K.Y.H., Lin, A.Y.C., Reinhard, M., 2010. Impacts of emerging organic contaminants on freshwater resources: Review of recent occurrences, sources, fate and effects. Sci. Total Environ. 408, 6062–6069. https://doi.org/10.1016/j.scitotenv.2010.09.026

Patrolecco, L., Ademollo, N., Capri, S., Pagnotta, R., Polesello, S., 2010. Occurrence of priority hazardous PAHs in water , suspended particulate matter , sediment and common eels (Anguilla anguilla) in the urban stretch of the River Tiber (Italy). Chemosphere 81, 1386–1392. https://doi.org/10.1016/j.chemosphere.2010.09.027

Pelletier, M., Burgess, R.M., Ho, K.T., Kuhn, A., Mckinney, R.A., Ryba, S.A., 1997. Phototoxicity of individual polycyclic aromatic hydrocarbons and petroleum to marine invertebrate larvae and juveniles. Environ. Toxicol. Chem. 16, 2190–2199. https://doi.org/10.1002/etc.5620161029

Peng, X., Zhang, G., Zheng, L., Mai, B., Zeng, S., 2005. The vertical variations of hydrocarbon pollutants and organochlorine pesticide residues in a sediment core in Lake Taihu , East China. Geochemistry Explor. Environ. Anal. 5, 99–104. https://doi.org/10.1144/1467-7873/03-038

Pérez-tejeda, P., Vanes, C., Maestre, A., 1990. Solubility of Naphthalene in Water + Alcohol Solutions at Various Temperatures. J. Chem. Eng. Data 35, 244–246. https://doi.org/10.1021/je00061a007

Pergal, M.M., Tešić, Ž.L., Popović, A.R., 2013. Polycyclic aromatic hydrocarbons: Temperature driven formation and behavior during coal combustion in a coal-fired power plant. Energy and Fuels 27, 6273–6278. https://doi.org/10.1021/ef401467z

Perraudin, E., Ne Budzinski, H., Villenave, E., 2007. Identification and quantification of ozonation products of anthracene and phenanthrene adsorbed on silica particles. Atmos. Environ. 41, 6005–6017. https://doi.org/10.1016/j.atmosenv.2007.03.010

Phuleria, H.C., Geller, M.D., Fine, P.M., Sioutas, C., 2006. Size-resolved emissions of organic tracers from light- and heavy-duty vehicles measured in a California roadway tunnel. Environ. Sci. Technol. 40, 4109–4118. https://doi.org/10.1021/es052186d

Pierce, R.C., Katz, M., 1975. Dependency of polynuclear aromatic hydrocarbon content on size distribution of atmospheric aerosols. Environ. Sci. Technol. 9, 347–353. https://doi.org/10.1021/es60102a004

Pies, C., Hoffmann, B., Petrowsky, J., Yang, Y., Ternes, T.A., Hofmann, T., 2008. Characterization and source identification of polycyclic aromatic hydrocarbons (PAHs) in river bank soils. Chemosphere 72, 1594–1601. https://doi.org/10.1016/J.CHEMOSPHERE.2008.04.021

Qi, L., Yuan, Y., 2011. Characteristics and the behavior in electrostatic precipitators of high-alumina coal fly ash from the Jungar power plant, Inner Mongolia, China. J. Hazard. Mater. 192, 222–225. https://doi.org/10.1016/j.jhazmat.2011.05.012

Qi, T., Zhou, L., Zhang, X., Ren, X., 2012. Regional economic output and employment impact of coal-to-liquids (CTL) industry in China: An input-output analysis. Energy 46, 259–263. https://doi.org/10.1016/j.energy.2012.08.024

Qiao, M., Huang, S., Wang, Z., 2008. Partitioning Characteristics of PAHs Between Sediment and Water in a Shallow Lake *. J Soil Sediments 8, 69–73. https://doi.org/10.1065/jss2008.03.279

Qiao, M., Wang, C., Huang, S., Wang, D., Wang, Z., 2006. Composition , sources , and potential toxicological significance of PAHs in the surface sediments of the Meiliang Bay , Taihu Lake , China. Environ. Int. 32, 28–33. https://doi.org/10.1016/j.envint.2005.04.005

Qin, B., 2008. Lake Taihu, China: dynamics and environmental change. Springer Science & Business Media.

Qin, B., Hu, W., Gao, G., Luo, L., Zhang, J., 2004. Dynamics of sediment resus- pension and the conceptual schema of nutrient release in the large shallow Lake Taihu , China. Chinese Sci. Bull. 49, 54–64. https://doi.org/10.1360/03wd0174

Qin, B., Li, W., Zhu, G., Zhang, Y., Wu, T., Gao, G., 2015. Cyanobacterial bloom management through integrated monitoring and forecasting in large shallow eutrophic Lake Taihu (China). J. Hazard. Mater. 287, 356–363. https://doi.org/10.1016/j.jhazmat.2015.01.047

Qin, B., Xu, P., Wu, Q., Luo, L., Zhang, Y., 2007. Environmental issues of Lake Taihu, China. Kluwer Academic Publishers. https://doi.org/10.1007/s10750-006-0521-5

Qin, B., Zhu, G., Gao, G., Zhang, Y., Li, W., Paerl, H.W., Carmichael, W.W., 2010. A drinking water crisis in Lake Taihu, China: Linkage to climatic variability and lake management. Environ. Manage. 45, 105–112. https://doi.org/10.1007/s00267-009-9393-6

Qin, B., Zhu, G., Zhang, L., Luo, L., Gao, G., Gu, B., 2006. Estimation of internal nutrient release in large shallow Lake Taihu , China. Sci. China Ser. D Earth Sci. 49, 38–50. https://doi.org/10.1007/s11430-006-8104-x

Qin, N., He, W., Kong, X.Z., Liu, W.X., He, Q.S., Yang, B., Wang, Q.M., Yang, C., Jiang, Y.J., Jorgensen, S.E., Xu, F.L., Zhao, X.L., 2014. Distribution, partitioning and sources of polycyclic aromatic hydrocarbons in the water-SPM-sediment system of Lake Chaohu, China. Sci. Total Environ. 496, 414–423. https://doi.org/10.1016/j.scitotenv.2014.07.045

Qu, W., Dickman, M., Fan, C., Wang, S., Su, C., Zhang, L., Zou, H., 2002. Distribution , sources and potential toxicological significance of polycyclic aromatic hydrocarbons (PAHs) in Taihu Lake sediments , China. Hydrobiologia 485, 163–171. https://doi.org/10.1023/A:1021301909296

Readman, J.W., Fillmann, G., Tolosa, I., Bartocci, J., Villeneuve, J.P., Catinni, C., Mee, L.D., 2002. Petroleum and PAH contamination of the Black Sea. Mar. Pollut. Bull. 44, 48–62. https://doi.org/10.1016/S0025-326X(01)00189-8

Readman, J.W., Mantoura, R.F.C., Rhead, M.M., Brown, L., 1982. Aquatic distribution and heterotrophic degradation of Polycyclic Aromatic Hydrocarbons (PAH) in the Tamar Estuary. Estuar. Coast. Shelf Sci. 14, 369–389. https://doi.org/10.1016/S0272-7714(82)80009-7

Ren, G., Teng, Y., Ren, W., Dai, S., Li, Z., 2016. Pyrene dissipation potential varies with soil type and associated bacterial community changes. https://doi.org/10.1016/j.soilbio.2016.08.007

Rogge, W.F., Hildemann, L.M., Mazurek, M.A., Cass, G.R., Simoneit, B.R.T., 1993. Sources of Fine Organic Aerosol. 2. Noncatalyst and Catalyst-Equipped Automobiles and Heavy-Duty Diesel Trucks. Environ. Sci. Technol. 27, 636–651. https://doi.org/10.1021/es00041a007

Rowntree, K., Foster, I., 2012. A reconstruction of historical changes in sediment sources, sediment transfer and sediment yield in a small, semi-arid Karoo catchment, South Africa. Zeitschrift für Geomorphol. Suppl. Issues 56, 87–100. https://doi.org/10.1127/0372-8854/2012/s-00074

Sanseverino, J., Applegate, B.M., King, J.M.H., Sayler', G.S., 1993. Plasmid-Mediated Mineralization of Naphthalene, Phenanthrene, and Anthracene Downloaded from. Appl. Environ. Microbiol. 59, 1931–1937.

Sarria-villa, R., Ocampo-duque, W., Páez, M., Schuhmacher, M., 2016. Presence of PAHs in water and

sediments of the Colombian Cauca River during heavy rain episodes , and implications for risk assessment. Sci. Total Environ. 540, 455–465. https://doi.org/10.1016/j.scitotenv.2015.07.020

Schauer, J.J., Kleeman, M.J., Cass, G.R., Simoneit, B.R.T., 2002. Measurement of emissions from air pollution sources. 5. C1 - C32 organic compounds from gasoline-powered motor vehicles. Environ. Sci. Technol. 36, 1169–1180. https://doi.org/10.1021/es0108077

Schützendübel, A., Majcherczyk, A., Johannes, C., Hüttermann, A., 1999. Degradation of fluorene, anthracene, phenanthrene, fluoranthene, and pyrene lacks connection to the production of extracellular enzymes by Pleurotus ostreatus and Bjerkandera adusta. Int. Biodeterior. Biodegrad. 43, 93–100. https://doi.org/10.1016/S0964-8305(99)00035-9

Shao, M., Tang, X., Zhang, Y., Li, W., 2006. City clusters in China air and surface water pollution. Front. Ecol. Environ. 4, 353–361. https://doi.org/10.1890/1540-9295(2006)004[0353:CCICAA]2.0.CO;2

Shen, G., Tao, S., Wei, S., Zhang, Y., Wang, R., Wang, B., Li, W., Shen, H., Huang, Y., Chen, Y., Chen, H., Yang, Y., Wang, W., Wang, X., Liu, W., Simonich, S.L.M., 2012. Emissions of Parent, Nitro, and Oxygenated Polycyclic Aromatic Hydrocarbons from Residential Wood Combustion in Rural China. Environ. Sci. Technol. 46, 8123–8130. https://doi.org/10.1021/es301146v

Shen, G., Wang, W., Yang, Y., Ding, J., Xue, M., Min, Y., Zhu, C., Shen, H., Li, W., Wang, B., Wang, R., Wang, X., Tao, S., Russell, A.G., 2011. Emissions of PAHs from indoor crop residue burning in a typical rural stove: Emission factors, size distributions, and gas-particle partitioning. Environ. Sci. Technol. 45, 1206–1212. https://doi.org/10.1021/es102151w

Shen, G., Wang, W., Yang, Y., Zhu, C., Min, Y., Xue, M., Ding, J., Li, W., Wang, B., Shen, H., Wang, R., Wang, X., Tao, S., 2010a. Emission factors and particulate matter size distribution of polycyclic aromatic hydrocarbons from residential coal combustions in rural Northern China. Atmos. Environ. 44, 5237–5243. https://doi.org/10.1016/j.atmosenv.2010.08.042

Shen, G., Wang, W., Yang, Y., Zhu, C., Min, Y., Xue, M., Ding, J., Li, W., Wang, B., Shen, H., Wang, R., Wang, X., Tao, S., 2010b. Emission factors and particulate matter size distribution of polycyclic aromatic hydrocarbons from residential coal combustions in rural Northern China. Atmos. Environ. 44, 5237–5243. https://doi.org/10.1016/j.atmosenv.2010.08.042

Shen, X., Ma, L.J.C., 2005. Privatization of rural industry and de facto urbanization from below in southern Jiangsu, China. Geoforum 36, 761–777. https://doi.org/10.1016/j.geoforum.2005.01.005

Shen, X., Yao, Z., Zhang, Q., Wagner, D.V., Huo, H., Zhang, Y., Zheng, B., He, K., 2015. Development of database of real-world diesel vehicle emission factors for China. J. Environ. Sci. (China) 31, 209–220. https://doi.org/10.1016/j.jes.2014.10.021

Shuttleworth, K.L., Cerniglia, C.E., 1995. Environmental Aspects of PAH Biodegradation. Appl. Biochem. Biotechnol. 54, 291–302. https://doi.org/10.1007/BF02787927

Silliman, J.E., Meyers, P.A., Eadie, B.J., 1998. Perylene : an indicator of alteration processes or precursor materials ? Org. Geochem. 29, 1737–1744. https://doi.org/10.1016/S0146-6380(98)00056-4

Silliman, J.E., Meyers, P.A., Eadie, B.J., Klump, V.J., 2001. A hypothesis for the origin of perylene based on its low abundance in sediments of Green Bay, Wisconsin. Chem. Geol. 177, 309–322. https://doi.org/10.1016/S0009-2541(00)00415-0

Slater, G.F., Benson, A.A., Marvin, C., Muir, D., 2013. PAH fluxes to Siskiwit revisited: Trends in fluxes and sources of pyrogenic PAH and perylene constrained via radiocarbon analysis. Environ. Sci. Technol. 47, 5066–5073. https://doi.org/10.1021/es400272z

Slmonich, S.L., Hites, R.A., 1994. Vegetation-Atmosphere Partitioning of Polycyclic Aromatic Hydrocarbons. Environ. Sci. Techno 28, 939–943. https://doi.org/10.1021/es00054a028

Sofowote, U.M., Hung, H., Rastogi, A.K., Westgate, J.N., Su, Y., Sverko, E., D'Sa, I., Roach, P., Fellin, P., Mccarry, B.E., 2010. The gas / particle partitioning of polycyclic aromatic hydrocarbons collected at a sub-Arctic site in Canada. Atmos. Environ. 44, 4919–4926. https://doi.org/10.1016/j.atmosenv.2010.08.028

Soma, Y., Tanaka, A., Soma, M., Kawai, T., 1996. Photosynthetic pigments and perylene in the sediments of southern basin of Lake Baikal. Org. Geochem. 24, 553–561. https://doi.org/10.1016/0146-6380(96)00036-8

Somtrakoon, K., Suanjit, S., Pokethitiyook, P., Kruatrachue, M., Lee, H., Upatham, S., 2008. Phenanthrene stimulates the degradation of pyrene and fluoranthene by Burkholderia sp. VUN10013. World J. Microbiol. Biotechnol. 24, 523–531. https://doi.org/10.1007/s11274-007-9503-7

Søndergaard, M., Kristensen, P., Jeppesen, E., 1992. Phosphorus release from resuspended sediment in the shallow and wind-exposed Lake Arresø, Denmark. Hydrobiologia 228, 91–99. https://doi.org/10.1007/BF00006480

Sun, J.H., Wang, G.L., Chai, Y., Zhang, G., Li, J., Feng, J., 2009. Distribution of polycyclic aromatic hydrocarbons (PAHs) in Henan Reach of the Yellow River, Middle China. Ecotoxicol. Environ. Saf. 72, 1614–1624. https://doi.org/10.1016/j.ecoenv.2008.05.010

Suzuki, N., Yessalina, S., Kikuchi, T., 2010. Probable fungal origin of perylene in Late Cretaceous to Paleogene terrestrial sedimentary rocks of northeastern Japan as indicated from stable carbon isotopes. Org. Geochem. 41, 234–241. https://doi.org/10.1016/J.ORGGEOCHEM.2009.11.010

Swartjes, F.A., 1999. Risk-based assessment of soil and groundwater quality in the Netherlands: Standards and remediation urgency. Risk Anal. 19, 1235–1249. https://doi.org/10.1111/j.1539-6924.1999.tb01142.x

Tan, P. qiang, Zhong, Y. mei, Hu, Z. yuan, Lou, D. ming, 2017. Size distributions, PAHs and inorganic ions of exhaust particles from a heavy duty diesel engine using B20 biodiesel with different exhaust aftertreatments. Energy 141, 898–906. https://doi.org/10.1016/j.energy.2017.09.122

Tan, Y.L., Heit, M., 1981. Biogenic and abiogenic polynuclear aromatic hydrocarbons in sediments from two remote Adirondack lakes. Geochim. Cosmochim. Acta 45, 2267–2279. https://doi.org/10.1016/0016-7037(81)90076-4

Tang, J., Petersen, E.J., Huang, Q., Weber, W.J., 2007. Development of engineered natural organic sorbents for environmental applications: 3. Reducing PAH mobility and bioavailability in contaminated soil and sediment systems. Environ. Sci. Technol. 41, 2901–2907. https://doi.org/10.1021/es061736k

Tang, Z., Guo, J., Liao, H., Zhao, X., Wu, F., Zhu, Y., Zhang, L., Giesy, J.P., 2015. Spatial and temporal distribution and sources of polycyclic aromatic hydrocarbons in sediments of Taihu Lake , eastern China. Env. Sci Pollut Res 22, 5350–5358. https://doi.org/10.1007/s11356-014-3746-2

Tao, H., Gemmer, M., Jiang, J., Lai, X., 2012. Assessment of CMIP3 climate models and projected changes of precipitation and temperature in the Yangtze River Basin , China. Clim. Change 111, 737–751. https://doi.org/10.1007/s10584-011-0144-3

Tao, Y., Dan, D., Kun, L., Chengda, H., Haibing, C., Guo, F., Qiujin, X., 2018. environmental implications in Taihu lake , China * d 15 N and nutrient stoichiometry of water , aquatic organisms and. Environ. Pollut. 237, 166–173. https://doi.org/10.1016/j.envpol.2018.02.048

Tao, Y., Yao, S., Xue, B., Deng, J., Wang, X., Feng, M., Hu, W., 2010. Polycyclic aromatic hydrocarbons in surface sediments from drinking water sources of Taihu Lake , China : sources , partitioning and toxicological risk. J. Environ. Monit. 12, 2282–2289. https://doi.org/10.1039/c0em00144a

Tongo, I., Ezemonye, L., Akpeh, K., 2017. Levels , distribution and characterization of Polycyclic Aromatic Hydrocarbons (PAHs) in Ovia river , Southern Nigeria. J. Environ. Chem. Eng. 5, 504–512. https://doi.org/10.1016/j.jece.2016.12.035

Tsapakis, M., Stephanou, E.G., 2007. Diurnal Cycle of PAHs , Nitro-PAHs , and oxy-PAHs in a High Oxidation Capacity Marine Background Atmosphere. Environ. Sci. Technol 41, 8011–8017. https://doi.org/10.1021/es071160e

Tsapakis, M., Stephanou, E.G., 2005. Occurrence of gaseous and particulate polycyclic aromatic hydrocarbons in the urban atmosphere : study of sources and ambient temperature effect on the gas / particle concentration and distribution. Environ. Pollut. 133, 147–156. https://doi.org/10.1016/j.envpol.2004.05.012

Tzamkiozis, T., Ntziachristos, L., Samaras, Z., 2010. Diesel passenger car PM emissions: From Euro 1 to Euro 4 with particle filter. Atmos. Environ. 44, 909–916. https://doi.org/10.1016/j.atmosenv.2009.12.003

US Environmnetal Protection Agency, 1993. Provisional Guidance for Quantitative Risk Assessment of Polycyclic Aromatic Hydrocarbons.

van Vaeck, L., van Cauwenberghe, K., 1978. Cascade impactor measurements of the size distribution of the major classes of organic pollutants in atmospheric particulate matter. Atmos. Environ. 12, 2229–2239.

https://doi.org/10.1016/0004-6981(78)90179-8

Venkataraman, C., Lyons, J.M., Friedlander, S.K., 1994. Size Distributions of Polycyclic Aromatic Hydrocarbons and Elemental Carbon. 1. Sampling, Measurement Methods, and Source Characterization. Environ. Sci. Technol. 28, 555–562. https://doi.org/10.1021/es00053a005

Venkataraman, C., Negi, G., Brata Sardar, S., Rastogi, R., 2002. Size distributions of polycyclic aromatic hydrocarbons in aerosol emissions from biofuel combustion. J. Aerosol Sci. 33, 503–518. https://doi.org/10.1016/S0021-8502(01)00185-9

Venkatesan, M.I., 1988. Occurrence and possible sources of perylene in marine sediments-a review. Mar. Chem. 25, 1–27. https://doi.org/10.1016/0304-4203(88)90011-4

Venkatesan, M.I., Kaplan, I.R., 1987. The lipid geochemistry of antarctic marine sediments: bransfield strait. Mar. Chem. 21, 347–375. https://doi.org/10.1016/0304-4203(87)90056-9

Vila-Escalé, M., Vegas-Vilarrúbia, T., Prat, N., 2007. Release of polycyclic aromatic compounds into a Mediterranean creek (Catalonia, NE Spain) after a forest fire. Water Res. 41, 2171–2179. https://doi.org/10.1016/J.WATRES.2006.07.029

Vollmuth, S., Niessner, R., 1995. Degradation of PCDD, PCDF, PAH, PCB and chlorinated phenols during the destruction-treatment of landfill seepage water in laboratory model reactor (UV, Ozone, and UV/Ozone). Chemosphere 30, 2317–2331. https://doi.org/10.1016/0045-6535(95)00104-G

Wang, B., Teng, Y., Xu, Y., Chen, W., Ren, W., Li, Y., Christie, P., Luo, Y., 2018. Effect of mixed soil microbiomes on pyrene removal and the response of the soil microorganisms. Sci. Total Environ. 640–641, 9–17. https://doi.org/10.1016/j.scitotenv.2018.05.290

Wang, H., Wang, C., Wu, W., Mo, Z., Wang, Z., 2003. Persistent organic pollutants in water and surface sediments of Taihu Lake, China and risk assessment. Chemosphere 50, 557–562. https://doi.org/10.1016/S0045-6535(02)00484-8

Wang, P., Wang, C., 2014. 4 . 8 Water Quality in Taihu Lake and the Effects of the Water Transfer from the Yangtze River to Taihu Lake Project, Comprehensive Water Quality and Purification. Elsevier Ltd. https://doi.org/10.1016/B978-0-12-382182-9.00071-2

Wang, Q., Chen, Y., 2010. Energy saving and emission reduction revolutionizing China ' s environmental protection. Renew. Sustain. Energy Rev. 14, 535–539. https://doi.org/10.1016/j.rser.2009.08.006

Wang, R., Yousaf, B., Sun, R., Zhang, H., Zhang, J., Liu, G., 2016a. Emission characterization and ı 13 C values of parent PAHs and nitro-PAHs in size-segregated particulate matters from coal-fired power plants. J. Hazard. Mater. 318, 487–496. https://doi.org/10.1016/j.jhazmat.2016.07.030

Wang, R., Yousaf, B., Sun, R., Zhang, H., Zhang, J., Liu, G., 2016b. Emission characterization and δ13C values of parent PAHs and nitro-PAHs in size-segregated particulate matters from coal-fired power plants. J. Hazard. Mater. 318, 487–496. https://doi.org/10.1016/j.jhazmat.2016.07.030

Wang, X., Feng, Z., 2003a. Energy consumption with sustainable development in developing country: A case in Jiangsu, China. Energy Policy 31, 1679–1684. https://doi.org/10.1016/S0301-4215(02)00234-3

Wang, X., Feng, Z., 2003b. Energy consumption with sustainable development in developing country: a case in Jiangsu, China. Energy Policy 31, 1679–1684. https://doi.org/10.1016/S0301-4215(02)00234-3

Wang, X., Westerdahl, D., Hu, J., Wu, Y., Yin, H., Pan, X., Max Zhang, K., 2012. On-road diesel vehicle emission factors for nitrogen oxides and black carbon in two Chinese cities. Atmos. Environ. 46, 45–55. https://doi.org/10.1016/j.atmosenv.2011.10.033

Weissenfels, W.D., Klewer, H.-J., Langhoff, J., 1992. Adsorption of polycyclic aromatic hydrocarbons (PAHs) by soil particles: influence on biodegradability and biotoxicity, Appl Microbiol Biotechnol.

Westerholm, R., Hang, L., Egebäck, K.E., Grägg, K., 1989. Exhaust emission reduction from a heavy duty diesel truck, using a catalyst and a particulate trap. Fuel 68, 856–860. https://doi.org/10.1016/0016-2361(89)90120-8

Westerholm, R.N., Alsberg, T.E., Frommelin, Å.B., Strandell, M.E., Rannug, U., Winquist, L., Grigorladis, V., Egebäck, K.E., 1988. Effect of fuel polycyclic aromatic hydrocarbon content on the emissions of polycyclic aromatic hydrocarbons and other mutagenic substances from a gasoline-fueled automobile. Environ. Sci. Technol. 22, 925–930. https://doi.org/10.1021/es00173a010

Whitehouse, B.G., 1984. The effects of temperature and salinity on the aqueous solubility of polynuclear aromatic hydrocarbons. Mar. Chem. 14, 319–332. https://doi.org/10.1016/0304-4203(84)90028-8

Wik, A., Dave, G., 2009. Occurrence and effects of tire wear particles in the environment – A critical review and an initial risk assessment. Environ. Pollut. 157, 1–11. https://doi.org/10.1016/j.envpol.2008.09.028

Wilcke, W., Amelung, W., Martius, C., Garcia, M.V.B., Zech, W., 2000. Biological Sources of Polycyclic Aromatic Hydrocarbons (PAHs) in the Amazonian Rain Forest. J. Plant Nutr. Soil Sci. 163, 27–30. https://doi.org/10.1002/(SICI)1522-2624(200002)163:1<27::AID-JPLN27>3.0.CO;2-E

Wilhelm, S.W., Farnsley, S.E., LeCleir, G.R., Layton, A.C., Satchwell, M.F., DeBruyn, J.M., Boyer, G.L., Zhu, G., Paerl, H.W., 2011. The relationships between nutrients, cyanobacterial toxins and the microbial community in Taihu (Lake Tai), China. Harmful Algae 10, 207–215. https://doi.org/10.1016/J.HAL.2010.10.001

Williams, A., Jones, J.M., Ma, L., Pourkashanian, M., 2012. Pollutants from the combustion of solid biomass fuels. Prog. Energy Combust. Sci. 38, 113–137. https://doi.org/10.1016/j.pecs.2011.10.001

Wolf, A., Bergmann, A., Wilken, R.D., Gao, X., Bi, Y., Chen, H., Schüth, C., 2013. Occurrence and distribution of organic trace substances in waters from the Three Gorges Reservoir, China. Environ. Sci. Pollut. Res. 20, 7124–7139. https://doi.org/10.1007/s11356-013-1929-x

Wolkenstein, K., Gross, J.H., Falk, H., Schoeler, H.F., 2006. Preservation of hypericin and related polycyclic quinone pigments in fossil crinoids. Proc. R. Soc. B 273, 451–456. https://doi.org/10.1098/rspb.2005.3358

Wolter, M., Zadrazil, F., Martens, R., Bahadir, M., 1997. Degradation of eight highly condensed polycyclic aromatic hydrocarbons by Pleurotus sp. Florida in solid wheat straw substrate. Appl. Microbiol. Biotechnol. 48, 398–404. https://doi.org/10.1007/s002530051070

Wu, D., Zhang, F., Lou, W., Li, D., Chen, J., 2017. Chemical characterization and toxicity assessment of fi ne particulate matters emitted from the combustion of petrol and diesel fuels. Sci. Total Environ. 605–606, 172–179. https://doi.org/10.1016/j.scitotenv.2017.06.058

Wu, H.X., 2007. The Chinese GDP Growth Rate Puzzle : How Fast Has the Chinese Economy Grown ?*. Asian Econ. Pap. 6, 1–23. https://doi.org/10.1162/asep.2007.6.1.1

Wu, Y., 2012. Energy intensity and its determinants in China's regional economies. Energy Policy 41, 703–711. https://doi.org/10.1016/j.enpol.2011.11.034

Wu, Y., Zhang, S., Hao, J., Liu, H., Wu, X., Hu, J., Walsh, M.P., Wallington, T.J., Zhang, K.M., Stevanovic, S., 2017. On-road vehicle emissions and their control in China: A review and outlook. Sci. Total Environ. 574, 332–349. https://doi.org/10.1016/j.scitotenv.2016.09.040

Xie, Y.-X., Xiong, Z.-Q., Xing, G.-X., Sun, G.-Q., Zhu, Z.-L., 2007. Assessment of Nitrogen Pollutant Sources in Surface Waters of Taihu Lake Region*'. Pedosphere 17, 200–208. https://doi.org/10.1016/S1002-0160(07)60026-5

Xu, H., Paerl, H.W., Qin, B., Zhu, G., Gao, G., 2010. Nitrogen and phosphorus inputs control phytoplankton growth in eutrophic Lake Taihu, China. Limnol. Oceanogr. 55, 420–432. https://doi.org/10.4319/lo.2010.55.1.0420

Xu, J., Zhang, Y., Zhou, C., Guo, C., Wang, D., Du, P., Luo, Y., Wan, J., Meng, W., 2014. Distribution, sources and composition of antibiotics in sediment, overlying water and pore water from Taihu Lake, China. Sci. Total Environ. 497–498, 267–273. https://doi.org/10.1016/J.SCITOTENV.2014.07.114

Xu, L., Zhang, Q., Li, H., Viney, N.R., 2007. Modeling of Surface Runoff in Xitiaoxi Catchment , China. Water Resour. Manag. 21, 1313–1323. https://doi.org/10.1007/s11269-006-9083-6

Xu, Z., Wu, J., Li, H., Chen, Y., Xu, J., Xiong, L., Zhang, J., 2018. Characterizing heavy metals in combined sewer overflows and its influence on microbial diversity. Sci. Total Environ. 625, 1272–1282. https://doi.org/10.1016/j.scitotenv.2017.12.338

Xue, B., Yao, S., 2011. Recent sedimentation rates in lakes in lower Yangtze River basin. Quat. Int. 244, 248–253. https://doi.org/10.1016/J.QUAINT.2011.01.003

Yang, B., Zhou, L., Xue, N., Li, F., Li, Y., Vogt, R.D., Cong, X., Yan, Y., Liu, B., 2013. Source apportionment of polycyclic aromatic hydrocarbons in soils of Huanghuai Plain, China: Comparison of three receptor models. Sci. Total Environ. 443, 31–39. https://doi.org/10.1016/j.scitotenv.2012.10.094

Yang, D., Qi, S., Zhang, Y., Xing, X., Liu, H., Qu, C., Liu, J., Li, F., 2013. Levels , sources and potential risks of polycyclic aromatic hydrocarbons (PAHs) in multimedia environment along the Jinjiang River mainstream to Quanzhou Bay, China. Mar. Pollut. Bull. 76, 298–306. https://doi.org/10.1016/j.marpolbul.2013.08.016

Yang, H.-H., Lai, S.-O., Hsieh, L.-T., Hsueh, H.-J., Chi, T.-W., 2002. Profiles of PAH emission from steel and iron industries. Chemosphere 48, 1061–1074. https://doi.org/10.1016/S0045-6535(02)00175-3

Yang, H.-H., Lee, W.-J., Chen, S.-J., Lai, S.-O., 1998. PAH emission from various industrial stacks. J. Hazard. Mater. 60, 159–174. https://doi.org/10.1016/S0304-3894(98)00089-2

Yang, Y., Miller, D.J., Hawthorne, S.B., 1997. Toluene Solubility in Water and Organic Partitioning from Gasoline and Diesel Fuel into Water at Elevated Temperatures and Pressures. J. Chem. Eng. Data 9568, 908–913. https://doi.org/10.1021/je960395v

Yeh, A.G.O., Xu, J., Liu, K., 2011. China's post-reform urbanization: retrospect, policies and trends. IIED.

Yi, H., Guo, X., Hao, J., Duan, L., Li, X., 2006. Characteristics of Inhalable Particulate Matter Concentration and Size Distribution from Power Plants in China. J. Air Waste Manage. Assoc. 56, 1243–1251. https://doi.org/10.1080/10473289.2006.10464590

You, C.F., Xu, X.C., 2010. Coal combustion and its pollution control in China. Energy 35, 4467–4472. https://doi.org/10.1016/j.energy.2009.04.019

Yuan, H., An, S., Shen, J., Liu, E., 2014. The characteristic and environmental pollution records of phosphorus species in different trophic regions of Taihu Lake, China. Environ. Earth Sci. 71, 783–792. https://doi.org/10.1007/s12665-013-2480-2

Yuan, X., Zhang, M., Wang, Q., Wang, Y., Zuo, J., 2017. Evolution analysis of environmental standards: Effectiveness on air pollutant emissions reduction. J. Clean. Prod. 149, 511–520. https://doi.org/10.1016/j.jclepro.2017.02.127

Yue, X., Wu, Y., Hao, J., Pang, Y., Ma, Y., Li, Y., Li, B., Bao, X., 2015. Fuel quality management versus vehicle emission control in China, status quo and future perspectives. Energy Policy 79, 87–98. https://doi.org/10.1016/j.enpol.2015.01.009

Yunker, M.B., Macdonald, R.W., Vingarzan, R., Mitchell, R.H., Goyette, D., Sylvestre, S., 2002. PAHs in the Fraser River basin: a critical appraisal of PAH ratios as indicators of PAH source and composition. Org. Geochem. 33, 489–515. https://doi.org/10.1016/S0146-6380(02)00002-5

Zakaria, M.P., Takada, H., Tsutsumi, S., Ohno, K., Yamada, J., Kouno, E., Kumata, H., 2002. Distribution of polycyclic aromatic hydrocarbons (PAHs) in rivers and estuaries in Malaysia: a widespread input of petrogenic PAHs. Environ. Sci. Technol. 36, 1907–1918. https://doi.org/10.1021/es011278+

Zamani, M., Khorasani, N., Bakhtiari, A.R., Rezaei, K., 2015. Source identification of perylene in surface sediments and waterbird eggs in the Anzali Wetland , Iran. Environ. Pollut. 205, 23–32. https://doi.org/10.1016/j.envpol.2015.05.007

Zeng, R., Zhao, J., Zhang, R., Lin, N., 2005. Bacterial community in sediment from the Western Pacific ?Warm Pool? and its relationship to environment. Sci. China Ser. D 48, 282–290. https://doi.org/10.1360/03yd0531

Zhai, S., Hu, W., Zhu, Z., 2010. Ecological impacts of water transfers on Lake Taihu from the Yangtze River , China. Ecol. Eng. 36, 406–420. https://doi.org/10.1016/j.ecoleng.2009.11.007

Zhang, K., Wen, Z., 2008. Review and challenges of policies of environmental protection and sustainable development in China. J. Environ. Manage. 88, 1249–1261. https://doi.org/10.1016/j.jenvman.2007.06.019

Zhang, L., Shen, Q., Hu, H., Shao, S., Fan, C., 2011. Impacts of corbicula fluminea on oxygen uptake and nutrient fluxes across the sediment-water interface. Water. Air. Soil Pollut. 220, 399–411. https://doi.org/10.1007/s11270-011-0763-3

Zhang, T., Zou, H., 1998. Zhang, Zou - 1998 - Fiscal decentralization, public spending, and economic growth in China. J. Public Econ. 67, 221–240. https://doi.org/10.1016/S0047-2727(97)00057-1

Zhang, W.L., Tian, Z.X., Zhang, N., Li, X.Q., 1996. Nitrate pollution of groundwater in northern China. Agric. Ecosyst. Environ. 59, 223–231. https://doi.org/10.1016/0167-8809(96)01052-3

Zhang, X., Chen, C., Ding, J., Hou, A., Li, Y., Niu, Z., Su, X., Xu, Y., Laws, E.A., 2010. The 2007 water crisis in Wuxi, China: Analysis of the origin. J. Hazard. Mater. 182, 130–135. https://doi.org/10.1016/J.JHAZMAT.2010.06.006

Zhang, X.L., Tao, S., Liu, W.X., Yang, Y., Zuo, Q., Liu, S.Z., 2005. Source Diagnostics of Polycyclic Aromatic Hydrocarbons Based on Species Ratios: A Multimedia Approach. Environ. Sci. Technol 39, 9109–9114. https://doi.org/10.1021/es0513741

Zhang, Y., Guo, C., Xu, J., Tian, Y., Shi, G., Feng, Y.-C., 2012. Potential source contributions and risk assessment of PAHs in sediments from Taihu Lake , China : Comparison of three receptor models. Water Res. 46, 3065–3073. https://doi.org/10.1016/j.watres.2012.03.006

Zhang, Y., Lu, Y., Xu, J., Yu, T., Zhao, W., 2011. Spatial Distribution of Polycyclic Aromatic Hydrocarbons from Lake Taihu, China. Bull Env. Contam Toxicol 87, 80–85. https://doi.org/10.1007/s00128-011-0292-1

Zhang, Yuanxun, Schauer, J.J., Zhang, Yuanhang, Zeng, L., Wei, Y., Liu, Y., Shao, M., 2008. Characteristics of particulate carbon emissions from real-world Chinese coal combustion. Environ. Sci. Technol. 42, 5068–5073. https://doi.org/10.1021/es7022576

Zhao, X., Zhou, Y., Min, J., Wang, S., Shi, W., Xing, G., 2012. Nitrogen runoff dominates water nitrogen pollution from rice-wheat rotation in the Taihu Lake region of China. Agric. Ecosyst. Environ. 156, 1–11. https://doi.org/10.1016/j.agee.2012.04.024

Zhao, Y., Wang, S., Duan, L., Lei, Y., Cao, P., Hao, J., 2008. Primary air pollutant emissions of coal-fired power plants in China : Current status and future prediction. Atmos. Environ. 42, 8442–8452. https://doi.org/10.1016/j.atmosenv.2008.08.021

Zhao, Y., Wang, S., Nielsen, C.P., Li, X., Hao, J., 2010. Establishment of a database of emission factors for atmospheric pollutants from Chinese coal-fired power plants. Atmos. Environ. 44, 1515–1523. https://doi.org/10.1016/J.ATMOSENV.2010.01.017

Zheng, S., Wang, P., Wang, C., Hou, J., Qian, J., 2013. Distribution of metals in water and suspended particulate matter during the resuspension processes in Taihu Lake sediment, China. Quat. Int. 286, 94–102. https://doi.org/10.1016/j.quaint.2012.09.003

Zhong, J., You, B., Fan, C., Li, B., Zhang, L., Ding, S., 2008. Influence of Sediment Dredging on Chemical Forms and Release of Phosphorus. Pedosphere 18, 34–44. https://doi.org/10.1016/S1002-0160(07)60100-3

Zhong, Y., Luan, T., Lin, L., Liu, H., Tam, N.F.Y., 2011. Production of metabolites in the biodegradation of phenanthrene, fluoranthene and pyrene by the mixed culture of Mycobacterium sp. and Sphingomonas sp. Bioresour. Technol. 102, 2965–2972. https://doi.org/10.1016/j.biortech.2010.09.113

Literature data reference

Fig. 4.5a data reference

Light-duty vehicle

Alkurdi, F., Karabet, F. and Dimashki, M., 2013. Characterization, concentrations and emission rates of polycyclic aromatic hydrocarbons in the exhaust emissions from in-service vehicles in Damascus. Atmospheric Research, 120, pp.68-77. https://doi.org/10.1016/j.atmosres.2012.08.003

Cao, X., Hao, X., Shen, X., Jiang, X., Wu, B. and Yao, Z., 2017. Emission characteristics of polycyclic aromatic hydrocarbons and nitro-polycyclic aromatic hydrocarbons from diesel trucks based on on-road measurements. Atmospheric environment, 148, pp.190-196. https://doi.org/10.1016/j.atmosenv.2016.10.040

Herrington, J.S., Hays, M.D., George, B.J. and Baldauf, R.W., 2012. The effects of operating conditions on semivolatile organic compounds emitted from light-duty, gasoline-powered motor vehicles. Atmospheric environment, 54, pp.53-59. https://doi.org/10.1016/j.atmosenv.2012.02.043

Heavy-duty vehicle

Alkurdi, F., Karabet, F. and Dimashki, M., 2013. Characterization, concentrations and emission rates of polycyclic aromatic hydrocarbons in the exhaust emissions from in-service vehicles in Damascus. Atmospheric Research, 120, pp.68-77. https://doi.org/10.1016/j.atmosres.2012.08.003

Cao, X., Hao, X., Shen, X., Jiang, X., Wu, B. and Yao, Z., 2017. Emission characteristics of polycyclic aromatic hydrocarbons and nitro-polycyclic aromatic hydrocarbons from diesel trucks based on on-road measurements. Atmospheric environment, 148, pp.190-196. https://doi.org/10.1016/j.atmosenv.2016.10.040

Mi, H.H., Lee, W.J., Chen, C.B., Yang, H.H. and Wu, S.J., 2000. Effect of fuel aromatic content on PAH emission from a heavy-duty diesel engine. Chemosphere, 41(11), pp.1783-1790. https://doi.org/10.1016/S0045-6535(00)00043-6

Rogge, W.F., Hildemann, L.M., Mazurek, M.A., Cass, G.R. and Simoneit, B.R., 1993. Sources of fine organic aerosol. 2. Noncatalyst and catalyst-equipped automobiles and heavy-duty diesel trucks. Environmental science & technology, 27(4), pp.636-651. https://doi.org/10.1021/es00041a007

Westerholm, R., Hang, L., Egebäck, K.E. and Grägg, K., 1989. Exhaust emission reduction from a heavy duty diesel truck, using a catalyst and a particulate trap. Fuel, 68(7), pp.856-860. https://doi.org/10.1016/0016-2361(89)90120-8

Coal coking

Khaparde, V.V., Bhanarkar, A.D., Majumdar, D. and Rao, C.C., 2016. Characterization of polycyclic aromatic hydrocarbons in fugitive PM10 emissions from an integrated iron and steel plant. Science of the Total Environment, 562, pp.155-163. https://doi.org/10.1016/j.scitotenv.2016.03.153

Kong, S., Ji, Y., Li, Z., Lu, B. and Bai, Z., 2013. Emission and profile characteristic of polycyclic aromatic hydrocarbons in PM2. 5 and PM10 from stationary sources based on dilution sampling. Atmospheric environment, 77, pp.155-165. https://doi.org/10.1016/j.atmosenv.2013.04.073

Kong, S., Shi, J., Lu, B., Qiu, W., Zhang, B., Peng, Y., Zhang, B. and Bai, Z., 2011. Characterization of PAHs within PM10 fraction for ashes from coke production, iron smelt, heating station and power plant stacks in Liaoning Province, China. Atmospheric Environment, 45(23), pp.3777-3785. https://doi.org/10.1016/j.atmosenv.2011.04.029

Mu, L., Peng, L., Cao, J., He, Q., Li, F., Zhang, J., Liu, X. and Bai, H., 2013. Emissions of polycyclic aromatic hydrocarbons from coking industries in China. Particuology, 11(1), pp.86-93. https://doi.org/10.1016/j.atmosenv.2011.04.029

Mu, L., Peng, L., Liu, X., Song, C., Bai, H., Zhang, J., Hu, D., He, Q. and Li, F., 2014. Characteristics of polycyclic aromatic hydrocarbons and their gas/particle partitioning from fugitive emissions in coke plants. Atmospheric environment, 83, pp.202-210. https://doi.org/10.1016/j.atmosenv.2013.09.043

Yang, H.H., Lee, W.J., Chen, S.J. and Lai, S.O., 1998. PAH emission from various industrial stacks. Journal of

Hazardous materials, 60(2), pp.159-174. https://doi.org/10.1016/S0304-3894(98)00089-2

Coal power plant

Kong, S., Ji, Y., Li, Z., Lu, B. and Bai, Z., 2013. Emission and profile characteristic of polycyclic aromatic hydrocarbons in PM2. 5 and PM10 from stationary sources based on dilution sampling. Atmospheric environment, 77, pp.155-165. https://doi.org/10.1016/j.atmosenv.2013.04.073

Kong, S., Shi, J., Lu, B., Qiu, W., Zhang, B., Peng, Y., Zhang, B. and Bai, Z., 2011. Characterization of PAHs within PM10 fraction for ashes from coke production, iron smelt, heating station and power plant stacks in Liaoning Province, China. Atmospheric Environment, 45(23), pp.3777-3785. https://doi.org/10.1016/j.atmosenv.2011.04.029

Li, H., Liu, G. and Cao, Y., 2014. Content and distribution of trace elements and polycyclic aromatic hydrocarbons in fly ash from a coal-fired CHP plant. Aerosol Air Qual. Res, 14(4), pp.1179-1188. https://doi.org/10.4209/aaqr.2013.06.0216

Li, Z., Chen, L., Liu, S., Ma, H., Wang, L., An, C. and Zhang, R., 2016. Characterization of PAHs and PCBs in fly ashes of eighteen coal-fired power plants. Aerosol Air Qual. Res, 16, pp.3175-3186. https://doi.org/10.4209/aaqr.2016.10.0430

Pergal, M.M., Tešić, Z.L. and Popović, A.R., 2013. Polycyclic aromatic hydrocarbons: temperature driven formation and behavior during coal combustion in a coal-fired power plant. Energy & Fuels, 27(10), pp.6273-6278. https://doi.org/10.1021/ef401467z

Ruwei, W., Jiamei, Z., Jingjing, L. and Liu, G., 2013. Levels and patterns of polycyclic aromatic hydrocarbons in coal-fired power plant bottom ash and fly ash from Huainan, China. Archives of environmental contamination and toxicology, 65(2), pp.193-202. https://doi.org/10.1007/s00244-013-9902-8

Wang, R., Yousaf, B., Sun, R., Zhang, H., Zhang, J. and Liu, G., 2016. Emission characterization and δ13C values of parent PAHs and nitro-PAHs in size-segregated particulate matters from coal-fired power plants. Journal of hazardous materials, 318, pp.487-496. https://doi.org/10.1016/j.jhazmat.2016.07.030

Wang, R., Liu, G., Sun, R., Yousaf, B., Wang, J., Liu, R. and Zhang, H., 2018. Emission characteristics for gaseous-and size-segregated particulate PAHs in coal combustion flue gas from circulating fluidized bed (CFB) boiler. Environmental pollution, 238, pp.581-589. https://doi.org/10.1016/j.envpol.2018.03.051

Yang, H.H., Lee, W.J., Chen, S.J. and Lai, S.O., 1998. PAH emission from various industrial stacks. Journal of Hazardous materials, 60(2), pp.159-174. https://doi.org/10.1016/S0304-3894(98)00089-2

Zhou, H., Jin, B., Xiao, R., Zhong, Z. and Huang, Y., 2009. Distribution of polycyclic aromatic hydrocarbons in fly ash during coal and residual char combustion in a pressurized fluidized bed. Energy & Fuels, 23(4), pp.2031-2034. https://doi.org/10.1021/ef8008162

Residential coal combustion

Chen, Y., Bi, X., Mai, B., Sheng, G. and Fu, J., 2004. Emission characterization of particulate/gaseous phases and size association for polycyclic aromatic hydrocarbons from residential coal combustion. Fuel, 83(7-8), pp.781-790. https://doi.org/10.1016/j.fuel.2003.11.003

Chen, Y., Sheng, G., Bi, X., Feng, Y., Mai, B. and Fu, J., 2005. Emission factors for carbonaceous particles and polycyclic aromatic hydrocarbons from residential coal combustion in China. Environmental Science & Technology, 39(6), pp.1861-1867. https://doi.org/10.1021/es0493650

Lee, R.G., Coleman, P., Jones, J.L., Jones, K.C. and Lohmann, R., 2005. Emission factors and importance of PCDD/Fs, PCBs, PCNs, PAHs and PM10 from the domestic burning of coal and wood in the UK. Environmental science & technology, 39(6), pp.1436-1447. https://doi.org/10.1021/es048745i

Shen, G., Wang, W., Yang, Y., Zhu, C., Min, Y., Xue, M., Ding, J., Li, W., Wang, B., Shen, H. and Wang, R., 2010. Emission factors and particulate matter size distribution of polycyclic aromatic hydrocarbons from residential coal combustions in rural Northern China. Atmospheric Environment, 44(39), pp.5237-5243. https://doi.org/10.1016/j.atmosenv.2010.08.042

Wang, Y., Xu, Y., Chen, Y., Tian, C., Feng, Y., Chen, T., Li, J. and Zhang, G., 2016. Influence of different types of coals and stoves on the emissions of parent and oxygenated PAHs from residential coal combustion in China. Environmental pollution, 212, pp.1-8. https://doi.org/10.1016/j.envpol.2016.01.041

Yang, X., Liu, S., Xu, Y., Liu, Y., Chen, L., Tang, N. and Hayakawa, K., 2017. Emission factors of polycyclic and nitro-polycyclic aromatic hydrocarbons from residential combustion of coal and crop residue pellets. Environmental Pollution, 231, pp.1265-1273. https://doi.org/10.1016/j.envpol.2017.08.087

Zhang, Y., Schauer, J.J., Zhang, Y., Zeng, L., Wei, Y., Liu, Y. and Shao, M., 2008. Characteristics of particulate carbon emissions from real-world Chinese coal combustion. Environmental science & technology, 42(14), pp.5068-5073. https://doi.org/10.1021/es7022576

Wood combustion

Hedberg, E., Kristensson, A., Ohlsson, M., Johansson, C., Johansson, P.Å., Swietlicki, E., Vesely, V., Wideqvist, U. and Westerholm, R., 2002. Chemical and physical characterization of emissions from birch wood combustion in a wood stove. Atmospheric Environment, 36(30), pp.4823-4837. https://doi.org/10.1016/S1352-2310(02)00417-X

Hytönen, K., Yli-Pirilä, P., Tissari, J., Gröhn, A., Riipinen, I., Lehtinen, K.E.J. and Jokiniemi, J., 2009. Gas–particle distribution of PAHs in wood combustion emission determined with annular denuders, filter, and polyurethane foam adsorbent. Aerosol Science and Technology, 43(5), pp.442-454. https://doi.org/10.1080/02786820802716743

Khalili, N.R., Scheff, P.A. and Holsen, T.M., 1995. PAH source fingerprints for coke ovens, diesel and, gasoline engines, highway tunnels, and wood combustion emissions. Atmospheric environment, 29(4), pp.533-542.

Kim Oanh, N.T., Bætz Reutergårdh, L. and Dung, N.T., 1999. Emission of polycyclic aromatic hydrocarbons and particulate matter from domestic combustion of selected fuels. Environmental Science & Technology, 33(16), pp.2703-2709. https://doi.org/10.1016/1352-2310(94)00275-P

Lamberg, H., Nuutinen, K., Tissari, J., Ruusunen, J., Yli-Pirilä, P., Sippula, O., Tapanainen, M., Jalava, P., Makkonen, U., Teinilä, K. and Saarnio, K., 2011. Physicochemical characterization of fine particles from small-scale wood combustion. Atmospheric Environment, 45(40), pp.7635-7643. https://doi.org/10.1016/j.atmosenv.2011.02.072

Lee, R.G., Coleman, P., Jones, J.L., Jones, K.C. and Lohmann, R., 2005. Emission factors and importance of PCDD/Fs, PCBs, PCNs, PAHs and PM10 from the domestic burning of coal and wood in the UK. Environmental science & technology, 39(6), pp.1436-1447. https://doi.org/10.1021/es048745i

Rogge, W.F., Hildemann, L.M., Mazurek, M.A., Cass, G.R. and Simoneit, B.R., 1998. Sources of fine organic aerosol. 9. Pine, oak, and synthetic log combustion in residential fireplaces. Environmental Science & Technology, 32(1), pp.13-22. https://doi.org/10.1021/es960930b

Shen, G., Tao, S., Wei, S., Zhang, Y., Wang, R., Wang, B., Li, W., Shen, H., Huang, Y., Chen, Y. and Chen, H., 2012. Emissions of parent, nitro, and oxygenated polycyclic aromatic hydrocarbons from residential wood combustion in rural China. Environmental science & technology, 46(15), pp.8123-8130. https://doi.org/10.1021/es301146v

Tissari, J., Hytönen, K., Lyyränen, J. and Jokiniemi, J., 2007. A novel field measurement method for determining fine particle and gas emissions from residential wood combustion. Atmospheric Environment, 41(37), pp.8330-8344. https://doi.org/10.1016/j.atmosenv.2007.06.018

Fig. 4.5b data reference

Baek, S.O., Goldstone, M.E., Kirk, P.W.W., Lester, J.N. and Perry, R., 1991. Phase distribution and particle size dependency of polycyclic aromatic hydrocarbons in the urban atmosphere. Chemosphere, 22(5-6), pp.503-520. https://doi.org/10.1016/0045-6535(91)90062-I

Chen, Y., Bi, X., Mai, B., Sheng, G. and Fu, J., 2004. Emission characterization of particulate/gaseous phases and size association for polycyclic aromatic hydrocarbons from residential coal combustion. Fuel, 83(7-8), pp.781-790. https://doi.org/10.1016/j.fuel.2003.11.003

Degrendele, C., Okonski, K., Melymuk, L., Landlová, L., Kukučka, P., Čupr, P. and Klánová, J., 2014. Size specific distribution of the atmospheric particulate PCDD/Fs, dl-PCBs and PAHs on a seasonal scale: Implications for cancer risks from inhalation. Atmospheric environment, 98, pp.410-416. https://doi.org/10.1016/j.atmosenv.2014.09.001

Kaupp, H. and McLachlan, M.S., 1998. Atmospheric particle size distributions of polychlorinated dibenzo-p-dioxins and dibenzofurans (PCDD/Fs) and polycyclic aromatic hydrocarbons (PAHs) and their implications for wet and dry deposition. Atmospheric Environment, 33(1), pp.85-95.

https://doi.org/10.1016/S1352-2310(98)00129-0

Kaupp, H. and McLachlan, M.S., 2000. Distribution of polychlorinated dibenzo-P-dioxins and dibenzofurans (PCDD/Fs) and polycyclic aromatic hydrocarbons (PAHs) within the full size range of atmospheric particles. Atmospheric Environment, 34(1), pp.73-83. https://doi.org/10.1016/S1352-2310(99)00298-8

Oliveira, C., Martins, N., Tavares, J., Pio, C., Cerqueira, M., Matos, M., Silva, H., Oliveira, C. and Camões, F., 2011. Size distribution of polycyclic aromatic hydrocarbons in a roadway tunnel in Lisbon, Portugal. Chemosphere, 83(11), pp.1588-1596. https://doi.org/10.1016/j.chemosphere.2011.01.011

Van Vaeck, L., Broddin, G. and Van Cauwenberghe, K., 1979. Differences in particle size distributions of major organic pollutants in ambient aerosols in urban, rural, and seashore areas. Environmental Science & Technology, 13(12), pp.1494-1502. https://doi.org/10.1021/es60160a013

Wang, R., Liu, G., Sun, R., Yousaf, B., Wang, J., Liu, R. and Zhang, H., 2018. Emission characteristics for gaseous-and size-segregated particulate PAHs in coal combustion flue gas from circulating fluidized bed (CFB) boiler. Environmental pollution, 238, pp.581-589. https://doi.org/10.1016/j.envpol.2018.03.051

Wang, R., Yousaf, B., Sun, R., Zhang, H., Zhang, J. and Liu, G., 2016. Emission characterization and δ13C values of parent PAHs and nitro-PAHs in size-segregated particulate matters from coal-fired power plants. Journal of hazardous materials, 318, pp.487-496. https://doi.org/10.1016/j.jhazmat.2016.07.030

Zhang, K., Zhang, B.Z., Li, S.M., Zhang, L.M., Staebler, R. and Zeng, E.Y., 2012. Diurnal and seasonal variability in size-dependent atmospheric deposition fluxes of polycyclic aromatic hydrocarbons in an urban center. Atmospheric environment, 57, pp.41-48. https://doi.org/10.1016/j.atmosenv.2012.04.014

Fig. 4.6 data reference

Coal coking

Same as the literature data in Fig. 4.5a coal coking

Coal power plant

Literature data in Fig. 4.5a plus the following literature data:

Masclet, P., Bresson, M.A. and Mouvier, G., 1987. Polycyclic aromatic hydrocarbons emitted by power stations, and influence of combustion conditions. Fuel, 66(4), pp.556-562. https://doi.org/10.1016/0016-2361(87)90163-3

Sahu, S.K., Bhangare, R.C., Ajmal, P.Y., Sharma, S., Pandit, G.G. and Puranik, V.D., 2009. Characterization and quantification of persistent organic pollutants in fly ash from coal fueled thermal power stations in India. Microchemical Journal, 92(1), pp.92-96. https://doi.org/10.1016/j.microc.2009.02.003

Residential coal combustion

Literature data in Fig. 4.5a plus the following literature data:

Bi, X., Simoneit, B.R., Sheng, G. and Fu, J., 2008. Characterization of molecular markers in smoke from residential coal combustion in China. Fuel, 87(1), pp.112-119. https://doi.org/10.1016/j.fuel.2007.03.047

Kim Oanh, N.T., Bætz Reutergårdh, L. and Dung, N.T., 1999. Emission of polycyclic aromatic hydrocarbons and particulate matter from domestic combustion of selected fuels. Environmental Science & Technology, 33(16), pp.2703-2709. https://doi.org/10.1021/es980853f

Liu, W.X., Dou, H., Wei, Z.C., Chang, B., Qiu, W.X., Liu, Y. and Tao, S., 2009. Emission characteristics of polycyclic aromatic hydrocarbons from combustion of different residential coals in North China. Science of the total environment, 407(4), pp.1436-1446. https://doi.org/10.1016/j.scitotenv.2008.10.055

Wood combustion

Literature data in Fig. 4.5a plus the following literature data:

Gonçalves, C., Alves, C. and Pio, C., 2012. Inventory of fine particulate organic compound emissions from residential wood combustion in Portugal. Atmospheric Environment, 50, pp.297-306.

https://doi.org/10.1016/j.atmosenv.2011.12.013

Hays, M.D., Smith, N.D., Kinsey, J., Dong, Y. and Kariher, P., 2003. Polycyclic aromatic hydrocarbon size distributions in aerosols from appliances of residential wood combustion as determined by direct thermal desorption—GC/MS. Journal of Aerosol Science, 34(8), pp.1061-1084. https://doi.org/10.1016/S0021-8502(03)00080-6

Li, C.K. and Kamens, R.M., 1993. The use of polycyclic aromatic hydrocarbons as source signatures in receptor modeling. Atmospheric Environment. Part A. General Topics, 27(4), pp.523-532. https://doi.org/10.1016/0960-1686(93)90209-H

McDonald, J.D., Zielinska, B., Fujita, E.M., Sagebiel, J.C., Chow, J.C. and Watson, J.G., 2000. Fine particle and gaseous emission rates from residential wood combustion. Environmental Science & Technology, 34(11), pp.2080-2091. https://doi.org/10.1021/es9909632

Orasche, J., Schnelle-Kreis, J., Schön, C., Hartmann, H., Ruppert, H., Arteaga-Salas, J.M. and Zimmermann, R., 2013. Comparison of emissions from wood combustion. Part 2: Impact of combustion conditions on emission factors and characteristics of particle-bound organic species and polycyclic aromatic hydrocarbon (PAH)-related toxicological potential. Energy & Fuels, 27(3), pp.1482-1491. https://doi.org/10.1021/ef301506h

Schauer, J.J., Kleeman, M.J., Cass, G.R. and Simoneit, B.R., 2001. Measurement of emissions from air pollution sources. 3. C1− C29 organic compounds from fireplace combustion of wood. Environmental Science & Technology, 35(9), pp.1716-1728. https://doi.org/10.1021/es001331e

Appendix

Tab. 1 PAH concentration in the surface sediments (ng/g)

location	naph	2methylnaph	1methylnaph	acenaphthy	acenaphthe	fluorene	phen	anthra	fluor	pyrene
1-1	17.12	30.15	9.63	3.58	4.27	21.95	83.94	4.41	70.33	63.39
1-3	16.84	26.28	10.19	3.22	6.32	40.16	151.13	8.12	76.08	58.54
1-5	14.15	24.18	9.75	3.65	4.84	29.40	104.01	6.33	52.15	38.26
3-12	6.29	6.75	5.06	4.33	5.69	3.97	38.71	ND	20.34	15.34
3-13	16.74	19.33	11.81	5.15	ND	18.83	54.27	4.33	57.77	39.97
3-15	21.43	11.92	10.53	4.52	ND	29.47	65.14	3.93	49.50	37.88
3-16	34.33	22.06	11.78	9.53	3.30	21.64	75.06	9.74	73.08	53.72
3-17	25.09	16.14	7.95	3.50	3.25	19.04	56.83	6.79	51.63	40.92
3-18	55.40	28.08	13.44	10.13	4.77	37.96	105.24	34.59	120.69	94.71
3-20	26.87	19.26	11.05	8.79	3.05	39.30	102.53	7.59	95.82	66.90
3-21	13.37	13.90	8.72	5.45	ND	23.26	61.50	3.89	58.07	40.54
3-22	33.42	24.13	12.42	4.61	3.84	56.04	131.10	6.56	90.77	67.55
3-23	33.33	19.53	10.75	4.35	3.44	36.90	94.30	8.04	97.22	70.74
4-41	24.97	12.90	9.22	4.73	3.57	9.38	41.27	30.10	53.55	54.60
8-6	12.62	6.37	3.71	3.00	3.00	8.00	30.23	10.21	76.72	56.77
8-7	10.92	6.39	4.22	3.54	3.76	10.03	28.48	9.75	78.37	50.77
8-8	4.11	ND	5.14	ND	ND	ND	12.84	6.86	23.09	15.53
8-9	9.43	9.25	5.02	ND	ND	10.05	31.29	7.77	75.56	50.84
8-10	8.09	3.63	4.48	ND	3.01	3.97	18.35	3.95	41.52	28.88
8-11	18.68	10.71	4.49	3.92	3.59	12.99	45.52	12.43	112.81	81.09
8-19	11.10	7.21	3.56	3.31	3.14	6.75	28.34	7.81	70.45	47.60
8-21	9.88	6.55	3.32	4.06	ND	5.29	24.15	12.78	50.26	38.40
8-22	21.14	13.54	7.09	3.77	3.64	10.89	46.12	36.25	82.93	71.25
8-23	184.46	83.08	45.79	35.56	27.46	60.01	211.98	169.75	218.31	208.42
8-24	30.38	14.08	7.78	4.57	6.56	15.46	94.22	51.29	199.25	173.47

The other PAHs are in the following page. ND: below the quantification limit of the measurement, same labels in all of the appendix tables.

Tab. 1 PAH concentration in the surface sediments (ng/g)

location	BaA	chry	BbF	BkF	BeP	BaP	perylene	INcdP	DahA	BghiP
1-1	21.34	24.66	53.58	16.19	33.01	24.07	58.72	35.54	5.80	37.57
1-3	24.17	27.51	67.50	20.03	41.01	31.45	107.01	48.36	7.68	48.12
1-5	17.39	21.18	49.09	14.45	30.67	18.22	67.96	33.62	6.04	35.96
3-12	4.50	5.59	11.85	3.32	7.29	5.08	23.36	7.99	ND	9.04
3-13	15.43	20.77	51.89	14.38	33.29	25.25	176.91	28.34	7.17	44.04
3-15	19.86	20.91	44.49	15.59	28.09	24.77	57.49	26.88	6.30	29.96
3-16	30.32	35.90	91.29	36.35	47.82	39.19	187.11	54.51	15.09	71.99
3-17	15.19	17.69	50.21	14.80	25.83	23.69	219.11	31.36	8.79	49.32
3-18	49.90	51.91	137.21	41.55	73.75	67.36	94.45	108.09	30.65	139.58
3-20	29.31	37.70	89.83	30.55	49.44	61.97	127.49	51.33	13.79	108.08
3-21	17.75	21.85	53.68	16.20	34.77	60.43	258.87	29.97	6.98	93.59
3-22	25.40	29.67	72.56	20.62	38.72	41.76	134.43	44.17	11.86	74.02
3-23	30.06	34.68	84.36	30.10	43.23	51.07	121.08	57.06	15.45	82.76
4-41	22.54	26.03	73.89	23.79	50.98	31.08	57.52	73.94	26.48	59.67
8-6	29.00	30.52	81.55	23.76	54.63	34.74	201.19	61.95	13.92	62.03
8-7	24.80	27.39	75.68	21.41	49.22	32.42	254.66	59.12	13.12	64.48
8-8	7.08	8.62	21.69	5.72	14.33	10.66	37.91	17.39	3.90	20.26
8-9	24.86	28.07	71.53	18.58	44.72	34.03	166.55	49.85	10.40	58.05
8-10	12.92	15.40	46.02	10.95	27.77	17.75	103.60	37.94	7.87	38.28
8-11	42.49	41.97	115.04	34.74	71.95	55.38	72.34	87.23	19.25	88.95
8-19	22.79	25.78	74.38	21.63	49.16	30.28	133.13	58.59	13.21	59.57
8-21	18.33	17.98	52.55	12.01	35.69	20.70	205.47	37.36	8.59	41.66
8-22	34.35	34.79	93.78	25.28	62.27	44.37	89.55	72.05	16.88	74.96
8-23	107.13	122.92	207.46	63.08	128.85	111.37	90.79	144.46	38.65	133.21
8-24	106.56	104.22	212.41	61.79	131.17	135.00	77.53	156.07	39.28	153.27

Tab. 2 PAH concentration in the sediment cores (ng/g)

location	depth cm	naph	2methylnaph	1methylnaph	acenaphthy	acenaphthe	fluorene	phen	anthra	fluor	pyrene
ZS23	2	156.16	69.72	36.09	31.89	22.28	53.20	211.01	155.61	293.74	278.76
ZS23	4	171.94	62.25	35.14	28.82	20.33	51.13	190.74	169.66	234.03	225.59
ZS23	6	217.80	68.23	40.43	32.74	22.37	59.05	199.46	168.96	231.24	223.41
ZS23	8	182.94	57.80	32.09	29.58	20.24	57.88	199.30	171.07	229.67	226.70
ZS23	10	165.25	60.06	33.46	26.58	20.72	49.41	171.47	152.16	197.33	199.81
ZS23	12	233.78	81.81	48.49	37.56	27.71	62.99	204.76	175.58	194.47	196.67
ZS23	14	352.70	98.30	53.27	48.63	32.98	94.28	288.66	235.67	284.76	273.81
ZS23	16	151.57	54.72	28.72	25.42	17.91	51.36	180.34	165.92	263.53	254.69
ZS23	18	139.22	57.55	30.22	25.29	18.20	48.46	181.55	163.55	239.84	234.81
ZS23	20	153.75	55.31	29.56	26.64	18.38	52.93	181.57	169.94	195.92	201.52
ZS23	22	163.78	55.81	30.32	27.08	18.89	52.89	199.46	184.81	199.29	196.37
ZS23	24	271.82	111.13	55.81	52.85	32.40	71.01	254.22	223.50	260.60	251.67
ZS23	26	272.94	119.37	64.51	54.20	37.35	71.80	270.19	228.55	315.91	305.26
ZS23	28	137.56	61.10	30.71	27.10	18.89	51.52	201.90	159.10	289.56	269.86
ZS23	30	126.09	54.63	28.10	23.69	17.97	51.02	211.87	163.28	321.78	293.42
ZS23	32	122.80	50.64	25.00	19.76	16.38	51.24	211.47	146.26	336.57	306.52
ZS23	34	131.36	54.76	28.54	23.11	18.07	50.94	207.84	141.80	301.50	282.04
ZS23	36	118.16	51.71	29.57	20.27	17.63	42.38	156.89	128.18	215.00	208.72
ZS23	38	120.37	43.10	23.07	18.85	12.86	44.43	142.70	165.86	193.87	182.41
ZS23	40	144.12	45.01	24.44	19.94	12.52	48.65	150.33	219.31	246.09	232.89
ML43	2	9.76	6.81	5.50	ND	ND	6.55	26.24	7.47	46.62	36.28
ML43	4	8.37	6.61	4.02	ND	ND	6.64	24.64	7.47	47.51	39.28
ML43	6	7.39	5.70	4.49	ND	ND	6.09	25.13	6.71	49.39	40.78
ML43	8	9.03	6.42	4.27	ND	ND	6.14	24.68	5.95	49.78	40.64
ML43	10	8.59	4.69	3.42	ND	3.42	4.41	23.95	6.58	48.31	38.07
ML43	12	8.86	3.84	ND	ND	ND	5.69	18.46	4.50	36.28	27.01
ML43	14	4.34	3.79	ND	ND	ND	4.19	13.62	3.40	25.08	18.65
ML43	16	5.91	3.35	ND	ND	ND	4.16	16.83	3.05	21.37	15.89

The other PAHs are in the following page.

Tab. 2 PAH concentration in the sediment cores (ng/g)

location	depth cm	BaA	chry	BbF	BkF	BeP	BaP	perylene	INcdP	DahA	BghiP
ZS23	2	134.00	136.71	237.35	66.17	137.15	130.49	127.73	119.77	30.16	126.92
ZS23	4	107.55	121.38	199.90	51.86	118.11	107.91	105.26	102.41	26.49	103.83
ZS23	6	114.79	119.80	196.66	54.27	117.07	103.75	102.40	109.33	28.39	112.61
ZS23	8	114.20	117.88	192.91	52.71	115.58	106.42	104.90	104.53	26.05	110.66
ZS23	10	100.64	107.61	174.32	45.04	105.88	90.34	88.77	99.12	24.32	92.96
ZS23	12	96.86	103.02	171.69	45.24	101.89	91.41	90.41	98.82	25.05	102.62
ZS23	14	133.66	141.07	219.01	59.45	129.95	119.48	104.57	119.85	28.39	117.75
ZS23	16	133.85	140.93	228.38	57.86	136.31	141.28	134.07	124.48	31.45	149.93
ZS23	18	119.60	135.38	216.12	57.56	130.45	108.93	125.62	124.42	29.72	128.22
ZS23	20	105.86	111.38	182.45	48.84	109.04	93.29	96.22	113.58	26.38	108.87
ZS23	22	101.25	101.72	175.51	45.58	102.42	99.24	100.78	107.44	26.03	117.43
ZS23	24	112.17	116.69	196.53	54.53	116.14	108.29	101.92	122.95	27.70	126.11
ZS23	26	144.49	156.12	237.40	62.42	143.55	135.66	133.93	147.80	33.91	152.28
ZS23	28	141.68	161.48	254.55	68.13	156.72	162.09	188.68	154.65	35.13	193.86
ZS23	30	155.38	164.60	259.51	74.54	157.84	145.49	177.57	167.71	41.15	197.19
ZS23	32	163.20	169.42	271.55	66.45	162.83	150.93	208.76	168.94	39.07	199.59
ZS23	34	155.91	166.80	269.94	73.98	163.82	156.81	208.20	169.97	41.50	200.66
ZS23	36	107.30	113.06	198.81	52.84	122.36	110.05	182.93	130.57	29.36	148.20
ZS23	38	103.88	106.75	187.67	47.13	113.56	95.13	126.68	116.81	27.48	126.15
ZS23	40	128.19	133.86	229.00	62.19	137.83	108.47	104.56	143.73	32.69	142.82
ML43	2	13.94	17.10	49.57	14.57	32.41	18.25	144.51	26.48	5.41	30.27
ML43	4	15.40	17.67	53.94	14.60	34.45	18.68	154.87	28.13	6.37	31.38
ML43	6	15.74	17.03	52.50	14.08	33.24	19.51	147.84	27.72	5.83	30.98
ML43	8	16.45	19.07	57.09	16.71	35.99	16.83	154.76	31.71	6.22	33.16
ML43	10	15.91	18.13	52.01	15.49	32.30	18.68	139.13	27.36	5.49	29.80
ML43	12	11.73	12.04	39.65	10.53	23.17	11.16	139.87	18.91	3.77	19.51
ML43	14	7.35	8.19	25.55	7.90	14.57	8.74	142.07	11.55	3.04	11.60
ML43	16	6.44	6.38	21.53	6.27	11.09	6.34	171.04	10.09	3.06	10.75

Tab. 2 PAH concentration in the sediment cores (ng/g)

location	depth cm	naph	2methylnaph	1methylnaph	acenaphthy	acenaphthe	fluorene	phen	anthra	fluor	pyrene
ML35	2	23.21	11.17	8.00	4.48	3.82	10.93	44.37	11.88	92.48	66.70
ML35	4	28.95	15.78	9.65	4.15	3.33	11.55	43.48	11.66	92.25	66.64
ML35	6	24.87	13.17	7.85	4.12	3.13	12.47	46.87	10.88	91.85	66.03
ML35	8	19.70	10.77	6.53	4.34	3.49	12.06	45.92	11.21	96.32	69.47
ML35	10	18.71	9.20	6.33	5.65	3.90	11.08	42.13	12.53	115.80	88.97
ML35	12	17.15	12.38	7.04	3.62	3.47	14.67	59.97	12.70	109.68	80.65
ML35	14	16.13	8.90	6.04	3.00	3.59	12.04	42.68	10.75	99.13	70.23
ML35	16	17.14	9.29	6.64	3.94	3.54	15.34	86.34	9.50	101.34	72.74
ML35	18	13.21	7.35	3.55	3.03	3.03	9.69	33.51	10.47	95.30	70.37
ML35	20	15.62	9.27	8.30	3.98	3.13	10.84	40.49	10.86	101.82	72.74
ML35	22	39.61	13.22	13.46	4.48	6.66	10.62	36.97	10.95	87.97	64.93
ML35	24	6.59	3.41	3.70	3.15	7.44	6.80	21.72	4.59	40.22	31.37
ML35	26	6.85	3.24	3.01	ND	ND	4.21	16.15	4.34	12.63	11.96
ML35	28	7.51	3.29	3.61	3.08	ND	3.04	10.53	3.15	9.16	10.37
ML35	30	19.63	4.67	13.47	3.79	ND	4.05	11.86	3.03	9.73	9.33
ML35	32	5.83	ND	ND	3.86	ND	4.24	16.24	3.26	8.63	7.57
ML35	34	5.47	5.63	3.15	3.28	ND	3.13	13.07	3.30	7.57	7.12
ML35	36	4.90	3.70	4.17	ND	ND	3.61	11.23	3.11	6.00	5.17
ML35	38	6.33	4.52	ND	ND	ND	5.98	21.32	5.01	6.16	5.37
ML24	2	31.56	15.47	10.41	7.96	7.31	14.14	96.60	45.03	218.76	202.02
ML24	4	30.46	15.84	8.48	8.67	10.12	15.97	105.73	56.36	227.05	207.24
ML24	6	34.90	18.50	11.58	12.01	13.33	31.40	223.08	91.04	505.87	414.35
ML24	8	64.72	20.48	12.79	7.82	23.53	46.14	272.32	128.95	601.10	478.97
ML24	10	62.29	30.26	16.78	9.37	17.00	38.91	210.07	171.47	467.33	394.96
ML24	12	57.44	28.56	16.22	9.68	18.49	40.72	269.92	167.08	541.58	445.19
ML24	14	56.85	20.35	11.36	7.98	15.42	31.67	189.90	181.99	420.40	360.34
ML24	16	45.73	23.57	13.27	8.13	14.93	36.08	215.21	177.90	467.31	394.34
ML24	18	23.46	13.44	7.45	5.35	8.52	22.98	130.53	69.75	276.61	245.33

The other PAHs are in the following page.

Tab. 2 PAH concentration in the sediment cores (ng/g)

location	depth cm	BaA	chry	BbF	BkF	BeP	BaP	perylene	INcdP	DahA	BghiP
ML35	2	32.67	36.72	121.59	33.74	80.32	41.09	213.63	126.43	42.73	74.71
ML35	4	30.41	36.99	103.02	28.85	73.91	47.63	213.94	105.01	32.07	65.18
ML35	6	33.00	40.60	85.25	21.33	61.76	41.86	199.47	69.43	20.67	55.74
ML35	8	33.52	39.37	99.44	24.55	75.84	47.23	188.85	94.31	30.57	69.88
ML35	10	46.43	48.12	134.76	39.04	97.18	67.44	190.99	168.35	42.79	100.36
ML35	12	37.19	40.72	121.67	31.09	94.33	55.05	198.65	168.58	53.59	95.31
ML35	14	34.72	41.86	114.45	30.96	84.64	55.19	235.81	134.58	46.63	102.14
ML35	16	31.90	37.69	113.76	30.53	81.72	43.36	214.29	127.77	40.26	91.18
ML35	18	33.28	34.73	100.40	30.51	68.71	41.93	228.86	102.44	34.32	67.58
ML35	20	34.83	40.54	117.08	43.43	74.73	45.31	237.27	111.86	34.86	80.47
ML35	22	30.53	34.09	76.27	18.69	50.20	55.96	383.95	54.85	13.44	61.07
ML35	24	13.55	14.63	43.33	13.31	29.91	17.63	685.36	37.42	13.59	29.73
ML35	26	3.67	3.67	12.61	4.40	8.05	5.79	1074.00	10.89	5.37	8.98
ML35	28	3.66	4.05	7.54	3.03	5.35	5.07	953.42	5.12	ND	3.86
ML35	30	4.97	4.47	8.84	ND	7.21	ND	909.44	3.12	ND	3.86
ML35	32	3.69	3.53	6.80	3.11	4.22	3.01	633.05	3.32	ND	3.33
ML35	34	3.77	3.66	5.16	4.61	3.10	9.38	820.61	3.37	ND	3.19
ML35	36	3.93	3.95	4.63	3.15	3.39	3.14	762.21	3.41	ND	6.47
ML35	38	3.03	3.48	6.40	3.38	3.65	4.08	864.53	4.90	ND	4.39
ML24	2	94.78	79.37	252.48	78.96	143.69	127.60	61.02	299.57	73.94	197.21
ML24	4	125.36	122.83	277.84	87.02	173.39	141.64	76.75	314.33	74.84	272.40
ML24	6	260.81	223.18	489.43	151.90	302.45	281.82	107.18	621.11	149.99	565.32
ML24	8	283.48	252.41	561.51	169.91	340.20	333.21	121.17	699.89	161.04	598.13
ML24	10	212.03	203.59	411.93	130.70	259.41	249.71	92.91	482.49	118.80	452.22
ML24	12	248.50	262.57	526.47	160.36	321.12	285.32	99.70	541.80	138.84	497.11
ML24	14	198.67	184.91	384.89	114.14	235.27	234.77	90.46	376.83	97.09	364.59
ML24	16	199.43	195.59	347.50	108.43	217.33	211.11	73.98	292.84	84.68	266.81
ML24	18	124.26	120.84	215.59	71.46	134.60	127.54	57.85	180.52	50.30	159.87

Tab. 2 PAH concentration in the sediment cores (ng/g)

location	depth cm	naph	2methylnaph	1methylnaph	acenaphthy	acenaphthe	fluorene	phen	anthra	fluor	pyrene
GH4	2	11.87	10.60	5.79	3.57	3.57	10.63	31.56	9.71	84.32	65.03
GH4	4	12.53	7.90	3.54	3.65	4.15	8.51	26.47	8.47	73.02	55.36
GH4	6	12.47	6.15	4.64	3.42	3.97	7.64	23.65	6.96	67.60	50.90
GH4	8	12.54	5.93	4.81	3.49	5.03	7.32	22.44	7.21	59.97	45.25
GH4	10	11.81	5.82	4.05	3.48	3.90	7.49	22.34	7.33	62.06	46.05
GH4	12	10.12	5.72	3.57	3.60	3.04	7.26	21.83	7.23	60.87	46.10
GH4	14	18.13	10.53	5.91	3.28	5.55	9.97	32.48	11.44	90.29	67.50
GH4	16	43.48	47.74	29.89	3.20	7.38	22.43	65.02	17.49	139.60	109.64
GH4	18	24.12	12.74	7.08	3.62	5.19	14.89	44.10	14.43	138.94	105.05
GH4	20	20.64	14.39	6.81	3.12	4.82	15.54	49.33	15.37	139.21	110.35
GH4	22	18.07	9.84	4.44	3.05	3.54	10.61	37.14	10.92	103.02	82.68
GH4	24	9.88	4.50	3.46	3.29	3.13	6.26	24.35	6.58	65.73	54.22
GH4	26	7.05	4.25	ND	ND	ND	4.65	12.08	4.68	29.28	23.99
GH4	28	23.35	7.69	5.42	3.15	4.71	4.61	12.55	3.44	22.19	19.97
ZS42	2	11.56	9.40	4.48	4.37	3.66	7.65	57.44	9.78	42.04	34.23
ZS42	4	11.86	7.00	3.54	4.30	ND	6.63	32.00	10.05	39.46	33.06
ZS42	6	16.65	9.85	4.80	ND	3.23	6.74	42.04	13.54	48.49	39.41
ZS42	8	17.54	8.99	4.88	3.44	3.01	6.94	40.52	14.82	49.81	42.70
ZS42	10	13.95	8.16	4.04	ND	3.17	7.49	28.61	11.86	48.17	39.89
ZS42	12	8.64	6.27	4.80	ND	3.09	4.73	29.80	9.99	36.82	31.07
ZS42	14	5.87	3.23	3.47	ND	3.17	3.60	19.38	5.70	24.11	20.09
ZS42	16	6.38	3.28	3.07	ND	ND	5.73	22.91	4.72	23.04	17.23
ZS42	18	7.85	3.63	3.88	3.42	3.15	4.55	24.58	6.58	21.12	15.40
ZS42	20	7.48	4.67	ND	ND	3.07	5.07	23.94	3.25	16.90	11.10
ZS42	22	6.27	3.83	ND	ND	4.41	3.20	19.65	3.11	15.07	9.79
ZS42	24	4.94	3.06	3.68	ND	3.02	3.24	25.50	3.90	17.64	12.62

The other PAHs are in the following page.

Tab. 2 PAH concentration in the sediment cores (ng/g)

location	depth cm	BaA	chry	BbF	BkF	BeP	BaP	perylene	INcdP	DahA	BghiP
GH4	2	31.69	29.67	88.76	25.45	56.30	33.19	60.04	53.68	11.26	46.41
GH4	4	27.43	26.24	78.51	24.80	48.21	29.35	46.94	47.20	9.67	40.44
GH4	6	25.50	24.46	69.17	20.59	43.12	28.59	48.75	37.57	7.88	31.85
GH4	8	21.98	19.82	60.23	16.89	38.31	23.03	41.79	29.32	6.48	27.55
GH4	10	23.95	21.42	62.10	17.59	39.35	25.79	41.69	31.15	7.07	30.62
GH4	12	23.75	20.72	64.68	17.87	39.80	23.02	39.56	33.01	6.99	27.91
GH4	14	36.01	32.03	97.63	27.38	60.93	36.94	56.17	51.50	11.66	45.87
GH4	16	53.19	48.59	140.14	42.36	90.59	51.88	77.32	78.07	17.98	69.80
GH4	18	47.86	42.65	127.09	37.00	79.82	49.62	75.58	62.91	12.44	59.02
GH4	20	49.76	44.04	130.93	40.00	80.55	49.69	76.09	63.67	13.59	55.52
GH4	22	38.01	35.52	105.08	29.57	64.89	38.20	73.48	48.36	10.71	44.51
GH4	24	24.22	23.43	66.70	19.64	39.59	21.09	93.53	27.97	5.69	25.38
GH4	26	11.50	10.55	31.15	8.58	17.44	13.37	128.88	11.63	ND	10.68
GH4	28	6.10	5.34	15.62	3.79	8.73	6.16	87.60	3.96	ND	3.71
ZS42	2	16.15	17.11	46.23	15.59	31.42	20.56	149.25	27.94	7.00	38.91
ZS42	4	16.23	17.95	45.89	13.81	30.25	21.65	143.74	29.10	7.15	35.37
ZS42	6	18.10	20.94	52.41	12.42	34.00	22.53	200.75	28.51	8.37	46.97
ZS42	8	17.49	21.24	54.66	15.61	36.55	25.56	185.29	34.70	9.21	45.57
ZS42	10	18.41	23.21	51.34	16.08	33.49	22.30	181.01	24.69	7.38	42.59
ZS42	12	14.32	15.25	46.04	12.02	30.28	17.53	231.28	28.28	6.34	35.59
ZS42	14	7.34	7.62	22.22	6.18	14.70	10.29	263.81	12.29	ND	17.03
ZS42	16	5.13	7.88	23.66	7.70	14.28	7.49	325.84	12.40	4.90	14.99
ZS42	18	5.30	8.12	20.07	3.17	10.31	8.11	323.60	10.88	ND	15.14
ZS42	20	3.01	4.33	9.24	3.75	5.02	3.56	358.05	4.85	ND	6.03
ZS42	22	3.39	3.40	7.76	3.63	4.01	3.01	366.27	4.35	ND	4.33
ZS42	24	3.08	4.91	11.15	3.06	7.61	4.62	449.61	6.19	ND	8.89

Tab. 2 PAH concentration in the sediment cores (ng/g)

location	depth cm	naph	2methylnaph	1methylnaph	acenaphthy	acenaphthe	fluorene	phen	anthra	fluor	pyrene
ML36	2	11.38	8.61	5.20	3.40	3.83	7.68	38.00	7.04	71.21	52.81
ML36	4	14.05	10.56	5.97	3.44	3.73	8.51	45.39	7.07	76.57	54.69
ML36	6	15.36	6.74	8.32	3.57	3.49	8.63	34.75	7.45	75.97	54.22
ML36	8	11.70	8.76	6.49	3.86	3.80	5.77	37.72	6.65	78.57	56.84
ML36	10	14.69	7.84	5.91	3.46	3.16	8.48	41.16	8.10	81.31	59.35
ML36	12	19.05	13.28	11.14	3.98	3.69	10.26	55.08	7.91	79.37	59.11
ML36	14	12.49	7.00	8.68	4.03	5.09	6.73	38.38	7.40	79.47	58.59
ML36	16	12.02	5.79	4.98	3.13	3.58	7.86	62.56	7.32	98.33	73.55
ML36	18	20.97	7.37	7.19	3.52	3.68	7.78	46.00	9.19	93.25	71.17
ML36	20	9.57	3.39	3.40	ND	3.20	3.85	28.34	5.01	51.41	38.78
ML36	22	ND	ND	ND	ND	ND	3.89	8.28	3.11	5.00	3.46
ML36	24	7.07	3.66	ND	ND	ND	5.33	12.85	3.06	6.08	4.28
GH38	2	5.79	4.68	3.48	3.01	ND	5.17	23.40	3.64	41.36	28.47
GH38	4	5.80	3.94	ND	ND	ND	4.87	21.97	3.09	19.11	12.75
GH38	6	5.04	ND	ND	ND	ND	4.64	11.59	3.11	6.86	5.62
GH38	8	5.28	ND	ND	ND	ND	6.29	12.41	3.14	6.46	4.92
GH38	10	4.62	ND	ND	ND	ND	4.69	10.74	3.19	6.97	5.85
GH38	12	5.99	ND	ND	ND	ND	5.79	13.07	3.90	15.48	12.38
GH38	14	5.19	ND	ND	ND	ND	4.61	9.39	3.19	6.75	6.28
GH38	16	4.56	ND	ND	ND	ND	4.70	8.85	3.12	6.36	6.75
GH38	18	4.83	ND	ND	ND	ND	ND	5.50	3.05	7.38	5.91
GH38	20	5.45	3.06	3.47	ND	ND	5.18	20.10	3.85	44.33	32.79
GH38	22	5.36	3.81	3.43	ND	3.11	4.60	22.87	4.71	53.75	41.14
GH38	24	6.18	3.56	3.74	ND	ND	4.68	21.98	5.02	52.00	37.89
GH38	26	5.70	3.53	ND	ND	ND	4.91	18.59	3.79	41.24	30.21
GH38	28	4.02	ND	ND	ND	ND	3.45	10.67	3.51	26.12	21.28
GH38	30	7.64	3.91	ND	ND	3.18	3.55	20.07	3.78	41.22	29.35

The other PAHs are in the following page.

Tab. 2 PAH concentration in the sediment cores (ng/g)

location	depth cm	BaA	chry	BbF	BkF	BeP	BaP	perylene	INcdP	DahA	BghiP
ML36	2	24.71	28.12	78.56	22.30	52.13	30.43	113.12	52.52	12.94	49.81
ML36	4	27.87	30.78	86.42	18.99	54.35	33.65	118.36	55.81	12.57	52.36
ML36	6	28.04	28.89	85.56	21.62	54.84	28.34	115.76	57.40	13.45	49.53
ML36	8	26.79	28.68	85.34	24.77	54.32	30.00	113.79	56.59	12.94	54.90
ML36	10	29.71	31.55	89.07	25.08	57.65	35.43	110.85	50.91	14.39	42.26
ML36	12	27.10	27.09	80.44	22.09	51.17	30.61	106.50	43.60	10.32	37.07
ML36	14	28.48	29.78	83.15	23.69	52.25	31.84	98.48	45.12	11.36	38.03
ML36	16	34.37	36.53	100.28	29.43	63.08	33.43	104.32	57.19	13.74	52.03
ML36	18	35.20	36.11	101.40	28.24	61.26	39.66	103.59	44.20	11.36	39.75
ML36	20	19.95	20.31	58.45	17.26	35.26	19.95	73.36	26.54	6.73	24.76
ML36	22	3.95	4.25	ND	ND	ND	ND	ND	3.08	ND	3.02
ML36	24	3.62	5.83	6.39	ND	3.15	ND	9.14	3.78	ND	3.98
GH38	2	12.04	13.66	28.67	8.88	24.06	15.59	636.46	18.20	3.75	22.75
GH38	4	4.87	5.56	15.82	4.57	9.56	6.28	898.04	8.22	ND	8.09
GH38	6	3.45	4.29	7.21	ND	6.50	ND	1045.52	7.50	ND	7.75
GH38	8	3.15	3.82	6.18	ND	4.28	ND	1126.35	6.80	ND	7.43
GH38	10	3.73	4.24	7.26	ND	7.21	ND	1068.07	6.20	ND	7.13
GH38	12	4.92	5.89	15.78	4.61	9.10	4.11	837.95	6.19	ND	7.00
GH38	14	3.00	3.10	7.20	ND	4.23	4.57	845.58	3.08	ND	3.36
GH38	16	3.67	3.88	6.54	ND	7.02	ND	946.60	3.00	ND	3.12
GH38	18	3.77	3.18	7.03	ND	4.56	5.16	359.68	3.58	ND	3.82
GH38	20	14.80	16.29	44.46	13.99	28.35	16.21	487.34	21.86	4.57	21.22
GH38	22	17.99	18.63	52.84	15.41	32.71	21.62	301.09	29.68	5.78	28.46
GH38	24	17.69	18.09	57.29	16.46	33.61	19.92	151.21	30.78	6.23	27.40
GH38	26	13.13	13.84	43.13	11.17	25.48	14.19	137.34	22.94	4.21	22.19
GH38	28	10.08	11.03	32.53	10.11	20.46	14.68	123.55	17.69	4.39	18.57
GH38	30	14.76	15.97	45.75	14.06	28.02	16.92	201.95	23.57	5.01	21.69

Tab. 2 PAH concentration in the sediment cores (ng/g)

location	depth cm	naph	2methylnaph	1methylnaph	acenaphthy	acenaphthe	fluorene	phen	anthra	fluor	pyrene
ML6	2	21.01	9.23	4.67	4.06	3.47	8.10	41.20	13.78	97.63	76.08
ML6	4	11.54	8.54	5.51	3.83	3.24	8.74	39.39	12.92	95.74	74.29
ML6	6	31.48	9.23	8.80	3.37	3.46	9.44	40.97	13.70	92.54	72.12
ML6	8	20.19	6.93	4.74	2.65	3.30	10.63	37.41	13.33	88.16	68.18
ML6	10	11.80	6.61	5.74	3.56	3.20	8.71	36.33	12.80	87.77	67.46
ML6	12	18.55	8.10	5.84	3.96	3.23	10.49	38.49	13.14	84.97	64.43
ML6	14	21.45	8.74	7.44	3.48	3.09	10.48	43.18	15.29	97.03	74.33
ML6	16	18.59	7.29	5.31	3.40	3.32	9.58	39.58	14.46	99.60	76.95
ML6	18	14.84	7.36	5.15	3.32	3.05	9.22	38.93	14.92	98.91	78.40
ML6	20	10.29	6.46	6.90	3.17	3.31	8.83	39.77	14.28	97.29	80.46
ML6	22	11.73	5.48	5.18	3.14	3.25	6.74	32.91	11.42	75.37	66.15
ML6	24	10.22	5.71	3.10	3.35	3.45	5.62	30.27	9.16	61.07	51.46
ML6	26	9.57	4.93	3.60	3.61	3.54	4.73	26.34	7.52	53.40	44.69
ML6	28	4.43	ND	ND	ND	ND	3.67	11.26	3.12	12.76	10.07
ML6	30	3.88	ND	ND	ND	ND	3.79	10.01	3.08	7.09	5.30
GH11	2	24.93	12.96	9.73	4.28	3.82	10.13	43.60	8.50	97.04	71.39
GH11	4	18.35	10.25	7.74	3.68	3.16	8.56	37.47	8.11	94.03	69.38
GH11	6	11.76	5.32	5.46	3.43	3.88	7.50	38.91	6.55	85.22	64.20
GH11	8	6.72	4.08	4.87	ND	ND	5.81	19.45	3.62	35.15	27.58
GH11	10	3.47	3.98	ND	ND	ND	4.60	13.36	3.28	22.51	17.39
GH11	12	3.67	ND	ND	ND	ND	3.31	6.15	4.54	ND	ND

The other PAHs are in the following page.

Tab. 2 PAH concentration in the sediment cores (ng/g)

location	depth cm	BaA	chry	BbF	BkF	BeP	BaP	perylene	INcdP	DahA	BghiP
ML6	2	39.71	40.43	104.96	30.49	63.01	41.80	154.65	59.80	13.18	55.46
ML6	4	37.17	39.98	100.30	27.98	62.01	42.97	149.32	60.06	12.80	55.41
ML6	6	36.62	37.66	100.56	28.27	61.83	44.13	148.51	56.55	12.33	51.88
ML6	8	37.07	38.61	99.55	26.97	61.99	42.13	145.07	56.53	12.07	54.44
ML6	10	37.60	39.98	113.06	29.99	74.79	49.18	148.83	109.37	26.81	100.72
ML6	12	35.21	37.73	99.89	23.16	67.33	41.15	144.97	82.77	20.75	78.30
ML6	14	38.05	40.59	110.07	26.00	74.04	46.85	145.51	98.37	25.61	93.18
ML6	16	40.07	40.68	114.84	29.71	72.55	47.96	142.49	94.31	24.49	90.65
ML6	18	40.80	42.63	123.40	31.33	80.14	50.54	148.82	109.64	25.60	102.44
ML6	20	40.02	45.23	118.15	33.56	74.94	52.67	138.60	88.74	22.70	85.05
ML6	22	30.02	33.71	90.52	24.45	55.08	38.15	158.14	65.08	16.55	61.22
ML6	24	26.94	28.90	73.40	22.07	45.59	31.90	182.24	54.36	14.07	49.44
ML6	26	22.69	23.14	58.71	17.67	35.33	26.39	181.45	40.79	9.63	39.89
ML6	28	5.01	5.16	11.99	3.15	7.27	5.43	54.21	7.79	3.16	8.33
ML6	30	3.20	3.49	5.33	ND	5.00	ND	15.99	6.04	ND	6.73
GH11	2	30.67	31.76	118.10	37.24	72.57	41.01	55.71	93.97	26.32	61.50
GH11	4	34.27	32.27	125.35	36.71	75.51	46.01	66.79	121.28	27.48	86.29
GH11	6	29.35	27.54	112.78	35.07	67.31	42.84	45.58	121.82	29.17	77.25
GH11	8	14.37	11.96	49.38	16.95	29.23	22.08	25.71	48.39	13.37	32.39
GH11	10	10.97	9.56	31.44	10.15	18.41	15.91	13.39	31.53	11.49	22.88
GH11	12	3.61	3.46	ND	ND	ND	ND	ND	3.62	ND	3.31

Tab. 2 PAH concentration in the sediment cores (ng/g)

location	depth cm	naph	2methylnaph	1methylnaph	acenaphthy	acenaphthe	fluorene	phen	anthra	fluor	pyrene
ML7	2	20.65	10.12	5.37	3.77	3.73	9.55	34.51	11.18	102.32	90.68
ML7	4	21.15	9.82	6.69	3.59	3.05	10.63	37.07	12.00	90.32	77.37
ML7	6	19.05	8.90	6.86	3.63	3.88	10.20	33.95	10.49	81.28	69.85
ML7	8	18.02	9.74	6.62	3.74	3.03	10.79	36.19	11.08	86.23	73.90
ML7	10	20.09	10.03	7.18	3.05	3.62	11.38	43.09	12.90	106.62	90.72
ML7	12	20.22	8.57	6.01	3.20	3.00	11.98	39.46	12.03	105.99	88.43
ML7	14	22.57	10.86	6.09	3.86	3.78	14.54	41.56	13.45	99.65	82.97
ML7	16	18.72	8.92	5.32	3.95	3.45	11.51	36.79	13.27	98.50	83.38
ML7	18	16.19	8.71	6.63	3.79	3.14	10.70	33.93	11.27	88.61	74.37
ML7	20	18.24	9.26	6.43	3.94	3.37	12.53	39.37	13.86	111.00	94.52
ML7	22	19.32	9.02	6.43	3.87	3.43	11.55	42.16	14.67	124.57	104.32
ML7	24	22.22	9.87	6.57	3.74	3.56	14.70	53.70	17.44	113.41	93.82
ML7	26	18.35	9.73	6.23	3.09	4.03	12.58	44.62	16.17	132.29	113.97
ML7	28	21.87	10.85	7.34	3.96	3.84	12.88	48.33	16.36	139.08	119.38
ML7	30	20.19	12.23	7.20	3.63	5.45	12.15	44.90	15.87	127.56	112.17
ML7	32	19.21	11.53	7.02	3.11	3.84	11.96	45.81	16.12	129.98	111.58
ML7	34	21.13	11.31	7.01	3.41	4.07	12.77	46.93	16.66	134.58	116.39

The other PAHs are in the following page.

Tab. 2 PAH concentration in the sediment cores (ng/g)

location	depth cm	BaA	chry	BbF	BkF	BeP	BaP	perylene	INcdP	DahA	BghiP
ML7	2	93.44	87.01	226.78	66.87	149.44	114.88	165.98	215.42	44.52	185.30
ML7	4	46.83	42.53	122.45	33.77	82.21	56.70	156.95	110.23	23.79	101.71
ML7	6	46.37	44.74	125.46	37.14	84.71	50.74	146.46	107.68	23.43	89.86
ML7	8	45.78	43.25	123.88	35.21	80.70	49.66	143.65	108.87	20.59	85.95
ML7	10	53.41	47.91	135.26	42.44	88.70	58.29	152.13	111.59	24.18	91.97
ML7	12	50.73	46.94	128.61	39.68	87.59	48.21	141.87	94.81	20.63	76.19
ML7	14	58.05	52.17	152.12	46.30	103.81	64.07	184.76	126.85	29.05	107.03
ML7	16	51.30	47.70	136.69	38.13	92.71	50.37	147.59	105.15	23.05	80.01
ML7	18	41.06	37.24	112.28	32.82	74.58	38.85	123.96	78.63	18.34	62.22
ML7	20	59.80	55.11	153.60	41.62	103.12	55.00	151.31	113.91	21.14	80.36
ML7	22	61.33	54.34	156.25	42.15	99.89	60.52	168.14	102.80	21.96	84.91
ML7	24	55.84	54.54	131.21	34.64	83.32	50.49	131.85	79.36	17.76	67.93
ML7	26	64.83	55.13	153.21	49.68	98.21	55.78	168.13	99.65	21.35	75.58
ML7	28	64.24	58.70	159.61	47.02	100.75	65.83	198.89	100.73	23.75	84.44
ML7	30	60.16	53.70	149.99	46.20	94.57	61.53	190.67	91.51	21.13	76.02
ML7	32	61.03	54.78	138.75	41.03	86.23	56.70	199.09	75.32	17.04	65.16
ML7	34	62.93	59.38	145.19	42.22	90.65	63.72	218.61	83.39	17.98	71.30

Tab. 3 PAH concentration in the water samples (ng/L)

location	naph	2methylnaph	1methylnaph	acenaphthy	acenaphthe	fluorene	phen	anthra	fluor	pyrene
11-2	81.84	46.10	27.18	ND	ND	ND	13.99	ND	ND	ND
11-3	55.53	48.50	18.83	ND	ND	ND	ND	ND	ND	ND
11-12	96.07	45.58	25.59	ND	ND	ND	ND	ND	ND	ND
11-13	112.47	56.31	31.18	ND	ND	ND	11.51	ND	ND	ND
11-14	109.31	50.27	29.18	ND	ND	ND	ND	ND	ND	ND
11-15	48.25	32.29	20.33	ND	ND	ND	ND	ND	ND	ND
11-18	60.38	62.98	21.03	ND	ND	ND	ND	ND	ND	ND
11-20	41.62	42.22	19.16	ND	ND	ND	ND	ND	ND	ND
11-21	51.24	34.18	19.57	ND	ND	ND	ND	ND	ND	ND
11-23	57.93	35.78	21.16	ND	ND	ND	ND	ND	ND	ND
6-1	255.34	262.39	165.85	ND	ND	23.98	46.86	ND	ND	ND
6-2	289.67	261.37	176.13	ND	ND	32.64	51.47	ND	ND	ND
6-5	379.00	362.97	233.63	ND	10.67	28.42	30.16	ND	ND	ND
6-6	396.71	367.30	233.80	ND	12.42	28.75	48.80	ND	ND	ND
6-7	393.13	386.71	247.58	ND	12.98	27.12	29.20	ND	ND	ND
6-8	403.23	398.67	245.01	ND	13.18	30.36	37.98	ND	ND	ND
6-9	434.72	387.20	260.57	10.14	15.53	32.37	35.78	ND	ND	ND
6-10	373.41	311.60	208.16	ND	12.05	24.74	39.18	ND	ND	ND
6-11	746.66	761.80	484.70	11.01	21.69	51.40	41.50	ND	ND	ND
6-12	483.07	439.36	294.71	ND	10.12	28.74	23.39	ND	ND	ND
6-13	358.75	327.86	213.10	ND	ND	23.47	22.96	ND	ND	ND

Tab. 3 PAH concentration in the water samples (ng/L)

location	naph	2methylnaph	1methylnaph	acenaphthy	acenaphthe	fluorene	phen	anthra	fluor	pyrene
2-2	118.88	69.36	38.94	ND	ND	12.16	33.27	ND	ND	ND
2-4	97.85	72.39	41.89	ND	ND	15.01	39.45	ND	ND	ND
2-6	62.39	56.89	33.38	ND	ND	12.74	20.90	ND	ND	ND
2-9	66.70	66.57	36.49	ND	ND	14.17	23.37	ND	ND	ND
2-11	58.39	51.87	34.75	ND	ND	ND	20.35	ND	ND	ND
2-14	91.26	62.19	51.58	ND	10.39	26.92	34.20	13.10	ND	ND
2-21	487.00	62.40	32.32	ND	ND	18.12	27.60	ND	ND	ND
2-22	483.15	61.92	32.46	ND	ND	18.00	23.19	ND	ND	ND
2-23	520.48	62.17	33.71	ND	ND	18.50	26.85	ND	ND	ND
2-24	491.00	87.69	44.51	ND	ND	18.55	27.14	ND	ND	ND
9-2	318.31	595.93	269.95	ND	ND	11.48	29.52	ND	ND	ND
9-3	488.26	1235.23	563.71	ND	ND	15.04	29.81	ND	ND	ND
9-4	423.70	1026.78	460.95	ND	ND	13.03	33.69	ND	ND	ND
9-6	440.91	1111.41	508.97	ND	ND	15.90	34.73	ND	ND	ND
9-7	559.06	1347.05	605.13	ND	10.27	17.93	32.23	ND	ND	ND
9-8	341.20	601.94	265.84	ND	ND	13.15	29.14	ND	ND	ND
9-10	392.01	738.69	329.47	ND	ND	13.79	33.17	ND	ND	ND
9-11	359.56	477.20	188.30	ND	ND	ND	15.55	ND	ND	ND
9-12	612.86	1018.76	446.67	ND	14.08	20.34	44.59	ND	11.88	14.47
9-14	417.68	685.01	304.72	ND	ND	14.14	28.21	ND	ND	ND

Acknowledgement

This research was based on the project of Sino-German water supply network supported by BMBF-SIGN 02WCL1336C and by the International Science & Technology Cooperation Program of China (No. 2016YFE0123700). I am grateful for the four-year scholarship support from the China Scholarship Council.

I sincerely thank my supervisor prof. Dr. Christoph Schüth for guiding me in the last four years. Due to the topic change and the project delay, the current topic was completely new for me and started in the second year of my Ph.D., so I appreciate my supervisor's patient enlightenment and instruction to get my Ph.D. work accomplished. In addition, I thank him for supporting me after my scholarship ended.

Furthermore, I was motivated by my families and friends during the last years when I was depressed and frustrated. Because of your encouragement and comfort, I become tougher to face difficulties and challenges. It is so fortunate to have you in my life.

During Ph.D., I had four times of field campaign, I am thankful to my campaign partners for nice cooperation. The partners are from IWW Water Centre in Mülheim an der Ruhr, Working Group of Environmental Mineralogy & Env. System Analysis (ENMINSA), Karlsruhe Institute of Technology (KIT), Jiangnan University, Technologiezentrum Wasser (TZW), Nanjing Institute of Geography and Limnology (NIGLAS), Tongji University, Chinese Research Academy of Environmental Sciences, Hydroisotop GmbH. I especially thank KIT for supplying sediment core sampler. In addition, I thank Dr. Michael Schubert from Helmholtz-Zentrum für Umweltforschung – UFZ for helping in the sediment dating measurement.

Last but not the least, I thank our lab technicians, Claudia Cosma, Stefanie Schmidt, Neumann Zahra for instructions in my laboratory work. Meanwhile, I thank all other colleagues from our hydrogeology group and some colleagues from our Institute of Applied Geosciences, it was nice and happy to work with you guys in the last years.

My heartfelt gratitude to all of you!!!